3D Dynamo Notes

A.D. Richmond and A. Maute

Draft, 2025 January 19

Contents

Chapter 1

Overview

The model assumes that the electric field $\mathbf{E}$ is electrostatic and exactly perpendicular to the main geomagnetic field $\mathbf{B}_0$, and that the electric current density $\mathbf{J}$ is divergence-free. The model provides an solution for the ionospheric dynamo equations

$$\mathbf{E} = -\nabla\Phi \tag{1.1}$$

$$\nabla \cdot \mathbf{J} = 0 \tag{1.2}$$

$$\mathbf{J} = \sigma_P \mathbf{E} + \sigma_H \mathbf{b}_0 \times \mathbf{E} + \mathbf{J}^D + \mathbf{J}_\parallel \tag{1.3}$$

where Φ is the electrostatic potential, σ_P and σ_H are the Pedersen and Hall conductivities, $\mathbf{J}_\parallel$ is the current density along $\mathbf{B}_0$, $\mathbf{b}_0$ is a unit vector along $\mathbf{B}_0$, and $\mathbf{J}^D$ is the dynamo source current. The Pedersen and Hall conductivities are

$$\sigma_P = \frac{Ne}{B_0}\left(\frac{\nu_{in}\Omega_i}{\nu_{in}^2 + \Omega_i^2} + \frac{\nu_{en\perp}\Omega_e}{\nu_{en\perp}^2 + \Omega_e^2}\right) \tag{1.4}$$

$$\sigma_H = \frac{Ne}{B_0}\left(\frac{\Omega_e^2}{\nu_{en\perp}^2 + \Omega_e^2} - \frac{\Omega_i^2}{\nu_{in}^2 + \Omega_i^2}\right) \tag{1.5}$$

where N is the ion and electron number density, e is the magnitude of the electron charge, ν_{in} is the ion-neutral collision frequency, $\nu_{en\perp}$ is the electron-neutral collision frequency

for motions perpendicular to the magnetic field, and Ω_i and Ω_e are the ion and electron gyrofrequencies

$$\Omega_i = eB_0/m_i \tag{1.6}$$

$$\Omega_e = eB_0/m_e \tag{1.7}$$

where m_i and m_e are the ion and electron masses. The dynamo source current is (see *Richmond*, 2016)

$$\mathbf{J}^D = \sigma_P \mathbf{u} \times \mathbf{B_0} + \sigma_H B_0 \mathbf{u}_\perp + \mathbf{J}_{pg} \tag{1.8}$$

where $\mathbf{u}_\perp$ is the component of wind velocity perpendicular to $\mathbf{B}_0$, and $\mathbf{J}_{pg}$ is the current driven by gravity and plasma pressure gradient forces perpendicular to the magnetic field:

$$\mathbf{J}_{pg} = \frac{\nu_{in}\Omega_i \mathbf{F}_{pgi\perp} - \Omega_i^2 \mathbf{b}_0 \times \mathbf{F}_{pgi\perp}}{B_0(\Omega_i^2 + \nu_{in}^2)} + \frac{-\nu_{en\perp}\Omega_e \mathbf{F}_{pge\perp} - \Omega_e^2 \mathbf{b}_0 \times \mathbf{F}_{pge\perp}}{B_0(\Omega_e^2 + \nu_{en\perp}^2)} \tag{1.9}$$

$$\mathbf{F}_{pgi\perp} = \{\mathbf{b}_0 \times [N m_i \mathbf{g} - \nabla(N k_B T_i)]\} \times \mathbf{b}_0 \tag{1.10}$$

$$\mathbf{F}_{pge\perp} = \{\mathbf{b}_0 \times [N m_e \mathbf{g} - \nabla(N k_B T_i)]\} \times \mathbf{b}_0 \tag{1.11}$$

where $\mathbf{g}$ is the acceleration of gravity, k_B is the Boltzmann constant, and T_i and T_e are the ion and neutral temperatures. (The vector multiplication of the force vectors in (1.10) and (1.11) by $\{\mathbf{b}_0 \times ....\} \times \mathbf{b}_0$ serves to extract the components of the force vectors perpendicular to $\mathbf{b}_0$.)

Geomagnetic field lines are assumed to be equipotentials (Φ is constant along them) through the thickness of the ionosphere. Field lines that intersect the ionosphere at middle and low latitudes are further assumed to have the same Φ at their conjugate locations along a field line in the southern and northern hemispheres. Some interhemispheric difference of Φ is allowed at high latitudes, with the magnitude of the allowed difference generally increasing with absolute magnetic latitude.

The lower boundary condition is a specification of vertical current density from the global atmospheric electric circuit, which is small and usually neglected. The upper boundary condition can take different forms, but basically involves a specification or calculation of vertical current density at the top of the ionosphere, where the current flows essentially

parallel to $\mathbf{B}_0$. At both the lower and upper boundaries it is assumed that the globally integrated vertical current density is zero, so that no electric charge is transferred between the ionosphere and either the Earth or space. The algorithm to solve for Φ makes use of this assumption and requires Φ to have no discontinuities. The solution for Φ contains an arbitrary constant that has no effect on the physics. Φ at any single location can be arbitrarily specified, such as setting it to 0 at the north magnetic pole.

Whereas $\mathbf{J}$ is three dimensional, Φ is two dimensional with respect to coordinates that vary only in the directions perpendicular to $\mathbf{B}_0$. For this reason the model uses a coordinate system organized with respect to the geomagnetic field, so that the solution for Φ involves only a two-dimensional partial differential equation.

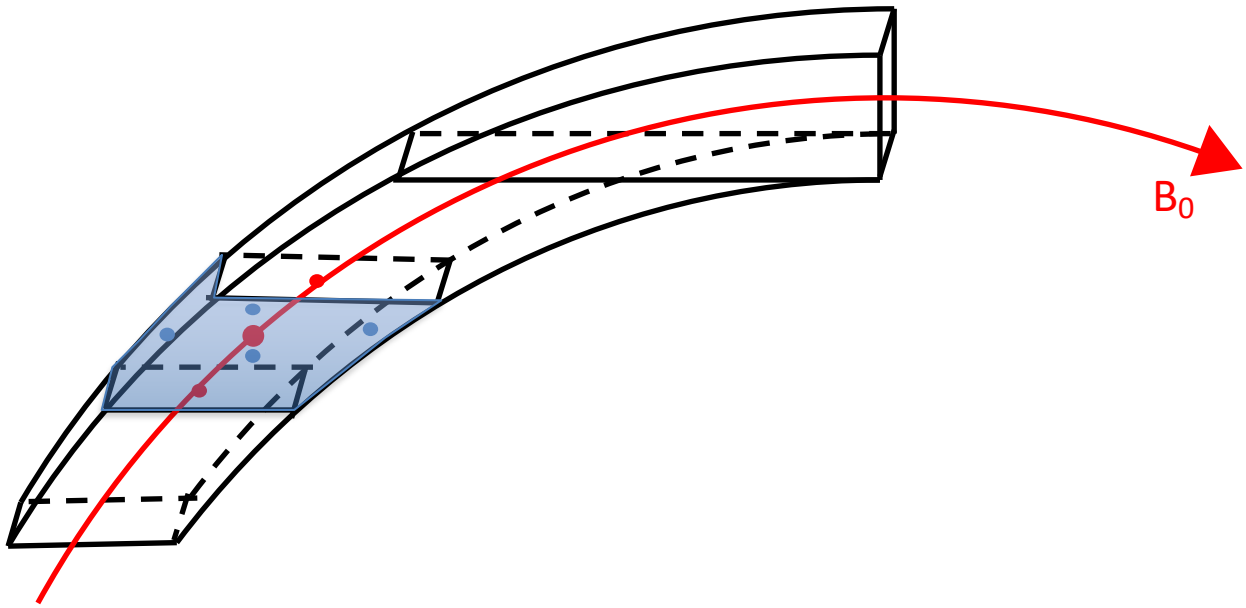

Figure 1.1: Schematic diagram of a geomagnetic flux tube and elemental volumes along it as used in the dynamo model. The light-blue-shaded elemental volume has 4 faces aligned with the main geomagnetic field; current densities are calculated at the blue points near the centers of these faces. Vertical currents are determined for the lower and upper horizontal faces (except for a volume at the apex of a field line, where vertical current is determined for the lower face and cross-equatorial current is determined for the equatorial face).

The model takes input values of $\mathbf{J}^D$ throughout the ionosphere, together with the specified lower and upper boundary conditions, to solve (1.1)-(1.3) for the two-dimensional electric potential Φ on a dense set of geomagnetic field lines. From Φ the model then calculates $\mathbf{E}$ from (1.1) and the components of $\mathbf{J}$ perpendicular to $\mathbf{B}_0$ from (1.3). $\mathbf{J}_\parallel$ is determined by

requiring the three-dimensional current density to be divergence-free.

A three-dimensional grid of points is set up, organized by magnetic longitude and latitude (which are both constant on a field line) and by geometric altitude above the Earth's oblate spheroidal surface. Elemental volumes are set up with respect to these coordinates, as in the example of Figure 1.1. Most of the elemental volumes have 6 faces, but the elemental volumes next to the geomagnetic poles and equator have only 5 faces. When integrated over an elemental volume, (1.2) requires that the net current flowing into or out of the volume through its faces must be 0. Geomagnetic field lines pass through only 2 of these faces, at the bottom and top (except for the top-most volume on a field line, where field lines pass through the bottom and the equatorial face). For the remaining 3 or 4 faces the electric current density normal to each face is expressed in terms of the Φ values on nearby field lines, using (1.3) and finite-difference approximations to express the negative gradient of Φ, i.e., the electric field. This current density normal to the face is multiplied by the area of the face to get an estimate of the total current flowing through the face. The net current flowing into the elemental volume through these 3 or 4 faces, plus the current flowing upward through the bottom face, equals the current flowing out of the top face (or the equatorial face for the top-most volume along a field line). The vertical outflow at the top of one elemental volume is the inflow at the bottom of the elemental volume just above along the same field line. Thus the vertical current density at any top face can be determined by summing the net inflows across the sides of all the elemental volumes below along that field line, plus the upward inflow at the lower-most volume on the field line (which is zero unless lower-atmosphere sources of currents are considered). This vertical current density is expressed in terms of the Φ values on the geomagnetic-field line in question and its neighbors. By applying the boundary conditions and the condition for current continuity across the magnetic equator in the ionosphere we arrive at a set of linear equations for the discretized Φ values that are then solved for those values. With Φ determined the model then calculates $\mathbf{E}$ and $\mathbf{J}$. From the distribution of $\mathbf{J}$ it can then calculate the associated magnetic perturbations below and within the ionosphere.

Chapter 2

Coordinates

Multiple coordinate systems are used. Model conductivities, winds, and plasma density and pressure generally come from models organized by geographic coordinates, and are transferred to magnetic coordinates. Geographic coordinates are also used for calculating magnetic perturbations from the simulated electric current densities.

For electrodynamics we use two coordinate systems aligned with strongly organizing properties of the physical system, which facilitates efficient calculations. The first geomagnetic coordinate system, used to calculate the electric potential, is based on Modified Magnetic Apex (MMA) coordinates as defined by *Richmond* (1995) (hereafter R95). MMA longitude ϕ_m and latitude λ_m are constant along geomagnetic-field lines. For the third MMA coordinate we use geographic height above Earth's surface, h, which strongly organizes winds, conductivities, and forces on the plasma. (This differs from R95, which uses geomagnetic potential for the third MMA coordinate.) The second geomagnetic coordinate system we use is Quasi-Dipole (QD) coordinates as defined by R95. QD longitude ϕ_q is identical to MMA longitude ϕ_m, while QD latitude λ_q is related to MMA latitude λ_m by a factor that depends on h and on the reference height for MMA coordinates h_R:

$$\cos\lambda_q = \left(\frac{R_E + h}{R_E + h_R}\right)^{\frac{1}{2}} \cos\lambda_m \tag{2.1}$$

where R_E is the mean Earth radius. Unlike MMA latitude, QD latitude is not constant along field lines but rather varies only slowly with height and would be constant in height and identical with geomagnetic dipole latitude if the field were a perfect dipole and the Earth were perfectly spherical. At the reference height h_R (typically 80 km for our model) MMA coordinates are identical to QD coordinates. Figure 2.1 shows a map of QD coordinates for epoch 2020 at an altitude of 250 km. We use the International Geomagnetic Reference Field (IGRF; *Alken et al.,* 2021) to determine the main geomagnetic field $\mathbf{B}_0$ in terms of the magnetic potential V_0:

$$\mathbf{B}_0 = -\nabla V_0 \tag{2.2}$$

The reference oblate spheroid for the Earth in the IGRF has an equatorial radius 6.37816×10^6 m and a flatness 1/298.25, which corresponds to an ellipticity $\sqrt{(2 - 1./298.25)/298.25}$. The magnetic coordinates evolve slowing in time; the Atlantic region experiences some of the fastest changes, where the magnetic equator moves northward at roughly 1° geographic latitude per decade.

The rest of this chapter focusses on the coordinates used to calculate the electric potential. The first coordinate for our dynamo model is ϕ_m, while our second coordinate is not λ_m itself, but rather $\rho \equiv \cos\lambda_m$, which varies in a more convenient fashion near the magnetic equator. Our third coordinate is height h. Define
h = height above the Earth's oblate spheroidal surface
R_E = mean Earth radius (6.37122×10^6 m)
h_R = reference height at the base of the dynamo region, typically 80 km or 80000 m
h_A = apex height of the geomagnetic field line passing through the point in question
$R \equiv R_E + h_R$ = reference radius value
$r \equiv R_E + h$ (for a non-spherical Earth this does not equal distance from Earth's center).
ϕ_m = Modified Magnetic Apex longitude, defined as the geomagnetic dipole longitude of the field-line apex.
λ_m = Modified Magnetic Apex (MMA) latitude

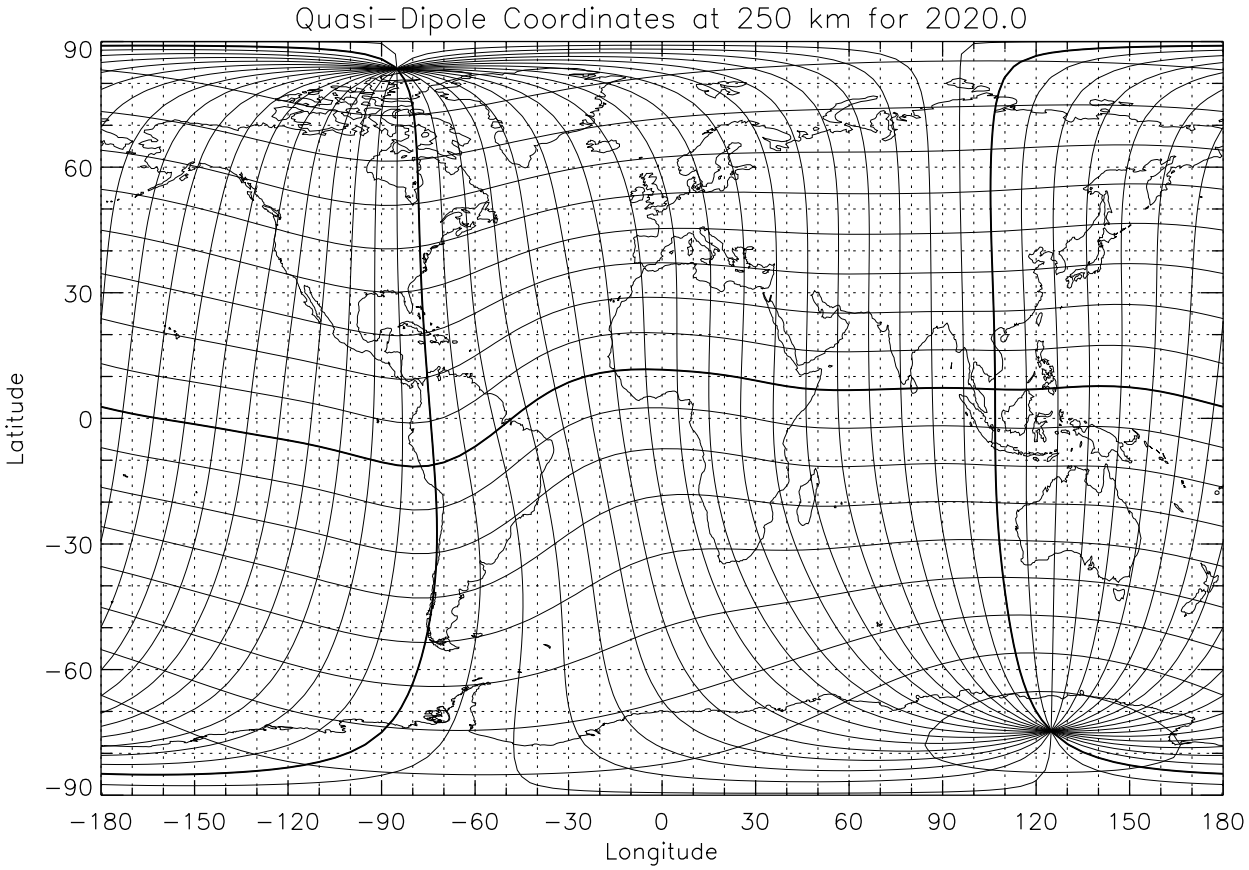

Figure 2.1: QD latitude and longitude at 10° intervals, at an altitude of 250 km for epoch 2020.0. The thickend contours show the QD equator and the QD longitudes of 0° (Americas) and 180° (East Asia).

The relation among ρ, h_A, and λ_m is

$$\rho = \left(\frac{R}{R_E + h_A}\right)^{\frac{1}{2}} = \cos\lambda_m, \tag{2.3}$$

Differentials of h_A and ρ are related by

$$dh_A = -\frac{2R}{\rho^3}d\rho \tag{2.4}$$

We use the ρ-dependent quantities $\cos I_m$ and $\sin I_m$ defined by R95 as

$$\cos I_m = \frac{\rho}{\sqrt{4 - 3\rho^2}} \tag{2.5}$$

$$\sin I_m = \pm\left(\frac{1 - \rho^2}{1 - \frac{3}{4}\rho^2}\right)^{\frac{1}{2}} \tag{2.6}$$

In this report the upper sign of the pair $\pm$ or $\mp$ always applies to the northern magnetic hemisphere, and the lower sign applies to the southern magnetic hemisphere.

Our use of h as the third coordinate, as opposed to the use of geomagnetic potential V_0 by R95, creates differences in some of the base vectors between the two treatments. The base vectors $\mathbf{d}_1,\ \mathbf{d}_2,\ \mathbf{d}_3,\ \mathbf{e}_1,\ \mathbf{e}_2,\ \mathbf{e}_3$ of R95 are defined such that they would be orthonormal at the reference radius R for a purely dipole geomagnetic field on a perfectly spherical Earth. In this report the analogous base vectors $\mathbf{d}'_1,\ \mathbf{d}'_2,\ \mathbf{e}'_3$ are identical to $\mathbf{d}_1,\ \mathbf{d}_2,\ \mathbf{e}_3$, but our base vectors $\mathbf{d}'_3,\ \mathbf{e}'_1,\ \mathbf{e}'_2$ differ from $\mathbf{d}_3,\ \mathbf{e}_1,\ \mathbf{e}_2$ of R95, and the former are neither unitary nor orthogonal to the remainder of their respective sets, even for a purely dipole geomagnetic field on a perfectly spherical Earth. Instead, they are defined such that the triple vector product $\mathbf{d}'_1 \cdot \mathbf{d}'_2 \times \mathbf{d}'_3$ is unity, as is $\mathbf{d}_1 \cdot \mathbf{d}_2 \times \mathbf{d}_3$. This property ensures that

$$\mathbf{d}'_i \cdot \mathbf{e}'_j = \delta_{ij} = \begin{cases} 1 & \text{if} \quad i = j \\ 0 & \text{if} \quad i \neq j \end{cases} \tag{2.7}$$

Our base vectors are:

$$\mathbf{d}'_1 \ = \ \mathbf{d}_1 = R\rho\nabla\phi_m \tag{2.8}$$

$$\mathbf{d}_2' = \mathbf{d}_2 = \frac{-\rho^3 \nabla h_A}{\sqrt{4-3\rho^2}} = \frac{R\nabla\rho}{\sqrt{1-\frac{3}{4}\rho^2}} \tag{2.9}$$

$$\mathbf{d}_3' = \frac{-\nabla h}{D\sin I} = \frac{-\mathbf{k}}{D\sin I} \tag{2.10}$$

$$D \equiv |\mathbf{d}_1 \times \mathbf{d}_2| \tag{2.11}$$

where $\mathbf{k}$ is a unit upward vector and I is the inclination of the geomagnetic field below the horizontal, and

$$\mathbf{e}_1' = \mathbf{d}_2 \times \mathbf{d}_3' = \frac{R\ \mathbf{k}\times\nabla\rho}{D\sin I\sqrt{1-\frac{3}{4}\rho^2}} = \left(\frac{r}{R}\right)^{\frac{3}{2}} \frac{\mathbf{f}_1}{F} \tag{2.12}$$

$$\mathbf{e}_2' = \mathbf{d}_3' \times \mathbf{d}_1 = \frac{-R\rho\ \mathbf{k}\times\nabla\phi_m}{D\sin I} = -\left(\frac{R}{r}\right)^{\frac{3}{2}} \frac{\mathbf{f}_2}{D\sin I} \tag{2.13}$$

$$\mathbf{e}_3' = \mathbf{e}_3 = \mathbf{d}_1 \times \mathbf{d}_2 = D\mathbf{b}_0 \tag{2.14}$$

$$F \equiv |\mathbf{f}_1 \times \mathbf{f}_2| \tag{2.15}$$

where F, $\mathbf{f}_1$, and $\mathbf{f}_2$ are quantities related to QD coordinates defined in R95, and $\mathbf{b}_0$ is a unit vector along $\mathbf{B}_0$. Note that $\mathbf{f}_1$ and $\mathbf{f}_2$ are horizontal base vectors that would have unit length for a purely dipole geomagnetic field on a perfectly spherical Earth at all altitudes, where F would also be 1. Although the factor $\sin I$ in the denominator of (2.10) and (2.13) causes these equations to fail at the magnetic equator, where $I = 0$, we do not need to apply them right at the equator.

The volume factor W' and area vectors $\mathbf{a}_1$, $\mathbf{a}_2$, and $\mathbf{a}_3$, which are used to calculate gradients and divergences, are

$$W' = |\mathbf{k}\cdot\nabla\phi_m \times \nabla\rho|^{-1} = \left|\mathbf{k}\cdot\left(\frac{\mathbf{d}_1}{R\rho}\right)\times\left(\frac{\sqrt{1-\frac{3}{4}\rho^2}\ \mathbf{d}_2}{R}\right)\right|^{-1} = \left|\frac{D\sin I\sqrt{1-\frac{3}{4}\rho^2}}{R^2\rho}\right|^{-1}$$

$$= \frac{R^2\rho}{D|\sin I|\sqrt{1-\frac{3}{4}\rho^2}} = \frac{R^2(\frac{r}{R})^3\rho}{F\sqrt{1-\frac{r}{R}\rho^2}} \tag{2.16}$$

$$\mathbf{a}_1' = W'\nabla\phi_m = \frac{R\ \mathbf{d}_1}{D|\sin I|\sqrt{1-\frac{3}{4}\rho^2}} = \frac{R(\frac{r}{R})^3\ \mathbf{d}_1}{F\sqrt{1-\frac{r}{R}\rho^2}} \tag{2.17}$$

$$\mathbf{a}_2' = W'\nabla\rho = \frac{R\rho\ \mathbf{d}_2}{D|\sin I|} = \frac{R(\frac{r}{R})^3\rho\sqrt{1-\frac{3}{4}\rho^2}\ \mathbf{d}_2}{F\sqrt{1-\frac{r}{R}\rho^2}} \tag{2.18}$$

$$\mathbf{a}_3' = W'\ \mathbf{k} = \frac{\pm R^2\rho\ \mathbf{k}}{D\sin I\sqrt{1-\frac{3}{4}\rho^2}} = \frac{\mp R^2\rho\ \mathbf{d}_3'}{\sqrt{1-\frac{3}{4}\rho^2}} = \frac{R^2(\frac{r}{R})^3\rho\ \mathbf{k}}{F\sqrt{1-\frac{r}{R}\rho^2}} \tag{2.19}$$

Although the factor $\sin I$ in the denominator of (2.16)-(2.19) causes these equations to fail at the magnetic equator, we do not need to apply these equations right at the equator.

In terms of the above quantities, (1.1) is

$$\begin{aligned}\mathbf{E} &= -\frac{1}{W'}\left[\mathbf{a}_1'\frac{\partial\Phi}{\partial\phi_m} + \mathbf{a}_2'\frac{\partial\Phi}{\partial\rho} + \mathbf{a}_3'\frac{\partial\Phi}{\partial h}\right] \\ &= -\frac{\mathbf{d}_1}{R\rho}\frac{\partial\Phi}{\partial\phi_m} - \frac{\sqrt{1-\frac{3}{4}\rho^2}\mathbf{d}_2}{R}\frac{\partial\Phi}{\partial\rho} - \mathbf{k}\frac{\partial\Phi}{\partial h}\end{aligned} \tag{2.20}$$

where each partial derivative is taken with the other two coordinate variables held constant. The model assumes that Φ is a function only of ϕ_m and ρ, and so $\partial\Phi/\partial h = 0$ when ϕ_m and ρ are constant, and the last term on the right-hand side of (2.20) vanishes.

Equation (1.2) gives

$$\nabla\cdot\mathbf{J} = \frac{1}{W'}\left[\frac{\partial(\mathbf{a}_1'\cdot\mathbf{J})}{\partial\phi_m} + \frac{\partial(\mathbf{a}_2'\cdot\mathbf{J})}{\partial\rho} + \frac{\partial(\mathbf{a}_3'\cdot\mathbf{J})}{\partial h}\right] = 0 \tag{2.21}$$

If we integrate $W'\nabla\cdot\mathbf{J}$ with respect to $\phi_m,\ \rho,\ h$ over a region of space $\phi_a < \phi_m < \phi_b$, $\rho_a < \rho < \rho_b$, $h_a < h < h_b$, noting that

$$\int_{\phi_a}^{\phi_b}\frac{\partial(\mathbf{a}_1'\cdot\mathbf{J})}{\partial\phi_m}d\phi_m = (\mathbf{a}_1'\cdot\mathbf{J})|_{\phi_m=\phi_b} - (\mathbf{a}_1'\cdot\mathbf{J})|_{\phi_m=\phi_a} \tag{2.22}$$

and similarly for integrations of derivatives of quantities with respect to ρ and h, we get

$$\begin{aligned}\int_{\phi_a}^{\phi_b}\int_{\rho_a}^{\rho_b}\int_{h_a}^{h_b} W'\nabla\cdot\mathbf{J}\ dh\ d\rho\ d\phi_m &= 0 = \\ \left[\int_{\rho_a}^{\rho_b}\int_{h_a}^{h_b}\mathbf{a}_1'\cdot\mathbf{J}\ dh\ d\rho\right]_{\phi_m=\phi_b} &- \left[\int_{\rho_a}^{\rho_b}\int_{h_a}^{h_b}\mathbf{a}_1'\cdot\mathbf{J}\ dh\ d\rho\right]_{\phi_m=\phi_a}\end{aligned}$$

$$+\left[\int_{\phi_a}^{\phi_b}\int_{h_a}^{h_b}\mathbf{a}_2'\cdot\mathbf{J}\;dh\;d\phi_m\right]_{\rho=\rho_b} \quad - \quad \left[\int_{\phi_a}^{\phi_b}\int_{h_a}^{h_b}\mathbf{a}_2'\cdot\mathbf{J}\;dh\;d\phi_m\right]_{\rho=\rho_a}$$
$$+\left[\int_{\phi_a}^{\phi_b}\int_{\rho_a}^{\rho_b}\mathbf{a}_3'\cdot\mathbf{J}\;d\rho\;d\phi_m\right]_{h=h_b} \quad - \quad \left[\int_{\phi_a}^{\phi_b}\int_{\rho_a}^{\rho_b}\mathbf{a}_3'\cdot\mathbf{J}\;d\rho\;d\phi_m\right]_{h=h_a} \tag{2.23}$$

The six integrals on the right-hand side of (2.23) represent the current leaving (or entering, if preceded by a minus sign) the specified region of space through one of six faces of the boundary of the region. The net current into the volume must be 0. Chapter 6 applies (2.23) to every elemental volume like that shaded blue in Figure 1.1.

Chapter 3

Relations Among Scalar Components of E, J, and $\mathbf{J}^D$

The electric field can be expressed as

$$\mathbf{E} = E_{d1}\mathbf{d}_1 + E_{d2}\mathbf{d}_2 = \frac{-\mathbf{a}_1}{W'}\frac{\partial\Phi}{\partial\phi_m} + \frac{-\mathbf{a}_2}{W'}\frac{\partial\Phi}{\partial\rho} \tag{3.1}$$

$$E_{d1} = \mathbf{E}\cdot\mathbf{e}'_1 = \mathbf{E}\cdot\mathbf{e}_1 = \frac{-\mathbf{e}_1\cdot\mathbf{a}'_1}{W'}\frac{\partial\Phi}{\partial\phi_m} = \frac{-1}{R\rho}\frac{\partial\Phi}{\partial\phi_m} \tag{3.2}$$

$$E_{d2} = \mathbf{E}\cdot\mathbf{e}'_2 = \mathbf{E}\cdot\mathbf{e}_2 = \frac{-\mathbf{e}_2\cdot\mathbf{a}'_2}{W'}\frac{\partial\Phi}{\partial\rho} = \frac{-\sqrt{1-\frac{3}{4}\rho^2}}{R}\frac{\partial\Phi}{\partial\rho} \tag{3.3}$$

The current density can be written as

$$\begin{aligned}\mathbf{J} &= J'_{e1}\mathbf{e}'_1 + J'_{e2}\mathbf{e}'_2 + J'_{e3}\mathbf{e}'_3 \\ &= J_{e1}\mathbf{e}'_1 + J_{e2}\mathbf{e}'_2 + J'_{e3}\mathbf{e}_3\end{aligned} \tag{3.4}$$

$$J_{e1} = \mathbf{d}'_1\cdot\mathbf{J} = \mathbf{d}_1\cdot\mathbf{J} \tag{3.5}$$

$$J_{e2} = \mathbf{d}'_2\cdot\mathbf{J} = \mathbf{d}_2\cdot\mathbf{J} \tag{3.6}$$

$$J'_{e3} = \mathbf{d}'_3\cdot\mathbf{J} = \frac{-J_r}{D\sin I} \tag{3.7}$$

where the second line of (3.4) makes use of the facts that $J_{e1} = J'_{e1},\ J_{e2} = J'_{e2},\ \mathbf{e}_3 = \mathbf{e}'_3$. As in R95, relations of $J_{e1},\ J_{e2}$ with $E_{d1},\ E_{d2}$ are found by taking the dot products of (1.3) and (1.8) with $\mathbf{d}_1$ and $\mathbf{d}_2$:

$$J_{e1} = \sigma_P d_1^2 E_{d1} - (\sigma_H D - \sigma_P \mathbf{d}_1 \cdot \mathbf{d}_2) E_{d2} + J_{e1}^D \tag{3.8}$$

$$J_{e2} = (\sigma_H D + \sigma_P \mathbf{d}_1 \cdot \mathbf{d}_2) E_{d1} + \sigma_P d_2^2 E_{d2} + J_{e2}^D \tag{3.9}$$

$$J_{e1}^D = \sigma_P d_1^2 u_{e2} B_{e3} + (\sigma_H D - \sigma_P \mathbf{d}_1 \cdot \mathbf{d}_2) u_{e1} B_{e3} + J_{e1}^{pg} \tag{3.10}$$

$$J_{e2}^D = (\sigma_H D + \sigma_P \mathbf{d}_1 \cdot \mathbf{d}_2) u_{e2} B_{e3} - \sigma_P d_2^2 u_{e1} B_{e3} + J_{e2}^{pg} \tag{3.11}$$

$$B_{e3} = B_0 / D \tag{3.12}$$

On geomagnetic field lines with apexes near the lower boundary of the dynamo region the current density component J_{e2} is nearly vertical and very small, representing current from the global atmospheric electrical circuit at the location of the magnetic equator. This is in a region where the ratio of Hall to Pedersen conductivity is large. A vertical polarization electric field sets up to prevent the vertical current density from departing from its lower-boundary value. This vertical electric field drives a zonal Hall current, in the same manner that the equatorial electrojet current is established around 100 km altitude, but the lower boundary is below the main electrojet current. Nevertheless, we can take advantage of this phenomenon to simplify the nature of the dynamo equations and improve their numerical behavior near the equatorial lower boundary, as follows. Assume J_{e2} is known near the boundary (equal to 0 unless there are lower-atmospheric sources). Solve (3.9) for E_{d2} at the equatorial lower boundary:

$$E_{d2} = [J_{e2} - J_{e2}^D - (\sigma_H D + \sigma_P \mathbf{d}_1 \cdot \mathbf{d}_2) E_{d1}] / (\sigma_P d_2^2) \tag{3.13}$$

Using (3.13) in (3.8) yields

$$J_{e1} = \sigma_C E_{d1} + J_{e1}^{Deq} \tag{3.14}$$

$$\sigma_C = \sigma_P d_1^2 + \frac{(\sigma_H D - \sigma_P \mathbf{d}_1 \cdot \mathbf{d}_2)(\sigma_H D + \sigma_P \mathbf{d}_1 \cdot \mathbf{d}_2)}{\sigma_P d_2^2} \tag{3.15}$$

$$J_{e1}^{Deq} = J_{e1}^{D} - \frac{(\sigma_H D - \sigma_P \mathbf{d}_1 \cdot \mathbf{d}_2)}{\sigma_P d_2^2}(J_{e2} - J_{e2}^{D}) \tag{3.16}$$

where σ_C is effectively the Cowling conductivity and J_{e1}^{Deq} is effectively the source term for eastward current near the equatorial boundary. Since $J_{e2} = \mathbf{d}_2' \cdot \mathbf{J}$ and since according to (2.9) $\mathbf{d}_2'$ is practically a unit downward vector at the equatorial boundary [$\rho = 1$, where $\nabla(h_A)$ is nearly a vertical unit vector], J_{e2} in (3.16) can be replaced by $-J_r$ to give

$$J_{e1}^{Deq} = J_{e1}^{D} + \frac{(\sigma_H D - \sigma_P \mathbf{d}_1 \cdot \mathbf{d}_2)}{\sigma_P d_2^2}(J_r + J_{e2}^{D}) \quad \text{at } \rho = 1 \tag{3.17}$$

where J_r is assumed known (=0 unless current comes from the global atmospheric electrical circuit). At this location $\mathbf{d}_1 \cdot \mathbf{d}_2$ is also nearly zero.

Chapter 4

Grid Set-Up in Magnetic Apex Coordinates

4.1 Overview

We want a grid with adequate vertical and horizontal resolution to capture significant variations of winds and conductivities with height and latitude. The grid described here is for so-called "P points", aligned with geomagnetic-field lines on which the electric potential is calculated. The P points are at the approximate centers of elemental volumes, of which the faces are used to calculate current inflow and outflow that is required to balance for each elemental volume.

The grid is equally spaced in Magnetic Apex longitude ϕ_m [= `ylonm` in the code], with I_{max} [= `nmlon`] points in longitude:

$$\phi_i = \frac{2\pi}{I_{max}}(i-1) - \pi \tag{4.1}$$

Grid points are unequally spaced with respect to h and ρ. There are K [= `nhgt_fix`] height levels h_k, from h_1 at the bottom to h_K at the top, and J [= `nmlat_h`] field lines at each

longitude, with ρ values from $\rho_1 = 0$ at the poles to $\rho_J = 1$ for a field line whose apex just touches the bottom of the model at height h_1.

At a given magnetic longitude each height surface h_k is touched by the apex of one geomagnetic-field line at the magnetic equator. This point defines the value of ρ for P points along that field line:

$$\rho_{J-k+1} = \sqrt{\frac{R}{R_E + h_k}} \tag{4.2}$$

Thus the height and magnetic-latitude grids are coupled to each other for field lines with apexes up to the top of the model at h_K, though they are no longer coupled for field lines with apexes above h_K for which $j < J - K + 1$.

This chapter first describes a highly flexible way to define the grid spacing with respect to ρ in Section 4.2, and then describes a simpler parameterization in Section 4.3. A summary recipe for the flexible grid with suggested default parameters is given at the end of Section 4.2. Once the ρ grid is specified, the height grid h_k is determined for $k = 1, K$ from

$$h_k = \frac{R}{\rho^2_{J-k+1}} - R_E \tag{4.3}$$

4.2 Flexible ρ grid

A field line is defined by its magnetic-apex longitude ϕ_m and by its magnetic-apex latitude

$$\lambda_m = \pm \cos^{-1} \rho \tag{4.4}$$

[λ_m = `ylat_m` in `subroutine gen_highres_grid`, file `grid.f90`] or its apex height

$$h_A = \frac{R}{\cos^2 \lambda_m} - R_E = \frac{R}{\rho^2} - R_E \tag{4.5}$$

For defining the apex height/latitude grid it will also be useful to introduce another variable y that is related to h_A, λ_m and ρ in a different manner in different regions. At low latitudes (Regions I and II described below) y is defined to be a rough representation of the number

of atmospheric pressure scale heights that h_A lies above h_R. For field lines intersecting the E-region ionosphere at middle latitudes (Region IV), a unit change of y corresponds to $1/D$ radians of λ_m. In the center of the auroral region (Region VI) a unit chnage of y is reduced to $1/F$ radians of λ_m, and in the polar cap (Region VIII) it is $1/H$ radians. Regions III, V, and VII are transitions between their respective neighbors, designed such that the derivatives of y with respect to λ_m and ρ are continuous, so that there are smooth transitions of grid spacings between regions. In this way we can simplify the construction of finite-difference derivatives with respect to ρ by assuming every grid point lies approximately midway between its neighbors. The relation of y to h_A, λ_m, and ρ for each region is detailed below.

Region I, $0 < y < y_b$ $\quad$ [y_b specified ≈ 5]
$h_R < h_A < h_b$ $\quad$ [h_R specified $\approx 80,000$ m, h_b calculated $\approx 110,000$ m]

$$h_A = h_R + H_s y \qquad [H_s \text{ specified} \approx 6,000 \text{ m}] \tag{4.6}$$

$$y = \frac{h_A - h_R}{H_s} \tag{4.7}$$

Region II, $y_b < y < y_c$ $\quad$ [y_c specified ≈ 18]

$$h_A = h_R + H_s y + \frac{1}{2}\frac{dH}{dy}(y - y_b)^2 \qquad \left[\frac{dH}{dy} \text{ specified} \approx 6,000 \text{ m}\right] \tag{4.8}$$

Differentiate h_A with respect to y:

$$\frac{dh_A}{dy} = H_s + \frac{dH}{dy}(y - y_b) \tag{4.9}$$

Rewrite (4.8) as a quadratic equation in $(y - y_b)$:

$$\frac{1}{2}\frac{dH}{dy}(y - y_b)^2 + H_s(y - y_b) + [H_s y_b + h_R - h_A] = 0 \tag{4.10}$$

for which the desired solution of $(y - y_b)$ in terms of h_A is

$$y - y_b = \frac{1}{dH/dy}\left\{-H_s + \left[H_s^2 - 2\frac{dH}{dy}(H_s y_b + h_R - h_A)\right]^{\frac{1}{2}}\right\} \tag{4.11}$$

The maximum apex height for Region II (and minimum apex height for Region III), where $y = y_c$, is

$$h_c = h_R + H_s y_c + \frac{1}{2}\frac{dH}{dy}(y_c - y_b)^2 \tag{4.12}$$

Region III, $y_c < y < y_1$

Whereas y_c is a specified number, y_1 is determined from λ_1, which is the specified value of λ_m at the boundary between Regions III and IV. The formula for determining y_1 from λ_1 is found below. In terms of two constants B and C to be determined, let h_A in Region III be related to y as

$$h_A = h_c + \frac{C}{B}\left\{\exp[B(y - y_c)] - 1\right\} \tag{4.13}$$

Differentiate h_A with respect to y:

$$\frac{dh_A}{dy} = C\exp[B(y - y_c)] \tag{4.14}$$

Equate (4.9) with (4.14) at $y = y_c$ in order to determine C:

$$H_s + \frac{dH}{dy}(y_c - y_b) = C \tag{4.15}$$

In order to determine B, we will equate the values of $dy/d\lambda_m$ for Regions III and IV at $y = y_1$. First solve (4.13) for $y - y_c$ in terms of $h_A - h_c$:

$$y - y_c = \frac{1}{B}\ln\left\{\frac{B}{C}(h_A - h_c) + 1\right\} \tag{4.16}$$

Using (4.5) to replace h_A yields

$$y = y_c + \frac{1}{B}\ln\left\{\frac{B}{C}\left(\frac{R}{\cos^2\lambda_m} - R_E - h_c\right) + 1\right\}$$

$$= \quad y_c + \frac{1}{B}\ln\left(\frac{BR}{C}\right) + \frac{1}{B}\ln\left[\frac{1}{\cos^2\lambda_m} - \frac{R_E + h_c}{R} + \frac{C}{BR}\right] \tag{4.17}$$

Differentiate (4.17) with respect to λ_m:

$$\frac{dy}{d\lambda_m} = \frac{1}{B}\left[\frac{1}{\cos^2\lambda_m} - \frac{R_E + h_c}{R} + \frac{C}{BR}\right]^{-1} \frac{2\sin\lambda_m}{\cos^3\lambda_m} \tag{4.18}$$

At $\lambda_m = \lambda_1$ [specified as $\approx 30^\circ$ in radians] equate (4.18) with D [specified as ≈ 10], which is the value of $dy/d\lambda_m$ in Region IV:

$$\frac{1}{B\left(\frac{1}{\cos^2\lambda_1} - \frac{R_E+h_c}{R}\right) + \frac{C}{R}}\left(\frac{2\sin\lambda_1}{\cos^3\lambda_1}\right) = D \tag{4.19}$$

Solve for B:

$$B\left(\frac{1}{\cos^2\lambda_1} - \frac{R_E + h_c}{R}\right) + \frac{C}{R} = \frac{2\sin\lambda_1}{D\cos^3\lambda_1}$$

$$B = \left(\frac{2\sin\lambda_1}{D\cos^3\lambda_1} - \frac{C}{R}\right) / \left(\frac{1}{\cos^2\lambda_1} - \frac{R_E + h_c}{R}\right) \tag{4.20}$$

Equation (4.20) defines B in terms of the specified values λ_1 and D, and the calculated values h_c from (4.12) and C from (4.15). The value of y_1 is determined by setting λ_m to λ_1 in (4.17):

$$y_1 = y_c + \frac{1}{B}\ln\left\{\frac{B}{C}\left[\frac{R}{\cos^2\lambda_1} - (R_E + h_c)\right] - 1\right\} \tag{4.21}$$

Region IV, $\lambda_1 < \lambda_m < \lambda_2$ [λ_1 specified $\approx 30^\circ$, λ_2 specified $\approx 50^\circ$ in radians]

Define

$$y \quad = \quad y_1 + D(\lambda_m - \lambda_1) \tag{4.22}$$

$$y_2 \quad = \quad y_1 + D(\lambda_2 - \lambda_1) \tag{4.23}$$

Differentiate (4.22) with respect to λ_m:

$$\frac{dy}{d\lambda_m} = D \tag{4.24}$$

Solve (4.22) for λ_m:

$$\lambda_m = \frac{y - y_1}{D} + \lambda_1 \tag{4.25}$$

Region V, $\lambda_2 < \lambda_m < \lambda_3$ $\quad$ [λ_3 specified $\approx 55°$ in radians]

Define

$$y = y_2 + D(\lambda_m - \lambda_2) + E(\lambda_m - \lambda_2)^2 \tag{4.26}$$

$$y_3 = y_2 + D(\lambda_3 - \lambda_2) + E(\lambda_3 - \lambda_2)^2 \tag{4.27}$$

where E will be calculated by equating $dy/d\lambda_m$ at the boundary y_3 between Regions V and VI. Differentiate (4.26) with respect to λ_m:

$$\frac{dy}{d\lambda_m} = D + 2E(\lambda_m - \lambda_2) \tag{4.28}$$

Rewrite (4.26) as a quadratic equation in $(\lambda_m - \lambda_2)$:

$$E(\lambda_m - \lambda_2)^2 + D(\lambda_m - \lambda_2) + (y_2 - y) = 0 \tag{4.29}$$

Solve (4.29) for λ_m:

$$\lambda_m = \lambda_2 + \frac{1}{2E}\left\{-D + \left[D^2 - 4E(y_2 - y)\right]^{\frac{1}{2}}\right\} \tag{4.30}$$

Region VI, $\lambda_3 < \lambda_m < \lambda_4$ $\quad$ [λ_4 specified $\approx 75°$ in radians]

Define

$$y = y_3 + F(\lambda_m - \lambda_3) \tag{4.31}$$

$$y_4 = y_3 + F(\lambda_4 - \lambda_3) \tag{4.32}$$

where F is specified [≈ 15]. Differentiate (4.31) with respect to λ_m:

$$\frac{dy}{d\lambda_m} = F \tag{4.33}$$

Solve (4.31) for λ_m:

$$\lambda_m = \frac{y - y_3}{F} + \lambda_3 \tag{4.34}$$

Equate (4.28) and (4.33) at $\lambda_m = \lambda_3$:

$$D + 2E(\lambda_3 - \lambda_2) = F \tag{4.35}$$

Solve (4.35) for E:

$$E = \frac{F - D}{2(\lambda_3 - \lambda_2)} \tag{4.36}$$

Region VII, $\lambda_4 < \lambda_m < \lambda_5$ $\quad$ [λ_5 specified $\approx 82^\circ$ in radians]

Define

$$y = y_4 + F(\lambda_m - \lambda_4) - G(\lambda_m - \lambda_4)^2 \tag{4.37}$$

$$y_5 = y_4 + F(\lambda_5 - \lambda_4) - G(\lambda_5 - \lambda_4)^2 \tag{4.38}$$

where G will be calculated by equating $dy/d\lambda_m$ at the boundary y_5 between Regions VII and VIII. Differentiate (4.37) with respect to λ_m:

$$\frac{dy}{d\lambda_m} = F - 2G(\lambda_m - \lambda_4) \tag{4.39}$$

Rewrite (4.37) as a quadratic equation in $(\lambda_m - \lambda_2)$:

$$G(\lambda_m - \lambda_4)^2 - F(\lambda_m - \lambda_4) + (y - y_4) = 0 \tag{4.40}$$

Solve (4.40) for λ_m:

$$\lambda_m = \lambda_4 + \frac{1}{2G}\left\{F - \left[F^2 - 4G(y - y_4)\right]^{\frac{1}{2}}\right\} \tag{4.41}$$

Region VIII, $\lambda_5 < \lambda_m < \frac{\pi}{2}$

Define

$$y = y_5 + H(\lambda_m - \lambda_5) \tag{4.42}$$

where H is specified [≈ 10]. Solve for λ_m:

$$\lambda_m = \frac{y - y_5}{H} + \lambda_5 \tag{4.43}$$

Differentiate (4.43) with respect to λ_m:

$$\frac{dy}{d\lambda_m} = H \tag{4.44}$$

Equate (4.39) and (4.44) at $\lambda_m = \lambda_5$:

$$F - 2G(\lambda_5 - \lambda_4) = H \tag{4.45}$$

Solve (4.45) for G:

$$G = \frac{F - H}{2(\lambda_5 - \lambda_4)} \tag{4.46}$$

From (4.42) the value of y at $\lambda_m = \frac{\pi}{2}$ is

$$y_{\max} = y_5 + H\left(\frac{\pi}{2} - \lambda_5\right) \tag{4.47}$$

Summary recipe

To get h_A, λ_m, and ρ as a function of y, do the following.

1. Specify the following parameters, where suggested default values are given in parentheses:

H_s (6000 m)

dH/dy (6000 m)

D (10)

F (15)

H (10)

y_b (5)

y_c (18)

λ_1 ($30°\pi/180°$)

λ_2 ($50°\pi/180°$)

λ_3 ($55°\pi/180°$)

λ_4 ($75°\pi/180°$)

λ_5 ($82°\pi/180°$).

2. Calculate the following parameters in the order given from the specified equations, where the trailing numbers in parentheses are the values obtained using the default values of the specified parameters above:

Eq. (4.12) h_c (695,000 m)

Eq. (4.15) C (84,000 m)

Eq. (4.20) B (0.5921756)

Eq. (4.36) E ($90/\pi = 28.64789$)

Eq. (4.46) G (20.462778)

Eq. (4.21) y_1 (21.858392)

Eq. (4.23) y_2 (25.349051)

Eq. (4.27) y_3 (26.439882)

Eq. (4.32) y_4 (31.675870)

Eq. (4.38) y_5 (33.203033)

Eq. (4.47) $y_{\max}$ (34.599297).

3. Specify J [= `nmlat_h`], the number of latitude grid points from either pole ($j = 1$) to the equator ($j = J$). A suggested default value of J is 105, which when used with the other default parameters yields a height step below 110 km of 1996.1133 m and a latitude step at midlatitudes (30°-50°) and 80 km altitude of 0.0332686 radians or 1.9061478°. Increasing J will reduce both the height step size and the latitude step size.

4. Define $\Delta y = y_{\max}/(J-1)$, which for the various default values is 0.3326855.

5. Define latitude grid points uniformly spaced in y, with $y(j) = (J-j)\Delta y$.

6. For Region I [$0 \le y(j) < y_b$] calculate h_A from (4.7), ρ from (2.3), and λ_m from (4.4).

7. For Region II [$y_b \le y(j) < y_c$] calculate h_A from (4.8), ρ from (2.3), and λ_m from (4.4).

8. For Region III [$y_c \le y(j) < y_1$] calculate h_A from (4.13), ρ from (2.3), and λ_m from (4.4).

9. For Region IV [$y_1 \le y(j) < y_2$] calculate λ_m from (4.25), ρ from (2.3), and h_A from (4.5).

10. For Region V [$y_2 \le y(j) < y_3$] calculate λ_m from (4.30), ρ from (2.3), and h_A from (4.5).

11. For Region VI [$y_3 \le y(j) < y_4$] calculate λ_m from (4.34), ρ from (2.3), and h_A from (4.5).

12. For Region VII [$y_4 \le y(j) < y_5$] calculate λ_m from (4.41), ρ from (2.3), and h_A from

(4.5).
13. For Region VIII [$y_5 \leq y(j) \leq y_{\max}$] calculate λ_m from (4.43), ρ from (2.3), and h_A from (4.5).

For the suggested default parameter values, the midpoint value of j is 53 and the midpoint value of y is 17.299648, which lies in Region II, with h_A = 637,642 m, $\rho = 0.9593944$, and $\lambda_m = 16.383674°$. This field line lies in the equatorial ionosphere, as do more than half of all field lines for these grid parameters. It is the need for adequate height resolution that puts most of the grid field lines in the equatorial ionosphere.

4.3 Simplified ρ grid

The simplified grid described here sets the following parameters of the previous section to the values
$H_s = 6$ km
$dH/dy = 6$ km
$y_b = 5$
$\lambda_1 = \pi/6$ (30°)
$\lambda_2 = \pi/2$ (90°)
$\lambda_3 = \pi/2$
$\lambda_4 = \pi/2$
$\lambda_5 = \pi/2$
Parameters F, H are not used, because setting λ_2 through λ_5 to $\pi/2$ effectively extends the midlatitude Region IV all the way to the pole. We are then left with parameters D, λ_c, and J to be determined. These will be calculated from two new parameters Δ_H and Δ_{deg} defined below and from specification of h_c, the maximum apex height for Region II.

It is assumed that h_c is also approximately the top altitude of the dynamo region. Considering that F-region gravity and pressure-gradient currents can significantly affect electrodynamics at night, h_c should lie well above most of the F region, at least 600 km for moderate solar activity. (In the topside ionosphere gravity currents and pressure-gradient

currents tend to cancel each other, so their combined dynamo effects are often small and it is usually not necessary to go much higher than 800 km.) If h_A is set to h_c in (4.11), y_c is found to be

$$y_c = y_b + \frac{1}{dH/dy}\left\{-H_s + \left[H_s^2 - 2\frac{dH}{dy}(H_s y_b + h_R - h_c)\right]^{\frac{1}{2}}\right\} \tag{4.48}$$

If $h_c = 695$ km, $y_c = 18$ for the above choice of other parameters.

Δ_H roughly represents the vertical thickness of height layers in Regions I and II measured in fractions of a scale height, since y below y_c is roughly the number of neutral scale heights above the reference height h_R. A typical choice for Δ_H would be 1/3, which would produce layers 2 km thick below 110 km for the choice of parameters we have made in this section. Above 110 km the layers become increasingly thick, roughly in proportion to the increase of neutral scale height with altitude. Since h_c is approximately the top altitude of the dynamo region, the dynamo region will have approximately y_c/Δ_H layers, except that this number needs to be rounded off to the nearest integer. If we choose $y_c = 18$ and $\Delta_H = 1/3$, then the number of layers will be 54. The increment Δy approximately equals Δ_H, not only in the equatorial region but over the entire latitude range, since Δy is constant over the entire range.

For field lines with apexes up to $h_A = h_c$ their magnetic-apex latitudes λ_m along the $h = h_R$ surface at the base of the dynamo region are determined uniquely by the altitude spacing of height surfaces within the dynamo region. Only for field lines with apexes above h_c can we begin to determine the latitude spacing independently.

Δ_{deg} is specified to be approximately the spacing of grid points in degrees for magnetic apex latitudes between λ_1 and the pole. With reference to (4.24), the corresponding increment of y is

$$\Delta y = D\Delta_{\text{deg}}\frac{\pi}{180^\circ} \tag{4.49}$$

Since Δy approximately equals Δ_H, D can be calculated as

$$D = \frac{\Delta_H}{\Delta_{\text{deg}}}\frac{180^\circ}{\pi} \tag{4.50}$$

From (4.23) the maximum value of y at the pole is

$$y_{\max} = y_1 + D(\lambda_2 - \lambda_1) = y_1 + \frac{\Delta_H}{\Delta_{\deg}} 60^\circ \tag{4.51}$$

for our chosen other parameters, with y_1 determined from (4.15), (4.20), and (4.21).

The number of latitude grids points is

$$J = 1 + \text{Integer}\{y_{\max}/\Delta y\} \tag{4.52}$$

where $y_{\max}/\Delta y$ needs to be rounded off to the nearest integer. Δy then needs to be adjusted to give an integral number of grid spaces between the pole and equator:

$$(\Delta y)_{\text{adjusted}} = y_{\max}/(J-1) \tag{4.53}$$

The subsequent steps of defining the latitude grid are then:
Define latitude grid points uniformly spaced in y, with $y(j) = (J-j)(\Delta y)_{\text{adjusted}}$;
If $y(j) < y_1$ calculate h_A from (4.7), (4.8), or (4.13), and ρ from (2.3);
If $y(j) > y_1$ calculate λ_m from (4.25) and ρ from (2.3).

4.4 Indexing of field lines and elemental volumes

Label a field line on which $\Phi(i,j)$ will be calculated wih indices i (increasing eastward) and j (increasing equatorward/downward from 1 at either pole to J [= `nmlat_h`] at the bottom height surface h_1 at the equator). Label height surfaces with index k (increasing upward in both hemispheres from 1 to K [= `nhgt_fix`]). P points lie wherever a field line intersects or touches (at its apex) a height surface. If the apex height of a field line does not exceed h_K, then the k value of the P point at the apex (at the magnetic equator) is

$$k_e = J - j + 1 \tag{4.54}$$

[where k_e = `jns` in `subroutine gen_highres_grid`, file `grid.f90`]. If the apex height exceeds h_K, then the maximum value of k on the field line is K.

Construct a volume about the point (i, j, k) in each hemisphere, bounded by the surfaces of constant ϕ, ρ, h given by

$$\phi_{i-\frac{1}{2}} = \frac{1}{2}(\phi_{i-1} + \phi_i) \quad \text{(allow for wraparound)} \tag{4.55}$$

$$\phi_{i+\frac{1}{2}} = \frac{1}{2}(\phi_i + \phi_{i+1}) \quad \text{(allow for wraparound)} \tag{4.56}$$

$$\rho_{j-\frac{1}{2}} = \begin{cases} \rho_1 \ (= 0) & \text{if} \quad j = 1 \\ \frac{1}{2}(\rho_{j-1} + \rho_j) & \text{if} \quad j > 1 \end{cases} \tag{4.57}$$

$$\rho_{j+\frac{1}{2}} = \begin{cases} \frac{1}{2}(\rho_j + \rho_{j+1}) & \text{if} \quad j < J \\ \rho_J \ (= 1) & \text{if} \quad j = J \end{cases} \tag{4.58}$$

$$h_{k-\frac{1}{2}} = \begin{cases} h_1 \ (= h_R) & \text{if} \quad k = 1 \\ \frac{R}{\rho^2_{J-k+\frac{3}{2}}} - R_E & \text{if} \quad 1 \le k \le K \end{cases} \tag{4.59}$$

$$h_{k+\frac{1}{2}} = \frac{R}{\rho^2_{J-k+\frac{1}{2}}} - R_E \qquad 1 \le k \le K \tag{4.60}$$

Note that the two expressions in (4.59) give the same result for $k = 1$; the first expression is written explicitly here only to emphasize that $h_{\frac{1}{2}} = h_1$. [In the code $\phi_{i+\frac{1}{2}}$ is `ylonm_s(i)`, $\rho_{j+\frac{1}{2}}$ is `rho_s(j)`, and $h_{k-\frac{1}{2}}$ (not $h_{k+\frac{1}{2}}$) is `hgt_fix_r(k)`.]

Figure 4.1 shows the southern-hemisphere portion of a magnetic flux tube containing elemental volumes. Figure 4.2 show the bottom-most flux tube and its overlying neighbor at the magnetic equator just above the base of the model at height $h_1 = h_R$. We first describe Figure 4.1. The red line represents a geomagnetic-field line ($\mathbf{B}_0$) running through the center of the flux tube. The flux tube is viewed from the east, with only the southern-hemisphere portion shown. This field line intersects fixed-height surfaces at heights h_k [$1 \le k \le \min(K, k_e)$], for which the quadrilateral segments intersecting the flux tube are shown in shaded pink or light orange, and for which the intersection points (P points) are thick red dots. (Although displayed as rectangles, these quadrilateral segments are not generally

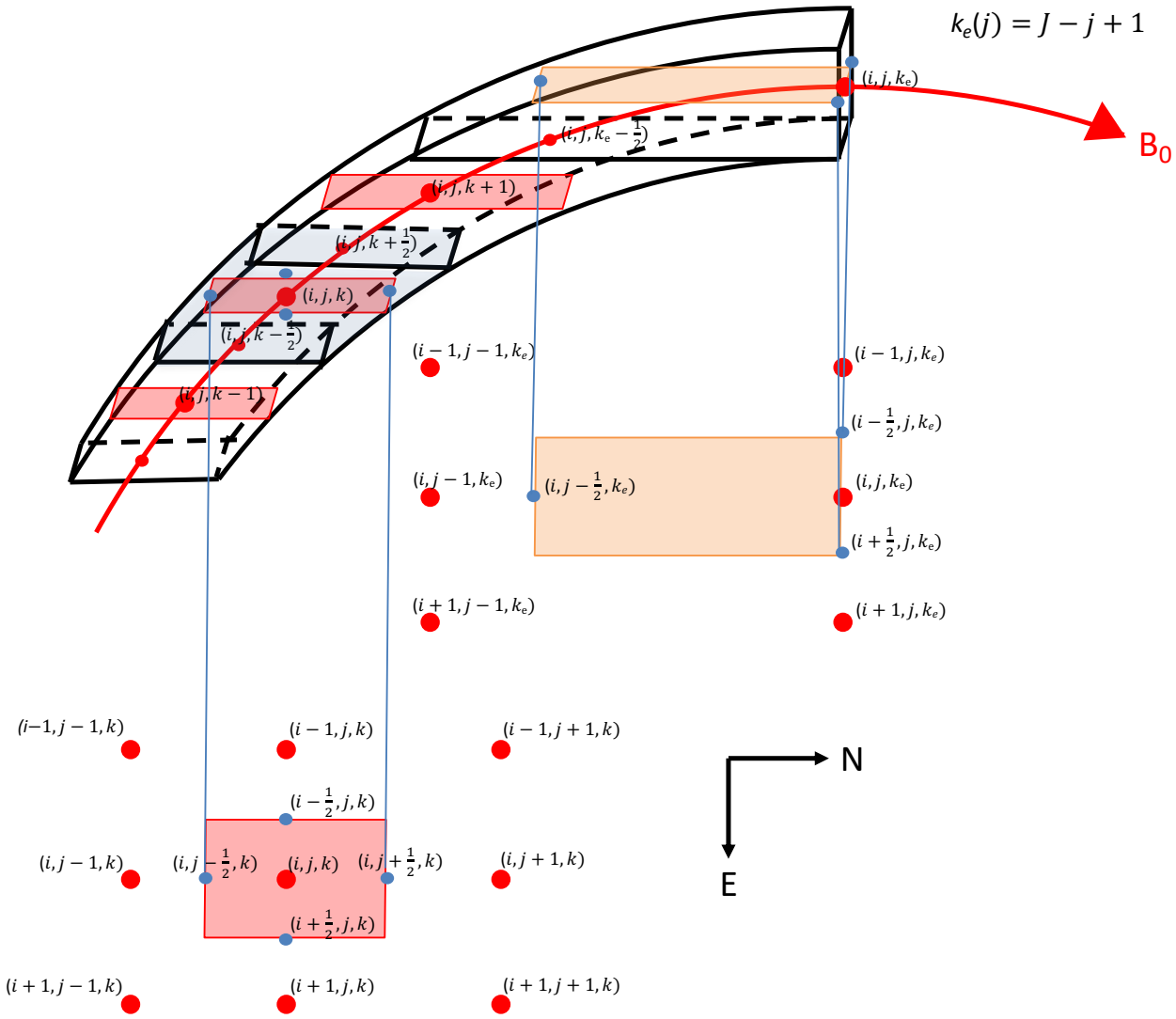

Figure 4.1: Schematic diagram of a flux tube as used in the dynamo model.

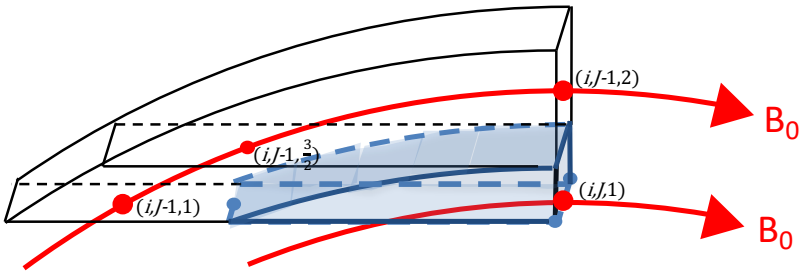

Figure 4.2: Schematic diagram of the bottom-most flux tube ($j = J$), shaded blue, with the overlying flux tube ($j = J - 1$).

rectangular.) For field lines that do not extend above the top of the model (where $h = h_{K+\frac{1}{2}}$), like the field line shown here, the highest height surface touched by the field line is at height h_{k_e}. The magnetic longitude of the central field line is ϕ_i, and its ρ value is ρ_j. For simplicity, points in the figure are labeled only by the subscripts of their respective (ϕ, ρ, h) coordinates.

Below the flux tube are shown two projections, as seen from above, of portions of two height surfaces. (In reality the points do not form a perfectly rectangular array.) For the lower height surface at $h = h_k$ nine thick-red grid points (P points) of intersecting field lines are shown, including the intersection with the central field line with coordinates ϕ_i, ρ_j and intersections with neighborng field lines to the west (ϕ_{i-1}), east (ϕ_{i+1}), above/poleward (ρ_{j-1}), and below/equatorward (ρ_{j+1}). Also shown is a reproduction of the pink quadrilateral representing the intersection of the height surface with the flux tube. The blue points on the edges of this quadrilateral are S1 (west-east) and S2 (south-north) points where conductivities, electric fields, and current densities are evaluated. [The thin vertical blue lines are associated with the blue points at $(i, j - \frac{1}{2}, k)$ and at $(i, j + \frac{1}{2}, k)$.]

For the upper height surface at $h = h_{k_e}$ six thick-red grid points (P points) of grazing or intersecting field lines are shown, including the apex of the central field line, the apexes of its neighbors to the east and west, and intersections of this height surface by the field line lying above/poleward (ρ_{j-1}) and by field lines to its west and east. Also shown is a reproduction of the orange quadrilateral representing the southern-hemisphere portion of the intersection of this height surface with the flux tube. The blue points at the left edge of this quadrilateral (S2 point) and at its equatorial corners (S1 points) are where conductivities, electric fields, and current densities are evaluated.

The volume element that is shaded light blue, which encloses the (i, j, k) grid point, has 6 sides through which the sum of current inflows must vanish. For the inflows normal to the 4 non-horizontal sides the current densities are calculated at the blue S1 (west-east) and S2 (south-north) points, approximately at the centers of the edges of the pink quadrilateral. For the vertical inflow the current densities are calculated at the small red points where the field line intersects the bottom and top faces of the volume.

The bottom-most and top-most elemental volumes of the half flux tube differ from those

at intermediate heights. The bottom-most volume does not extend below the thick-red P point, but rather has its lower face lying right on the height surface of the P point. This bottom-most elemental volume is not illustrated in Figure 4.1, but is seen for the $j = J - 1$ flux tube in Figure 4.2. The lower face of this bottom-most elemental volume is at height $h_1 = h_R$ and the upper face is at height $h_{\frac{3}{2}} = \frac{1}{2}(h_1 + h_2)$. The top-most elemental volume of the half flux tube in Figure 4.1 differs from the others in that it has only 5 faces, with the non-vertical inflows calculated from current densities evaluated at the blue points and the vertical inflow from below calculated at the small red point at the bottom face. Current flow across the magnetic equator is calculated at the right-most face of the elemental volume. For $j = J$, at the base of the model at the equator, this top-most elemental volume has its lower face lying on the height surface at $h_1 = h_R$, as seen in Figure 4.2.

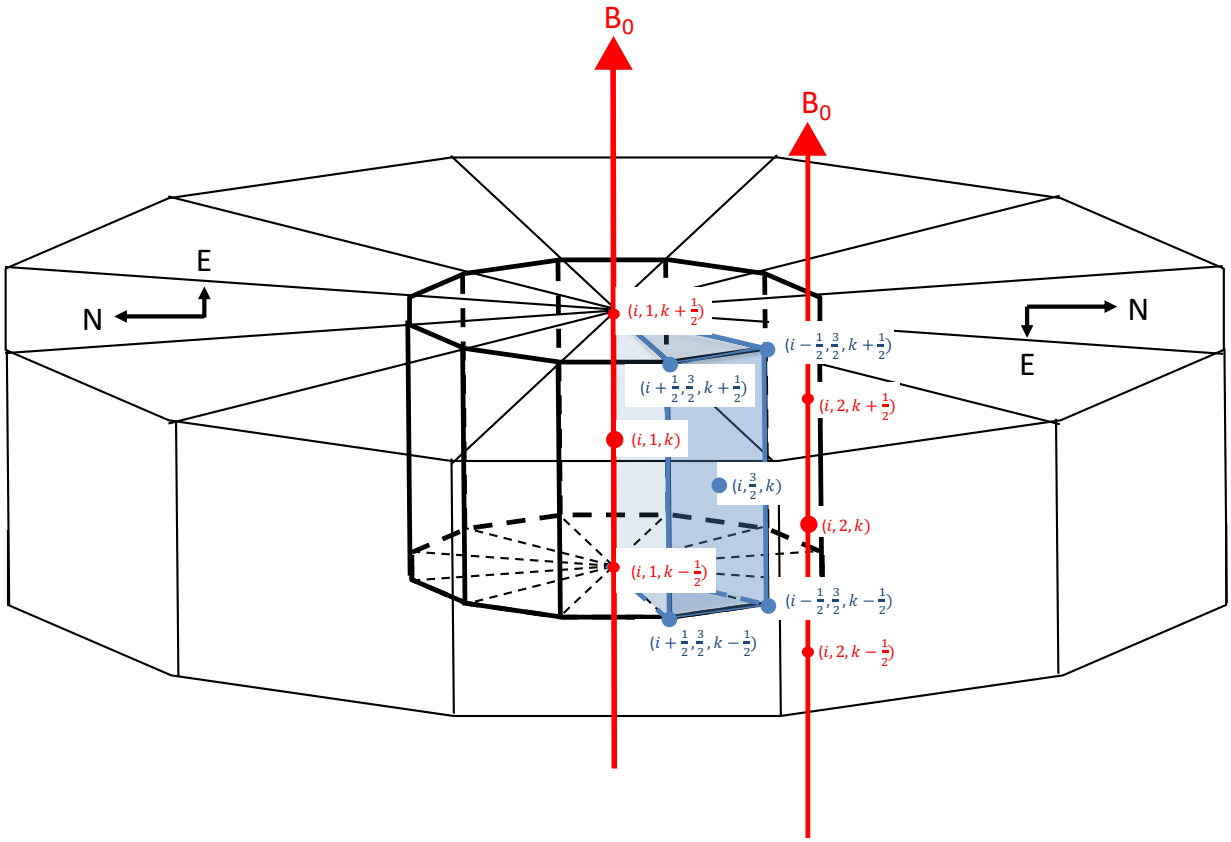

Figure 4.3: Schematic diagram of a flux tube element near the South Magnetic Pole and its neighbors.

Elemental flux-tube volumes at the poles are special cases, because they have neighbors only on their western, eastern, and equatorward sides, as represented by the blue-shaded

volume in Figure 4.3 for the South Magnetic Pole. That is, the bottom and top faces of their associated elemental volumes are triangles instead of quadrilaterals, and the polar field line lies at one vertex of the triangle instead of in its interior. These polar elemental volumes have only 5 faces. At a given height there is only a single polar grid point that represents both the field line $(i, 1, k)$ and its neighbors to the west $(i-1, 1, k)$ and east $(i+1, 1, k)$. Therefore, all of the triangular-wedge elemental volumes surrounding a pole are combined in the model into a single volume centered on the pole, having bottom and top faces with I_{max} segments along the edges, and having I_{max} vertical faces connecting the bottom and top faces. The i value of the polar field line is arbitrarily set to 1.

Number of P points on a field line. At high latitudes $(1 \leq j \leq J - K + 1)$ each field line identified with indices (i, j) intersects K height surfaces in one hemisphere. At low latitudes $(J - K + 1 \leq j \leq J)$ the number of height surfaces intersected by the field line in one hemisphere decreases by 1 as j increases by 1 and the apex drops one height level. Considering that the point at the apex applies to both the southern and northern hemispheres, these low-latitude field lines have a total of $2(J-j)+1$ grid points along them.

Number of P points on a height surface. The lowest height surface $(h = h_1)$ has J grid points between each pole and the equator, inclusive, at each longitude. Pole-to-pole there are $2J - 1$ grid points at each longitude, because there is only a single point at the equator that applies to both hemispheres. As we step up in height, each height surface loses one grid point per hemisphere at each longitude, so the number of grid points per longitude in one hemisphere is $J - k + 1$ and pole-to-pole is $2(J - k) + 1$.

Chapter 5

Calculation of Face Areas

The model is based on a calculation of currents flowing between neighboring elemental volumes, subject to boundary conditions at the bottom and top of the ionosphere. Current is strictly conserved by requiring the net current into or out of a volume to be zero, and by calculating the current flowing through a face separating two elemental volumes identically for each volume. The next chapter will describe how the face currents are calculated from the values of Φ on the chosen geomagnetic field lines. This chapter derives the areas of the faces through which current flows in each of three directions. The same methodology is used in both hemispheres. In the equations the upper value of $\pm$ or $\mp$ refers to the northern hemisphere, and the lower value to the southern hemisphere.

5.1 Eastward currents

Let $I_1(i-\frac{1}{2},j,k)$ be the current flowing eastward across the volume face at $\phi_{i-\frac{1}{2}}$:

$$I_1(i-\frac{1}{2},j,k) = \int_{r_{k-\frac{1}{2}}}^{r_{k+\frac{1}{2}}} \int_{\rho_{j-\frac{1}{2}}}^{\rho_j^+} \mathbf{a}_1' \cdot \mathbf{J}\; d\rho\; dr = \int_{r_{k-\frac{1}{2}}}^{r_{k+\frac{1}{2}}} \int_{\rho_{j-\frac{1}{2}}}^{\rho_j^+} \frac{R(\frac{r}{R})^3 J_{e1}\; d\rho\; dr}{F\sqrt{1-\frac{r}{R}\rho^2}} \tag{5.1}$$

where

$$\rho_j^+ = \begin{cases} \rho_{j+\frac{1}{2}}, & j < J-k+1 \quad \text{(not at equator)} \\ \left(\frac{R}{r}\right)^{\frac{1}{2}}, & j = J-k+1 \quad \text{(equatorial volume)} \end{cases} \tag{5.2}$$

Assume $\frac{J_{e1}}{F}\left(\frac{r}{R}\right)^{\frac{5}{2}}$ is approximately constant over the integration surface, equal to its value at $(i-\frac{1}{2},j,k)$:

$$I_1(i-\frac{1}{2},j,k) = \frac{RJ_{e1}(i-\frac{1}{2},j,k)}{F(i-\frac{1}{2},j,k)}\left(\frac{r_k}{R}\right)^{\frac{5}{2}} \int_{r_{k-\frac{1}{2}}}^{r_{k+\frac{1}{2}}} \int_{\rho_{j-\frac{1}{2}}}^{\rho_j^+} \frac{d\rho\ dr}{\sqrt{\frac{R}{r}-\rho^2}} \tag{5.3}$$

The integral with respect to ρ in (5.3), between the limits $\rho_{j-\frac{1}{2}}$ and ρ_j^+, can be expressed as the difference between two integrals that have the limits $(0,\rho_j^+)$ and $(0,\rho_{j-\frac{1}{2}})$:

$$\int_{\rho_{j-\frac{1}{2}}}^{\rho_j^+} \frac{d\rho}{\sqrt{\frac{R}{r}-\rho^2}} = \int_0^{\rho_j^+} \frac{d\rho}{\sqrt{\frac{R}{r}-\rho^2}} - \int_0^{\rho_{j-\frac{1}{2}}} \frac{d\rho}{\sqrt{\frac{R}{r}-\rho^2}} = \sin^{-1}\left(\sqrt{\frac{r}{R}}\ \rho_j^+\right) - \sin^{-1}\left(\sqrt{\frac{r}{R}}\ \rho_{j-\frac{1}{2}}\right) \tag{5.4}$$

Then the double integral in (5.3) is

$$\int_{r_{k-\frac{1}{2}}}^{r_{k+\frac{1}{2}}} \int_{\rho_{j-\frac{1}{2}}}^{\rho_j^+} \frac{d\rho\ dr}{\sqrt{\frac{R}{r}-\rho^2}} = \int_{r_{k-\frac{1}{2}}}^{r_{k+\frac{1}{2}}} \sin^{-1}\left(\sqrt{\frac{r}{R}}\ \rho_j^+\right) dr - \int_{r_{k-\frac{1}{2}}}^{r_{k+\frac{1}{2}}} \sin^{-1}\left(\sqrt{\frac{r}{R}}\ \rho_{j-\frac{1}{2}}\right) dr \tag{5.5}$$

Let us first evaluate the first integral on the right-hand side of (5.5); then the second integral can be found be replacing ρ_j^+ with $\rho_{j-\frac{1}{2}}$. Make a change of variables as

$$y = \sqrt{\frac{r}{R}}\rho_j^+ \tag{5.6}$$

so that

$$r = R\left(\frac{y}{\rho_j^+}\right)^2 \tag{5.7}$$

$$dr = \frac{2R}{(\rho_j^+)^2}\ y\ dy \tag{5.8}$$

$$\int_{r_{k-\frac{1}{2}}}^{r_{k+\frac{1}{2}}} \sin^{-1}\left(\sqrt{\frac{r}{R}}\ \rho_j^+\right) dr \quad = \quad \int_{\sqrt{\frac{r_{k-\frac{1}{2}}}{R}}\rho_j^+}^{\sqrt{\frac{r_{k+\frac{1}{2}}}{R}}\rho_j^+} \frac{2R}{(\rho_j^+)^2}\ y \sin^{-1} y\ dy$$

$$= \frac{R}{(\rho_j^+)^2}\left[\left(y^2-\frac{1}{2}\right)\sin^{-1}y+\frac{y}{2}\sqrt{1-y^2}\right]_{\sqrt{\frac{r_{k-\frac{1}{2}}}{R}}\rho_j^+}^{\sqrt{\frac{r_{k+\frac{1}{2}}}{R}}\rho_j^+} \quad (5.9)$$

Numerically, this solution is poorly behaved (small difference between two large numbers [NEED TO VERIFY THIS; IF THIS SOLUTION IS ADEQUATE, THE FOLLOWING APPROXIMATION IS NOT NEEDED]) as $\rho_j^+ \to 0$, and also as $r_{k+\frac{1}{2}} - r_{k-\frac{1}{2}} \to 0$. Therefore, let us approximate the integral as

$$\int_{r_{k-\frac{1}{2}}}^{r_{k+\frac{1}{2}}} \sin^{-1}\left(\sqrt{\frac{r}{R}}\rho_j^+\right) dr \approx (r_{k+\frac{1}{2}} - r_{k-\frac{1}{2}})\sin^{-1}\left(\sqrt{\frac{r^*}{R}}\rho_j^+\right) \quad (5.10)$$

where r^* is prescribed as follows. When ρ_j^+ is small (high-latitude field lines) the mean value of $\sin^{-1}(\sqrt{\frac{r}{R}}\rho_j^+)$ over the integration range is essentially $\sin^{-1}(\sqrt{\frac{r_{k-\frac{1}{2}}+r_{k-\frac{1}{2}}}{2R}}\rho_{j+\frac{1}{2}})$, so the appropriate value of r^* is $\frac{1}{2}(r_{k+\frac{1}{2}} + r_{k-\frac{1}{2}})$. (This is where field lines are nearly straight through the thin layer.) When ρ_j^+ approaches 1 (near-equatorial field lines), the curvature of field lines within the layer may not be negligible.

Note that the integral is essentially proportional to the area of a thin strip between $r_{k-\frac{1}{2}}$ and $r_{k+\frac{1}{2}}$ and between the pole and the field line at $\rho_{j+\frac{1}{2}}$. Define r_a as the value of r at the field-line apex,

$$r_a = \frac{R}{\rho_{j+\frac{1}{2}}^2} \quad (5.11)$$

If we approximate the field line as a parabola on a flat Earth satisfying $r = r_a - c\lambda_q^2$ (see Figure 5.1), then the area in the strip between $r_{k-\frac{1}{2}}$ and $r_{k+\frac{1}{2}}$ and between $\rho_{j+\frac{1}{2}}$ and the equator is

$$\frac{2}{3}\left[(r_a - r_{k-\frac{1}{2}})R\sqrt{\frac{r_a - r_{k-\frac{1}{2}}}{c}} - (r_a - r_{k+\frac{1}{2}})R\sqrt{\frac{r_a - r_{k+\frac{1}{2}}}{c}}\right] \equiv (r_{k+\frac{1}{2}} - r_{k-\frac{1}{2}})R\sqrt{\frac{r_a - r*}{c}} \quad (5.12)$$

where use is made of the relation that distance from the equator is $R\lambda_q = R\sqrt{(r_a - r)/c}$ and

where the equivalence sign indicates that (5.12) is the definition of $r*$. Solve (5.12) for $r*$:

$$r* = r_a - \frac{4}{9}\left[\frac{(r_a - r_{k-\frac{1}{2}})^{\frac{3}{2}} - (r_a - r_{k+\frac{1}{2}})^{\frac{3}{2}}}{r_{k+\frac{1}{2}} - r_{k-\frac{1}{2}}}\right]^2 \tag{5.13}$$

When the field-line apex is at the top of the thin layer, i.e., $r_a = r_{k+\frac{1}{2}}$, (5.13) gives $r* = \frac{5}{9}r_{k+\frac{1}{2}} + \frac{4}{9}r_{k-\frac{1}{2}}$. In the other extreme, when $r_a \to \infty$, $r* \to \frac{1}{2}(r_{k+\frac{1}{2}} + r_{k-\frac{1}{2}})$. The transition from the former toward the latter value of $r*$ is rapid as r_a increases. For the formula (5.13) to be numerically stable, r_a may not become too large.

Define a normalized area factor $A_1(j+\frac{1}{2},k)$ representing the normalized area in layer k between the pole and $\rho_{j+\frac{1}{2}}$:

$$A_1(j+\frac{1}{2},k) = \begin{cases} 0 & \text{if} \quad j = 0 \\ \frac{2}{\pi}\sin^{-1}\left(\rho_{j+\frac{1}{2}}\sqrt{\frac{r^*_{j+\frac{1}{2},k}}{R}}\right) & \text{if} \quad 1 \le j < J-k+1 \\ 1 & \text{if} \quad j = J-k+1 \quad \text{(equatorial element)} \end{cases} \tag{5.14}$$

where the dependence of r^* on j and k is as given by (5.11) and (5.13). [In `subroutine calc_mf` (file `areas.f90`) `a1(j+1,k)` is $A_1(j-\frac{1}{2},k)$, not $A_1(j+\frac{1}{2},k)$.] Then (5.3) becomes

$$I_1(i-\frac{1}{2},j,k) = \frac{RJ_{e1}(i-\frac{1}{2},j,k)}{F(i-\frac{1}{2},j,k)}\left(\frac{r_k}{R}\right)^{\frac{5}{2}}\frac{\pi}{2}\left[A_1(j+\frac{1}{2},k) - A_1(j-\frac{1}{2},k)\right](r_{k+\frac{1}{2}} - r_{k-\frac{1}{2}}) \tag{5.15}$$

Define a scaled area factor $M_1(i-\frac{1}{2},j,k)$ for this face of the elemental volume from

$$I_1(i-\frac{1}{2},j,k) = M_1(i-\frac{1}{2},j,k)J_{e1}(i-\frac{1}{2},j,k) \tag{5.16}$$

$$M_1(i-\frac{1}{2},j,k) = R\frac{\pi}{2}\left(\frac{r_k}{R}\right)^{\frac{5}{2}}\frac{\left[A_1(j+\frac{1}{2},k) - A_1(j-\frac{1}{2},k)\right](r_{k+\frac{1}{2}} - r_{k-\frac{1}{2}})}{F(i-\frac{1}{2},j,k)} \tag{5.17}$$

Note that $M_1 \times F$ is independent of longitude.

5.2 Equatorward/downward currents

Let $I_2(i, j-\frac{1}{2}, k)$ be the current flowing equatorward/downward across the volume face at $\rho_{j-\frac{1}{2}}$:

$$I_2(i,j-\frac{1}{2},k) = \int_{\phi_{i-\frac{1}{2}}}^{\phi_{i+\frac{1}{2}}} \int_{r_{k-\frac{1}{2}}}^{r_{k+\frac{1}{2}}} \mathbf{a}_2' \cdot \mathbf{J}\; dr\; d\phi = \int_{\phi_{i-\frac{1}{2}}}^{\phi_{i+\frac{1}{2}}} \int_{r_{k-\frac{1}{2}}}^{r_{k+\frac{1}{2}}} \frac{R(\frac{r}{R})^3 \rho_{j-\frac{1}{2}} \sqrt{1-\frac{3}{4}\rho^2_{j-\frac{1}{2}}}\; J_{e2}\; dr\; d\phi}{F\sqrt{1-\frac{r}{R}\rho^2_{j-\frac{1}{2}}}} \tag{5.18}$$

If $j = 1$ (5.18) represents equatorward current coming from the zero-width pole, where $\rho_{\frac{1}{2}} = 0$, so $I_2(i, \frac{1}{2}, k) = 0$. Assume that $(\frac{r}{R})^3 J_{e2}/F$ is approximately constant over the area of integration, equal to its value at $\phi_i, \rho_{j-\frac{1}{2}}, r_k$. Note that

$$\int_{r_{k-\frac{1}{2}}}^{r_{k+\frac{1}{2}}} \frac{dr}{\sqrt{1-\frac{r}{R}\rho^2}} = \frac{2R}{\rho^2}\left[\sqrt{1-\frac{r_{k-\frac{1}{2}}}{R}\rho^2} - \sqrt{1-\frac{r_{k+\frac{1}{2}}}{R}\rho^2}\;\right] \tag{5.19}$$

Then (5.18) can be written

$$I_2(i,j-\frac{1}{2},k) = M_2(i,j-\frac{1}{2},k) J_{e2}(i,j-\frac{1}{2},k) \tag{5.20}$$

where the scaled area for this face of the elemental volume is

$$M_2(i,j-\frac{1}{2},k) = \frac{2R^2(\frac{r_k}{R})^3\sqrt{1-\frac{3}{4}\rho^2_{j-\frac{1}{2}}}}{F(i,j-\frac{1}{2},k)\rho_{j-\frac{1}{2}}}\left[\sqrt{1-\frac{r_{k-\frac{1}{2}}}{R}\rho^2_{j-\frac{1}{2}}} - \sqrt{1-\frac{r_{k+\frac{1}{2}}}{R}\rho^2_{j-\frac{1}{2}}}\;\right](\phi_{i+\frac{1}{2}} - \phi_{i-\frac{1}{2}}) \tag{5.21}$$

$$M_2(i,\frac{1}{2},k) = 0 \tag{5.22}$$

Note that $M_2 \times F$ is independent of longitude if $(\phi_{i+\frac{1}{2}} - \phi_{i-\frac{1}{2}})$ is constant. For volumes on a field line not at the equator ($k < J - j + 1$), $M_2(i, j+\frac{1}{2}, k)$ is obtained from (5.21) by substituting $j - \frac{1}{2} \to j + \frac{1}{2}$. For the equatorial volume, the $j + \frac{1}{2}$ field line has zero length, so

$$M_2(i,j+\frac{1}{2},k) = 0,\;\; k = J - j + 1 \quad \text{(equatorial volume)} \tag{5.23}$$

5.3 Vertical currents

Let $I_3(i,j,k-\frac{1}{2})$ be the current flowing upward across the volume face at $r_{k-\frac{1}{2}}$:

$$I_3(k,j,k-\frac{1}{2}) = \int_{\phi_{i-\frac{1}{2}}}^{\phi_{i+\frac{1}{2}}} \int_{\rho_{j-\frac{1}{2}}}^{\rho_{j+\frac{1}{2}}} (\mp \mathbf{a}_3') \cdot \mathbf{J} \; d\rho \; d\phi = \int_{\phi_{i-\frac{1}{2}}}^{\phi_{i+\frac{1}{2}}} \int_{\rho_{j-\frac{1}{2}}}^{\rho_{j+\frac{1}{2}}} \frac{R^2(\frac{r}{R})^3 \rho J_r \; d\rho \; d\phi}{F\sqrt{1-\frac{r_{k-\frac{1}{2}}}{R}\rho^2}} \tag{5.24}$$

Assume that $(\frac{r}{R})^3 J_r/F$ is approximately constant over the area of integration, equal to its value at $(\phi_i, \rho_j, r_{k-\frac{1}{2}})$. Note that

$$\int_{\rho_{j-\frac{1}{2}}}^{\rho_{j+\frac{1}{2}}} \frac{\rho \; d\rho}{\sqrt{1-\frac{r_{k-\frac{1}{2}}}{R}\rho^2}} = \frac{R}{r_{k-\frac{1}{2}}} \left[\sqrt{1-\frac{r_{k-\frac{1}{2}}}{R}\rho_{j-\frac{1}{2}}^2} - \sqrt{1-\frac{r_{k-\frac{1}{2}}}{R}\rho_{j+\frac{1}{2}}^2} \; \right] \tag{5.25}$$

Then (5.24) can be written

$$I_3(i,j,k-\frac{1}{2}) = M_3(i,j,k-\frac{1}{2}) J_r(i,j,k-\frac{1}{2}) \tag{5.26}$$

where the scaled area for this face of the elemental volume is

$$M_3(i,j,k-\frac{1}{2}) = \frac{r_{k-\frac{1}{2}}^2}{F(i,j,k-\frac{1}{2})} \left[\sqrt{1-\frac{r_{k-\frac{1}{2}}}{R}\rho_{j-\frac{1}{2}}^2} - \sqrt{1-\frac{r_{k-\frac{1}{2}}}{R}\rho_{j+\frac{1}{2}}^2} \; \right] (\phi_{i+\frac{1}{2}} - \phi_{i-\frac{1}{2}}) \tag{5.27}$$

Note that $M_3 \times F$ is independent of longitude if $(\phi_{i+\frac{1}{2}} - \phi_{i-\frac{1}{2}})$ is constant. Define the normalized scaled area at $r_{k-\frac{1}{2}}$ from the pole to $\rho_{j+\frac{1}{2}}$ as

$$A_3(j+\frac{1}{2},k-\frac{1}{2}) = 1 - \sqrt{1-\frac{r_{k-\frac{1}{2}}}{R}\rho_{j+\frac{1}{2}}^2} = 1 - \sin|\lambda_q(j+\frac{1}{2},k-\frac{1}{2})| \tag{5.28}$$

Then

$$M_3(i,j,k-\frac{1}{2}) = \frac{r_{k-\frac{1}{2}}^2}{F(i,j,k-\frac{1}{2})} \left[A_3(j+\frac{1}{2},k-\frac{1}{2}) - A_3(j-\frac{1}{2},k-\frac{1}{2}) \right] (\phi_{i+\frac{1}{2}} - \phi_{i-\frac{1}{2}}) \tag{5.29}$$

[Note that $A_3(j-\frac{1}{2},k-\frac{1}{2}) = 0$ for $j=1$ (pole).] For the top elemental volume on a field line, define $I_3(k,j,k+\frac{1}{2})$ as the current flowing outward across the equatorial face (which is

not necessarily perpendicular to a field line).

Chapter 6

Relating $I_1,\ I_2,\ I_3$ to Φ

The net current flowing out of an elemental volume at (i, j, k) is

$$I_1(i+\frac{1}{2},j,k)-I_1(i-\frac{1}{2},j,k)+I_2(i,j+\frac{1}{2},k)-I_2(i,j-\frac{1}{2},k)+I_3(i,j,k+\frac{1}{2})-I_3(i,j,k-\frac{1}{2})=0 \tag{6.1}$$

This equation applies separately to the southern and northern hemispheres; later we sometimes use superscripts S and N to identify the hemisphere, when necessary. I_1 and I_2 can be calculated from Ohm's Law using (3.8)-(3.11) [or (3.14) and (3.17) in place of (3.8) and (3.10) at the equatorial boundary], along with (5.16), and (5.20). However, Ohm's Law does not give the local vertical current density, which has an important component associated with $\mathbf{J}_\parallel$, not described by Ohm's Law. Instead, I_3 will be determined from I_1 and I_2 by using (6.1) and stepping up along a field line, effectively integrating the vertical derivative of I_3 with respect to height, starting with a given lower boundary condition on I_3 at $h = h_1$. When I_3 at the upper boundary is matched to the specified upper-boundary condition (for field lines at middle and high latitudes) or to $-I_3$ from the upper boundary of the opposite hemisphere (for field lines at low latitudes), an equation is obtained relating the values of Φ on that field line and its neighbors. The set of such equations for all locations is then solved for the values of Φ on all field lines.

6.1 Electric-field components

In order to apply (6.1) we need finite-difference expressions for the electric-field components E_{d1} and E_{d2} at locations $(i-\frac{1}{2},j)$, $(i+\frac{1}{2},j)$, $(i,j-\frac{1}{2})$ and $(i,j+\frac{1}{2})$. We apply first-order finite differences to (3.2) and (3.3) to get

$$E_{d1}(i-\frac{1}{2},j) = \frac{\Phi(i-1,j)-\Phi(i,j)}{R\rho_j(\phi_i-\phi_{i-1})} \tag{6.2}$$

$$E_{d2}(i-\frac{1}{2},j) = \frac{\sqrt{1-\frac{3}{4}\rho_j^2}}{R}\frac{[\Phi(i-1,j-1)+\Phi(i,j-1)-\Phi(i-1,j+1)-\Phi(i,j+1)]}{2(\rho_{j+1}-\rho_{j-1})} \tag{6.3}$$

$$E_{d1}(i+\frac{1}{2},j) = \frac{\Phi(i,j)-\Phi(i+1,j)}{R\rho_j(\phi_i-\phi_{i-1})} \tag{6.4}$$

$$E_{d2}(i+\frac{1}{2},j) = \frac{\sqrt{1-\frac{3}{4}\rho_j^2}}{R}\frac{[\Phi(i,j-1)+\Phi(i+1,j-1)-\Phi(i,j+1)-\Phi(i+1,j+1)]}{2(\rho_{j+1}-\rho_{j-1})} \tag{6.5}$$

$$E_{d1}(i,j-\frac{1}{2}) = \frac{\Phi(i-1,j-1)+\Phi(i-1,j)-\Phi(i+1,j-1)-\Phi(i+1,j)}{2R\rho_{j-\frac{1}{2}}(\phi_{i+1}-\phi_{i-1})} \tag{6.6}$$

$$E_{d2}(i,j-\frac{1}{2}) = \frac{\sqrt{1-\frac{3}{4}\rho_{j-\frac{1}{2}}^2}}{R}\frac{[\Phi(i,j-1)-\Phi(i,j)]}{(\rho_j-\rho_{j-1})} \tag{6.7}$$

$$E_{d1}(i,j+\frac{1}{2}) = \frac{\Phi(i-1,j)+\Phi(i-1,j+1)-\Phi(i+1,j)-\Phi(i+1,j+1)}{2R\rho_{j+\frac{1}{2}}(\phi_{i+1}-\phi_{i-1})} \tag{6.8}$$

$$E_{d2}(i,j+\frac{1}{2}) = \frac{\sqrt{1-\frac{3}{4}\rho_{j+\frac{1}{2}}^2}}{R}\frac{[\Phi(i,j)-\Phi(i,j+1)]}{(\rho_{j+1}-\rho_j)} \tag{6.9}$$

These equations cannot always be applied directly at locations near the polar or equatorial lower boundaries, either because the equations would sometimes call for an undefined value of Φ at non-existent locations with $\rho=\rho_0$ or $\rho=\rho_{J+1}$, or they produce fractions where both the numerator and denominator are zero (when the denominator has either $\rho_{\frac{1}{2}}$ or ρ_1). Special considerations are then applied.

6.2 Eastward current component I_1

When $1 < j < J$, $I_1(i-\frac{1}{2},j,k)$ can be expressed in terms of neighboring Φ values by using (3.8), (3.10), (5.14)-(5.17), (6.2), and (6.3):

$$\begin{aligned} &I_1(i-\tfrac{1}{2},j,k) = \\ &\quad N_1^P(i-\tfrac{1}{2},j,k)[\Phi(i-1,j)-\Phi(i,j)] \\ &\quad - N_1^H(i-\tfrac{1}{2},j,k)[\Phi(i-1,j-1)+\Phi(i,j-1)-\Phi(i-1,j+1)-\Phi(i,j+1)] \\ &\quad + S_1(i-\tfrac{1}{2},j,k) \end{aligned} \tag{6.10}$$

$$N_1^P(i-\frac{1}{2},j,k) = \frac{M_1(i-\frac{1}{2},j,k)[\sigma_P d_1^2](i-\frac{1}{2},j,k)}{R\rho_j(\phi_i-\phi_{i-1})} \tag{6.11}$$

$$N_1^H(i-\frac{1}{2},j,k) = \frac{M_1(i-\frac{1}{2},j,k)[\sigma_H D-\sigma_P \mathbf{d}_1\cdot\mathbf{d}_2](i-\frac{1}{2},j,k)\sqrt{1-\frac{3}{4}\rho_j^2}}{2R(\rho_{j+1}-\rho_{j-1})} \tag{6.12}$$

$$S_1(i-\frac{1}{2},j,k) = M_1(i-\frac{1}{2},j,k)J_{e1}^D(i-\frac{1}{2},j,k) \tag{6.13}$$

An expression for $I_1(i+\frac{1}{2},j,k)$ is found by replacing i by $i+1$ in (6.10)-(6.13).

An expression for I_1 at the pole ($\rho = \rho_1 = 0$) is needed for calculating the distribution of eastward and upward currents near the pole, even though it will not be needed for calculating Φ. An adequate estimation of the polar I_1 values can be obtained by interpolating across the pole: first average $J_{e1}(i-\frac{1}{2},2,k)$ [that is, $I_1(i-\frac{1}{2},2,k)/M_1(i-\frac{1}{2},2,k)$] and $-J_{e1}(i'-\frac{1}{2},2,k)$, where $i'-\frac{1}{2}$ lies at the longitude 180° away, and then multiply this average by the local area factor $M_1(i-\frac{1}{2},1,k)$. (Note that since the direction of J_{e1} flips when stepping across the pole, it is $-J_{e1}$ rather than J_{e1} that we use for longitude index $i'-\frac{1}{2}$.) With $I_{\max}$ being the number of longitudes, the index i' is calculated as

$$i' = \begin{cases} i + I_{\max}/2, & i \le I_{\max}/2 \\ i - I_{\max}/2, & i > I_{\max}/2 \end{cases} \tag{6.14}$$

Then

$$I_1(i-\frac{1}{2},1,k)=\frac{1}{2}\left[\frac{I_1(i-\frac{1}{2},2,k)}{M_1(i-\frac{1}{2},2,k)}-\frac{I_1(i'-\frac{1}{2},2,k)}{M_1(i'-\frac{1}{2},2,k)}\right]M_1(i-\frac{1}{2},1,k) \tag{6.15}$$

At the equatorial boundary, $\rho=\rho_J$, we use (3.14) instead of (3.8) so that (6.10) remains applicable, but (6.11)-(6.13) become

$$N_1^P(i-\frac{1}{2},J,k)=\frac{M_1(i-\frac{1}{2},J,k)[\sigma_C d_1^2](i-\frac{1}{2},J,k)}{R\rho_J(\phi_i-\phi_{i-1})} \tag{6.16}$$

$$N_1^H(i-\frac{1}{2},J,k)=0 \tag{6.17}$$

$$S_1(i-\frac{1}{2},J,k)=M_1(i-\frac{1}{2},J,k)J_{e1}^{Deq}(i-\frac{1}{2},J,k) \tag{6.18}$$

where σ_C is given by (3.15) and J_{e1}^{Deq} is given by (3.17). An expression for $I_1(i+\frac{1}{2},J,k)$ is found by replacing i by $i+1$ in (6.10), (6.16)-(6.18).

6.3 Equatorward/downward current component I_2

When $1<j\le J$, $I_2(i,j-\frac{1}{2},k)$ can be expressed in terms of neighboring Φ values by using (3.9), (3.11), (5.20)-(5.23), (6.6), and (6.7):

$$\begin{aligned}&I_2(i,j-\tfrac{1}{2},k)=\\&\quad N_2^P(i,j-\tfrac{1}{2},k)[\Phi(i,j-1)-\Phi(i,j)]\\&\quad+\ N_2^H(i,j-\tfrac{1}{2},k)[\Phi(i-1,j-1)+\Phi(i-1,j)-\Phi(i+1,j-1)-\Phi(i+1,j)]\\&\quad+S_2(i,j-\tfrac{1}{2},k)\end{aligned} \tag{6.19}$$

$$N_2^P(i,j-\frac{1}{2},k)=\frac{M_2(i,j-\frac{1}{2},k)[\sigma_P d_2^2](i,j-\frac{1}{2},k)\sqrt{1-\frac{3}{4}\rho_{j-\frac{1}{2}}^2}}{R(\rho_j-\rho_{j-1})} \tag{6.20}$$

$$N_2^H(i,j-\frac{1}{2},k)=\frac{M_2(i,j-\frac{1}{2},k)[\sigma_H D+\sigma_P\mathbf{d}_1\cdot\mathbf{d}_2](i,j-\frac{1}{2},k)}{2R\rho_{j-\frac{1}{2}}(\phi_{i+1}-\phi_{i-1})} \tag{6.21}$$

$$S_2(i, j-\frac{1}{2}, k) = M_2(i, j-\frac{1}{2}, k) J^D_{e2}(i, j-\frac{1}{2}, k) \tag{6.22}$$

When (6.1) is applied at the pole ($j = 1$), (6.19)-(6.22) all give zero values, because $M_2(i, \frac{1}{2}, k) = 0$. An expression for $I_2(i, j+\frac{1}{2}, k)$ is found by replacing j by $j+1$ in (6.19)-(6.22). When (6.1) is applied at the equatorial lower boundary ($j = J$), where $M_2(i, J+\frac{1}{2}, k) = 0$,

$$I_2(i, J+\frac{1}{2}, k) = 0 \tag{6.23}$$

$$N^P_2(i, J+\frac{1}{2}, k) = 0 \tag{6.24}$$

$$N^H_2(i, J+\frac{1}{2}, k) = 0 \tag{6.25}$$

$$S_2(i, J+\frac{1}{2}, k) = 0. \tag{6.26}$$

6.4 Vertical current component I_3

The difference between upward currents at the top and bottom of an elemental volume is obtained from (6.1):

$$I_3(i, j, k+\frac{1}{2}) - I_3(i, j, k-\frac{1}{2}) = I_1(i-\frac{1}{2}, j, k) - I_1(i+\frac{1}{2}, j, k) + I_2(i, j-\frac{1}{2}, k) - I_2(i, j+\frac{1}{2}, k) \tag{6.27}$$

For $1 < j \leq J$ use (6.10) and (6.19) in (6.27) to get

$$
\begin{aligned}
& I_3(i,j,k+\tfrac{1}{2}) - I_3(i,j,k-\tfrac{1}{2}) \\
&= N_1^P(i-\tfrac{1}{2},j,k)[\Phi(i-1,j) - \Phi(i,j)] \\
&- N_1^H(i-\tfrac{1}{2},j,k)[\Phi(i-1,j-1) + \Phi(i,j-1) - \Phi(i-1,j+1) - \Phi(i,j+1)] \\
&+ S_1(i-\tfrac{1}{2},j,k) \\
&- N_1^P(i+\tfrac{1}{2},j,k)[\Phi(i,j) - \Phi(i+1,j)] \\
&+ N_1^H(i+\tfrac{1}{2},j,k)[\Phi(i,j-1) + \Phi(i+1,j-1) - \Phi(i,j+1) - \Phi(i+1,j+1)] \\
&- S_1(i+\tfrac{1}{2},j,k) \\
&+ N_2^P(i,j-\tfrac{1}{2},k)[\Phi(i,j-1) - \Phi(i,j)] \\
&+ N_2^H(i,j-\tfrac{1}{2},k)[\Phi(i-1,j-1) + \Phi(i-1,j) - \Phi(i+1,j-1) - \Phi(i+1,j)] \\
&+ S_2(i,j-\tfrac{1}{2},k) \\
&- N_2^P(i,j+\tfrac{1}{2},k)[\Phi(i,j) - \Phi(i,j+1)] \\
&- N_2^H(i,j+\tfrac{1}{2},k)[\Phi(i-1,j) + \Phi(i-1,j+1) - \Phi(i+1,j) - \Phi(i+1,j+1)] \\
&- S_2(i,j+\tfrac{1}{2},k)
\end{aligned}
\tag{6.28}
$$

Notice that whenever the second index of Φ for a term in (6.28) would be calculated to be either 0 (at the pole) or $J+1$ (at the equator), that non-existent value of Φ is multiplied by a quantity that has been set to 0.

Rearrange to collect terms for which Φ has like indices:

$$
\begin{aligned}
& I_3(i,j,k+\tfrac{1}{2}) - I_3(i,j,k-\tfrac{1}{2}) \\
&= c_1(i,j,k)\Phi(i+1,j) + c_2(i,j,k)\Phi(i+1,j+1) + c_3(i,j,k)\Phi(i,j+1) \\
&+ c_4(i,j,k)\Phi(i-1,j+1) + c_5(i,j,k)\Phi(i-1,j) + c_6(i,j,k)\Phi(i-1,j-1) \\
&+ c_7(i,j,k)\Phi(i,j-1) + c_8(i,j,k)\Phi(i+1,j-1) + c_9(i,j,k)\Phi(i,j) \\
&+ S(i,j,k)
\end{aligned}
\tag{6.29}
$$

$$
c_1(i,j,k) = N_1^P(i+\frac{1}{2},j,k) - N_2^H(i,j-\frac{1}{2},k) + N_2^H(i,j+\frac{1}{2},k) \tag{6.30}
$$

$$
c_2(i,j,k) = -N_1^H(i+\frac{1}{2},j,k) + N_2^H(i,j+\frac{1}{2},k) \tag{6.31}
$$

$$
c_3(i,j,k) = N_1^H(i-\frac{1}{2},j,k) - N_1^H(i+\frac{1}{2},j,k) + N_2^P(i,j+\frac{1}{2},k) \tag{6.32}
$$

$$
\begin{aligned}
c_4(i,j,k) &= N_1^H(i-\frac{1}{2},j,k) - N_2^H(i,j+\frac{1}{2},k) && (6.33)\\
c_5(i,j,k) &= N_1^P(i-\frac{1}{2},j,k) + N_2^H(i,j-\frac{1}{2},k) - N_2^H(i,j+\frac{1}{2},k) && (6.34)\\
c_6(i,j,k) &= -N_1^H(i-\frac{1}{2},j,k) + N_2^H(i,j-\frac{1}{2},k) && (6.35)\\
c_7(i,j,k) &= -N_1^H(i-\frac{1}{2},j,k) + N_1^H(i+\frac{1}{2},j,k) + N_2^P(i,j-\frac{1}{2},k) && (6.36)\\
c_8(i,j,k) &= N_1^H(i+\frac{1}{2},j,k) - N_2^H(i,j-\frac{1}{2},k) && (6.37)\\
c_9(i,j,k) &= -N_1^P(i+\frac{1}{2},j,k) - N_1^P(i-\frac{1}{2},j,k) - N_2^P(i,j-\frac{1}{2},k) - N_2^P(i,j+\frac{1}{2},k) && (6.38)
\end{aligned}
$$

$$
S(i,j,k) = S_1(i-\frac{1}{2},j,k) - S_1(i+\frac{1}{2},j,k) + S_2(i,j-\frac{1}{2},k) - S_2(i,j+\frac{1}{2},k) \qquad (6.39)
$$

For volume elements at the pole ($j = 1$) we sum (6.27) over all i so that the terms $I_1(i+\frac{1}{2},j,k) - I_1(i-\frac{1}{2},j,k)$ cancel each other out, and we note that $I_2(i,j-\frac{1}{2},k) = 0$ and that the polar potential $\Phi(i,1)$ has the same value for all i, so that

$$
I_3^p(k+\frac{1}{2}) - I_3^p(k-\frac{1}{2}) = -\sum_i I_2(i,\frac{3}{2},k) \qquad (6.40)
$$

$$
I_3^p(k+\frac{1}{2}) = \sum_i I_3(i,1,k+\frac{1}{2}) = \left[\sum_i M_3(i,1,k+\frac{1}{2})\right] J_r^p(k+\frac{1}{2}) \qquad (6.41)
$$

$$
I_3^p(k-\frac{1}{2}) = \sum_i I_3(i,1,k-\frac{1}{2}) = \left[\sum_i M_3(i,1,k-\frac{1}{2})\right] J_r^p(k-\frac{1}{2}) \qquad (6.42)
$$

where J_r^p is the upward current density at the pole. Summing (6.19) over i for $j = 2$ and noting that $\Phi(i-1,1) = \Phi(i+1,1)$ gives

$$
\begin{aligned}
\sum_i I_2(i,\frac{3}{2},k) &= \sum_i N_2^P(i,\frac{3}{2},k)[\Phi(i,1) - \Phi(i,2)]\\
&+ \sum_i N_2^H(i,\frac{3}{2},k)[\Phi(i-1,2) - \Phi(i+1,2)] + \sum_i S_2(i,\frac{3}{2},k) \qquad (6.43)
\end{aligned}
$$

Since the summation is over all i,

$$
\sum_i N_2^H(i,\frac{3}{2},k)\Phi(i-1,2) = \sum_i N_2^H(i+1,\frac{3}{2},k)\Phi(i,2) \qquad (6.44)
$$

$$\sum_i N_2^H(i,\frac{3}{2},k)\Phi(i+1,2) = \sum_i N_2^H(i-1,\frac{3}{2},k)\Phi(i,2) \tag{6.45}$$

so that

$$\sum_i N_2^H(i,\frac{3}{2},k)[\Phi(i-1,2) - \Phi(i+1,2)] = \sum_i [N_2^H(i+1,\frac{3}{2},k) - N_2^H(i-1,\frac{3}{2},k)]\Phi(i,2) \tag{6.46}$$

Combining (6.40)-(6.46) gives

$$I_3^p(k+\frac{1}{2}) - I_3^p(k-\frac{1}{2}) = \sum_i \chi_2(i,k)\Phi(i,2) - \chi^p(k)\Phi^p - \sum_i S_2(i,\frac{3}{2},k) \tag{6.47}$$

$$\chi_2(i,k) = N_2^P(i,\frac{3}{2},k) - N_2^H(i+1,\frac{3}{2},k) + N_2^H(i-1,\frac{3}{2},k) \tag{6.48}$$

$$\chi^p(k) = \sum_i N_2^P(i,\frac{3}{2},k) \tag{6.49}$$

$$\Phi^p = \Phi(i,1) \quad \text{for all } i \tag{6.50}$$

Chapter 7

Solving for Φ

On a given field line in one hemisphere the maximum value of k is

$$k_{max} = \begin{cases} K & \text{if} \quad j \leq J - K + 1 \\ J - j + 1 & \text{if} \quad j \geq J - K + 1 \end{cases} \tag{7.1}$$

From (6.29) and (9.1) the value of I_3 at this upper boundary is

$$\begin{aligned} & I_3(i, j, k_{max} + \tfrac{1}{2}) \\ & = \; C_1(i,j)\Phi(i+1,j) + C_2(i,j)\Phi(i+1,j+1) + C_3(i,j)\Phi(i,j+1) \\ & + C_4(i,j)\Phi(i-1,j+1) + C_5(i,j)\Phi(i-1,j) + C_6(i,j)\Phi(i-1,j-1) \\ & + C_7(i,j)\Phi(i,j-1) + C_8(i,j)\Phi(i+1,j-1) + C_9(i,j)\Phi(i,j) \\ & + S_{int}(i,j) + I_3(i,j,\tfrac{1}{2}) \end{aligned} \tag{7.2}$$

$$C_n = \sum_{k=1}^{k_{max}} c_n(i,j,k) \tag{7.3}$$

$$S_{int}(i,j) = \sum_{k=1}^{k_{max}} S(i,j,k) \tag{7.4}$$

These coefficients will be labelled with a superscript S or N as needed in later equations to distinguish their values in the southern or northern magnetic hemisphere, respectively.

At the pole,

$$I_3^p(K+\frac{1}{2}) = \sum_i X_2(i)\Phi(i,2) + C_9^p\Phi^p + S_{int}^p + I_3^p(\frac{1}{2}) \tag{7.5}$$

$$X_2(i) = \sum_{k=1}^{K} \chi_2(i,k) \tag{7.6}$$

$$C_9^p = \sum_{k=1}^{K} \chi^p(k) \tag{7.7}$$

$$S_{int}^p = -\sum_{k=1}^{K}\sum_i S_2(i,\frac{3}{2},k) \tag{7.8}$$

If I_3 at $k = k_{max}$ is known, (7.2) and (7.5) give us a set of linear equations to be solved for the gridded values $\Phi(i,j)$. However, because these equations have all been derived using only dfferences of Φ values, and represent a balance of current flow from one elemental volume to another, they are not independent equations. Furthermore, they are consistent with the addition of any arbitrary global constant value to every gridded value of Φ. To resolve these problems, we apply (7.5) only at the South Magnetic Pole, and replace (7.5) at the North Pole by

$$\Phi^{pN} = 0. \tag{7.9}$$

It should be noted that there is a constraint on $I_3(i,j,k_{max}+\frac{1}{2})$:

$$\sum_{S,N}\left[\sum_i\sum_{j=2}^{J} I_3(i,j,k_{max}+\frac{1}{2}) + I_3^p(K+\frac{1}{2})\right] = \sum_{S,N}\left[\sum_i\sum_{j=2}^{J} I_3(i,j,\frac{1}{2}) + I_3^p(\frac{1}{2})\right] \tag{7.10}$$

where the sum over S, N adds the values for the southern and northern magnetic hemispheres. This constraint ensures that there is no net current flowing into the global ionosphere. Furthermore, it ensures that Φ varies smoothly across the South Magnetic Pole, where the unused equation (7.5) would otherwise have enforced smoothness there.

The values of $I_3(i,j,k_{max}+\frac{1}{2})$ for conjugate points in the southern and northern hemispheres on a given geomagnetic field line, i.e., for the same values of i and j, generally depend on each other. At low and middle magnetic latitudes, for values of j greater than or equal to a particular midlatitude value J_M, the sum of the S and N values of $I_3(i,j,k_{max})$ vanishes

unless there is a net magnetospheric source of current $I_m(i,j)$ that can flow into either or both hemispheres. Furthermore, the model assumes that geomagnetic-field lines are perfect equipotentials all the way between hemispheres at these latitudes, so that Φ has the same value at southern and northern conjugate points. Adding (7.2) for both hemispheres for $j > J_M$ gives:

$$\begin{aligned} & C_1^T(i,j)\Phi(i+1,j) + C_2^T(i,j)\Phi(i+1,j+1) + C_3^T(i,j)\Phi(i,j+1) \\ + \; & C_4^T(i,j)\Phi(i-1,j+1) + C_5^T(i,j)\Phi(i-1,j) + C_6^T(i,j)\Phi(i-1,j-1) \\ + \; & C_7^T(i,j)\Phi(i,j-1) + C_8^T(i,j)\Phi(i+1,j-1) + C_9^T(i,j)\Phi(i,j) \\ + \; & S_{int}^T(i,j) + I_3^T(i,j,\tfrac{1}{2}) = I_m(i,j), \qquad j > J_M \end{aligned} \tag{7.11}$$

$$C_n^T \equiv C_n^S + C_n^N \tag{7.12}$$

$$S_{int}^T \equiv S_{int}^S + S_{int}^N \tag{7.13}$$

$$I_3^T \equiv I_3^S + I_3^N \tag{7.14}$$

For high-latitude regions ($j < J_M$) the model allows the conjugate values of Φ to differ between the hemispheres, increasingly so as we move to higher latitudes. Therefore, when $j = J_M$ (7.11) must be replaced by

$$\begin{aligned} & C_1^T(i,j)\Phi(i+1,j) + C_2^T(i,j)\Phi(i+1,j+1) + C_3^T(i,j)\Phi(i,j+1) \\ + \; & C_4^T(i,j)\Phi(i-1,j+1) + C_5^T(i,j)\Phi(i-1,j) + C_6^S(i,j)\Phi(i-1,j-1) \\ + \; & C_6^N(i,j)\Phi(i-1,j-1) + C_7^S(i,j)\Phi(i,j-1) + C_7^N(i,j)\Phi(i,j-1) \\ + \; & C_8^S(i,j)\Phi(i+1,j-1) + C_8^N(i,j)\Phi(i+1,j-1) + C_9^T(i,j)\Phi(i,j) \\ + \; & S_{int}^T(i,j) + I_3^T(i,j,\tfrac{1}{2}) = I_m(i,j), \qquad j = J_M \end{aligned} \tag{7.15}$$

For latitudes poleward of $j = J_M$ let us assume we have an imperfect model of a reference radial current $J_r^R(i,j)$ (superscript R stands for "reference") at $r = r_{K+\frac{1}{2}}$. Because this model is imperfect, we need to allow extra interhemispheric current to flow between conjugate points to prevent large spurious potential differences from developing between conjugate

points. Therefore, we assume

$$I_3(i,j,K+\frac{1}{2}) = I_3^R(i,j) + b(i,j)[\Phi(i,j) - \Phi^*(i,j)], \quad 2 < j < J_M \tag{7.16}$$

$$I_3^p(K+\frac{1}{2}) = I_3^{pR} + \beta[\Phi^p - \Phi^{p*}] \tag{7.17}$$

where Φ^* and Φ^{p*} are the conjugate potentials, b is a conductance that allows enough extra interhemispheric current to flow to prevent unreasonably large potential differences from developing, and

$$I_3^R(i,j) = M_3(i,j,K+\frac{1}{2})J^R(i,j) \tag{7.18}$$

$$I_3^{pR} = \left[\sum_i M_3(i,1,K+\frac{1}{2})\right] J^R(1,1) \tag{7.19}$$

$$\beta = \sum_i b(i,1) \tag{7.20}$$

Note that $J^R(i,1) = J^R(1,1)$ for all i. I_3^R and I_3^{pR} may need to be adjusted to ensure the constraint (7.10) is satisfied. Using (7.16) in (7.2) gives the following relation for each hemisphere:

$$\begin{aligned} &C_1(i,j)\Phi(i+1,j) + C_2(i,j)\Phi(i+1,j+1) + C_3(i,j)\Phi(i,j+1) \\ &+ C_4(i,j)\Phi(i-1,j+1) + C_5(i,j)\Phi(i-1,j) + C_6(i,j)\Phi(i-1,j-1) \\ &+ C_7(i,j)\Phi(i,j-1) + C_8(i,j)\Phi(i+1,j-1) + [C_9(i,j) - b(i,j)]\Phi(i,j) \\ &+ b(i,j)\Phi^*(i,j) + S_{int}(i,j) + I_3(i,j,\tfrac{1}{2}) - I_3^R(i,j) = 0, \quad 2 < j < J_M \end{aligned} \tag{7.21}$$

Using (7.17) in (7.5) gives

$$\sum_i X_2(i)\Phi(i,2) + [C_9^p - \beta]\Phi^p + \beta\Phi^{p*} + S_{int}^p + I_3^p(\frac{1}{2}) - I_3^{pR} = 0 \tag{7.22}$$

Although (7.22) is valid for both poles, we apply it only at the south magnetic pole, to keep our entire set of equations linearly independent.

Let us calculate the number of gridded Φ values and the number of independent equations. If we use single points at the poles instead of I_{max} points with equal potentials, then there are $I_{max}(J_M - 2) + 1$ high-latitude southern grid points, $I_{max}(J_M - 2) + 1$ high-latitude northern

grid points, and $I_{max}(J - J_M + 1)$ low-latitude grid points, for a total of $I_{max}(J + J_M - 3) + 2$ grid points. The $I_{max}(J + J_M - 3) + 2$ equations to solve for the gridded potentials are:
North pole:

$$\Phi^{pN} = 0 \tag{7.23}$$

South pole: Equation (7.22);
High latitudes ($2 \leq j < J_M$): Equation (7.21) for $i = 1, I_{max},\ j = 2, J_M - 1$ in both S and N hemispheres [$2I_{max}(J_M - 2)$ equations];
Midlatitude transition ($j = J_M$): Equation (7.15) for $i = 1, I_{max}$ [I_{max} equations];
Low latitudes ($J_M \leq j \leq J$): Equation (7.11) for $i = 1, I_{max},\ j = J_M, J$ [$I_{max}(J - J_M)$ equations].

Chapter 8

Ideas for constructing the array $b(i,j)$

The interhemispheric coupling factor $b(i,j)$ has the units of conductance. It must have the same value at conjugate points in the southern (S) and northern (N) hemispheres.

In (7.16) the term $b(i,j)[\Phi(i,j) - \Phi^*(i,j)]$ is antisymmetric between the S and N hemispheres, and so to evaluate how to choose values for $b(i,j)$ we look at the antisymmetric components of this equation. Although $I_3^R(i,j)$ may have an antisymmetric component, this antisymmetric component is generally poorly determined from observations, especially at middle latitudes, and its uncertainty will be comparable in magnitude to $b(i,j)[\Phi(i,j) - \Phi^*(i,j)]$, which should therefore be comparable to the magnitude of the antisymmetric component of $I_3(I,j,K+\frac{1}{2})$.

In fact, at middle and low latitudes $I_3^R(i,j)$ is usually ignored, so that $I_3(I,j,K+\frac{1}{2})$ equals $b(i,j)[\Phi(i,j)-\Phi^*(i,j)]$. At midlatitudes $I_3(i,j,K+\frac{1}{2})$ is basically the amount of field-aligned current flowing above the ionosphere through the (i,j) flux tube, which intersects the surface $r = r_{K+\frac{1}{2}}$ over a horizontal area given by $M_3(i,j,K+\frac{1}{2})$. That is,

$$I_3(i,j,K+\frac{1}{2}) = M_3(i,j,K+\frac{1}{2})J_r(i,j,K+\frac{1}{2}). \tag{8.1}$$

J_r is the divergence of the height-integrated horizontal current density below. A very rough

estimate of J_r can be obtained by considering only the Pedersen current driven by the electric field, ignoring the wind-driven current and the electric-field-driven Hall currrent. In a region where the Pedersen conductance

$$\Sigma_P(i,j) = \sum_{k=1}^{K} \left(h_{k+\frac{1}{2}} - h_{k-\frac{1}{2}} \right) \sigma_P(i,j,k) \tag{8.2}$$

is roughly constant, $J_r(i,j,K+\frac{1}{2})$ roughly has the magnitude of $\Sigma_P(i,j)$ times the magnitude of the Laplacian of the electric potential, which is very roughly $|\Phi|/L^2$, where $|\Phi|$ is a characteristic magnitude of Φ and L is a characteristic scale length of Φ. It will usually be the characteristic scale length in the north-south direction that has the greater influence on the magnitude of the Laplacian of Φ, as compared with that in the east-west direction, because L in the north-south direction is usually the smaller of the two scale lengths. Then the magnitude of the antisymmetric component of I_3 is very roughly

$$|I_3^{\text{antisymmetric}}(i,j,K+\frac{1}{2})| \approx \frac{|\Phi|}{L^2} M_3(i,j,K+\frac{1}{2}) \Sigma_P(i,j) \tag{8.3}$$

If Σ_P differs between the northern (N) and southern (S) hemispheres, the hemisphere with the smaller Σ_P will tend to limit J_r in both hemispheres. That is, it tends to be the average of the resistances $1/\Sigma_P$ in the two hemispheres that controls the field-aligned current. Thus (8.3) should be modified as

$$|I_3^{\text{antisymmetric}}(i,j,K+\frac{1}{2})| \approx \frac{|\Phi|}{L^2} \frac{2}{1/[M_3(i,j,K+\frac{1}{2})\Sigma_P(i,j)]^N + 1/[M_3(i,j,K+\frac{1}{2})\Sigma_P(i,j)]^S} \tag{8.4}$$

Let a characteristic magnitude of $[\Phi(i,j) - \Phi^*(i,j)]$ be $\Delta\Phi$. If (8.4) is equated to $b(i,j)\Delta\Phi$, then

$$b(i,j) \approx \frac{|\Phi|}{\Delta\Phi L^2} \times \frac{2}{1/[M_3(i,j,K+\frac{1}{2})\Sigma_P(i,j)]^N + 1/[M_3(i,j,K+\frac{1}{2})\Sigma_P(i,j)]^S} \tag{8.5}$$

To get an approximate value of Σ_P we note that the sum $C_3(i,j)+C_7(i,j)$, corresponding

to coef_ns2(i, j, isn, 3) + coef_ns2(i, j, isn, 7) in calc_coef.f90, is

$$C_3(i,j) + C_7(i,j) = \sum_{k=1}^{k_m} [N_2^P(i, j-\frac{1}{2}, k) + N_2^P(i, j+\frac{1}{2}, k)] \equiv 2\sum_{k=1}^{k_m} N_2^P(i,j,k) \tag{8.6}$$

From (6.20)

$$N_2^P(i,j,k) = \frac{M_2(i,j,k)[\sigma_P d_2^2](i,j,k)\sqrt{1-3\rho_j^2/4}}{R\Delta\rho(j)} \tag{8.7}$$

where

$$\Delta\rho(j) = (\rho_{j+1} - \rho_{j-1})/2 \tag{8.8}$$

is the width with respect to ρ of the jth flux tube.

$b(i,j)$ is applicable to upper midlatitudes, where $\rho_j < 1/2$, and where both $\sin I$ and $\sqrt{1-3\rho_j^2/4}$ are not too different from 1. d_2^2 is also not too different from 1. M_2 is the area of the meridional face of an elemental volume. Neglecting the tilt of this face (i.e., $\sin I \approx 1$) and approximating its width by $R\rho_j(\phi_{i+\frac{1}{2}} - \phi_{i-\frac{1}{2}})$, we find that $M_2(i,j,k)$ is roughly

$$M_2(i,j,k) \approx R\rho_j(\phi_{i+\frac{1}{2}} - \phi_{i-\frac{1}{2}})(h_{k+\frac{1}{2}} - h_{k-\frac{1}{2}}) \tag{8.9}$$

Then summing $N_2^P(i,j,k)$ in altitude gives approximately

$$\sum_{k=1}^{k_m} N_2^P(i,j,k) \approx \frac{R\rho_j(\phi_{i+\frac{1}{2}} - \phi_{i-\frac{1}{2}})\sum_{k=1}^{k_m}[(h_{k+\frac{1}{2}} - h_{k-\frac{1}{2}})\sigma_P(i,j,k)]}{R\Delta\rho(j)} = \frac{\rho_j(\phi_{i+\frac{1}{2}} - \phi_{i-\frac{1}{2}})\Sigma_P(i,j)}{\Delta\rho(j)} \tag{8.10}$$

Equations (8.6) and (8.10) give

$$\Sigma_P(i,j) \approx \frac{\Delta\rho(j)[C_3(i,j) + C_7(i,j)]}{2\rho_j(\phi_{i+\frac{1}{2}} - \phi_{i-\frac{1}{2}})} \tag{8.11}$$

$M_3(i,j,K+\frac{1}{2})$ is the area of the top horizontal face of the top elemental volume on a field line. Its longitudinal width is roughly $R\rho_j(\phi_{i+\frac{1}{2}} - \phi_{i-\frac{1}{2}})$ and its latitudinal width is roughly $R\Delta\rho(j)$, so

$$M_3(i,j,K+\frac{1}{2}) \approx R^2\rho_j(\phi_{i+\frac{1}{2}} - \phi_{i-\frac{1}{2}})\Delta\rho(j) \tag{8.12}$$

Combining (8.11) and (8.12) gives

$$M_3(i,j,K+\frac{1}{2})\Sigma_P(i,j) \approx \frac{[R\Delta\rho(j)]^2[C_3(i,j)+C_7(i,j)]}{2} \tag{8.13}$$

Using this in (8.5) yields

$$b(i,j) \approx \frac{R^2|\Phi|}{L^2\Delta\Phi} \times \frac{\Delta\rho(j)^2}{1/[C_3(i,j)+C_7(i,j)]^S + 1/[C_3(i,j)+C_7(i,j)]^N} \tag{8.14}$$

The quantity $R^2|\Phi|/L^2\Delta\Phi$ is now to be specified as a function of magnetic latitude, and perhaps also longitude, in a way that prevents interhemispheric potential differences on closed field lines from becoming too large at low, middle, and auroral latitudes, while allowing potential differences in the open-field regions of the polar caps to be unconstrained. In open-field regions $b(i,j)$ should be essentially 0.

At midlatitudes, large-scale electric potentials have a characteristic scale length L on the order of $R/3$. If we want to limit $\Delta\Phi/|\Phi|$ to, say, 1%, then $|\Phi|/\Delta\Phi$ might be roughly 100, which would give $R^2|\Phi|/L^2\Delta\Phi$ the value 900.

At auroral latitudes L for large-scale features is on the order of 3×10^5 m $\approx R/20$. Because of field-line potential drops and displacement of field-line footpoints owing to magnetospheric currents that distort field lines, we expect $|\Phi|/\Delta\Phi$ to be considerably smaller than at midlatitudes, maybe roughly 3. For these values, $R^2|\Phi|/L^2\Delta\Phi$ would be roughly 1200.

Given our very rough guesses for suitable values of $|\Phi|/\Delta\Phi$ and $(R/L)^2$ it may be reasonable to use the same value of $R^2|\Phi|/L^2\Delta\Phi$ for auroral latitudes as for midlatitudes, although testing will be necessary to determine what gives satisfactory, stable solutions. A value of 1000 is a reasonable first guess.

Concerning the transition of $b(i,j)$ between polar and auroral regions, there are a number of possibilities.

A. A simple option would be to pre-define a fixed transition region (say, 65-75° magnetic

latitude) over which b drops from the value (8.14) at the auroral edge to 0 at the polar-cap edge.

B. If the upper-boundary reference current J_r^R comes from an MHD magnetospheric model, that model may be able to determine the open-closed field-line boundary, and b could have a sharp transition to 0 everywhere poleward of that boundary, while taking the value (8.14) elsewhere.

C. A more complicated option than A might use a narrower, shifting transition region that takes into account polar-cap expansion and contraction, as defined either by geomagnetic indices or by an algorithm that finds the latitude of Region-1 currents.

Chapter 9

Current Densities on QD Grid

After Φ is determined, I_1 is calculated at $S1$ points using (6.10) or (6.15); I_2 is calculated at $S2$ points using (6.19); and the difference of I_3 between the top and bottom of volume elements is calculated from (6.27). I_3 at the top of any elemental volume is determined by summing the differences from the bottom of the model to the desired height h_k:

$$I_3(i,j,k+\frac{1}{2}) = \sum_{k'=1}^{k} [I_3(i,j,k'+\frac{1}{2}) - I_3(i,j,k'-\frac{1}{2})] + I_3(i,j,\frac{1}{2}) \tag{9.1}$$

where the lower-boundary value $I_3(i,j,\frac{1}{2})$ is typically specified as 0, but may come from a model of the global atmospheric electric circuit.

In this chapter I_1 and I_3 are remapped horizontally to new elemental volumes in QD coordinates, called "QD cells", and are used to calculate northward currents for these volumes by requiring current continuity. The currents are converted to current densities, and interpolated to the centers of the QD cells.

9.1 QD cells

The magnetic longitudes and the heights of QD cells in (ϕ, λ_q, r) coordinates, where λ_q is QD latitude, are identical with those of the elemental volumes defined in (ϕ, ρ, r) coordinates in Chapter 4. The grid spacing in magnetic longitude is uniform, with the value

$$\Delta\phi = \frac{2\pi}{I_{max}} \tag{9.2}$$

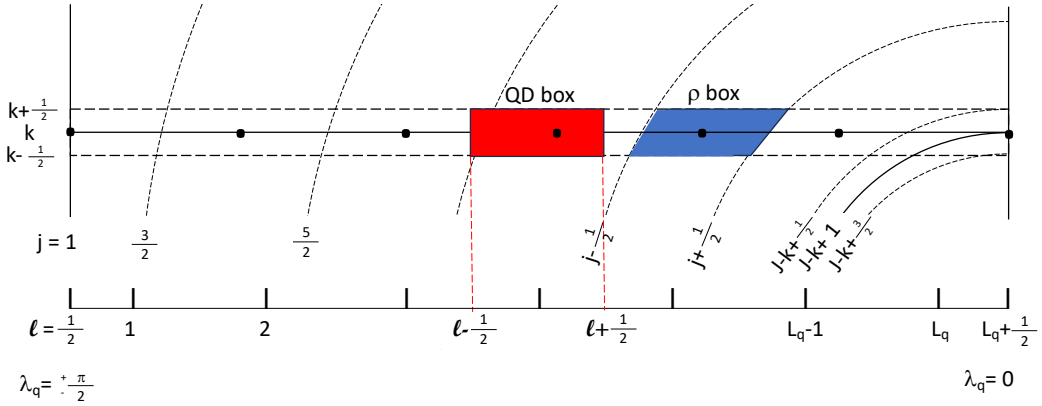

Figure 9.1: Schematic illustration of the west or east sides of an elemental volume in (ϕ, ρ, r) coordinates ("ρ" box) and of a QD cell ("QD box"). The horizontal strip at level k lies between $r = r_{k-\frac{1}{2}}$ and $r = r_{k+\frac{1}{2}}$. The black dots along it represent P points of the grid. The blue ρ box centered at $\rho = \rho_j$, $r = r_k$, is one element along the k strip, lying between two adjacent $S2$ geomagnetic field lines at $\rho = \rho_{j-\frac{1}{2}}$ and $\rho = \rho_{j+\frac{1}{2}}$. The red QD box centered at $\lambda_q = \lambda_{q\ell}$, of width $\Delta\lambda_q$, lies along the k strip between $\lambda_q = \lambda_{q(\ell-\frac{1}{2})}$ and $\lambda_q = \lambda_{q(\ell+\frac{1}{2})}$. ($\ell$ varies from $\frac{1}{2}$ at the pole to $L_q + \frac{1}{2}$ at the equator.) In general, the ρ and QD boxes have different latitude widths, and may overlap each other.

Figure 9.1 illustrates the sides of a QD cell (or "QD box") and of an elemental volume in (ϕ, ρ, r) coordinates (or "ρ box") on a surface of constant ϕ. The current remapping is done separately for each magnetic hemisphere. In QD coordinates ℓ is the latitude index for the

center of a QD cell, going from 1 for the cell closest to either the south or north magnetic pole to L_q for the cell next to the magnetic equator in that hemisphere. A layer centered at height h_k ($r = r_k$), lying between $r = r_{k-\frac{1}{2}}$ and $r = r_{k+\frac{1}{2}}$ is illustrated between the magnetic pole ($\lambda_q = \pm\frac{\pi}{2}$) and equator ($\lambda_q = 0$). Along this strip lie $(J - k)$ ρ boxes indexed by j, one of which is highlighted in blue, with polar edge at $\rho = \rho_{j-\frac{1}{2}}$ and equatorward edge at $\rho = \rho_{j+\frac{1}{2}}$. The QD boxes have equal widths in λ_q. One is highlighted in red, with polar edge at $\lambda_q = \lambda_{q(\ell-\frac{1}{2})}$ and equatorward edge at $\lambda_q = \lambda_{q(\ell+\frac{1}{2})}$. [In `subroutine remap_weights` (file `remap_wt.f90`) L_q is `nlat_qd_h-1` and $\lambda_{q(\ell-\frac{1}{2})}$ is `lat_qd_ed(l)`]. The pole has j index 1 but ℓ index $\frac{1}{2}$. The QD latitude increment is

$$\Delta\lambda_q = \frac{\pi}{2L_q} \tag{9.3}$$

The latitude edges of QD box ℓ have indices $\ell - \frac{1}{2}$ and $\ell + \frac{1}{2}$:

$$|\lambda_{q(\ell-\frac{1}{2})}| = \frac{\pi}{2} - (\ell - 1)\Delta\lambda_q \tag{9.4}$$

$$|\lambda_{q(\ell+\frac{1}{2})}| = \frac{\pi}{2} - \ell\Delta\lambda_q \tag{9.5}$$

9.2 Remapping eastward currents

Let $I_1^q(i - \frac{1}{2}, \ell, k)$ be the current flowing eastward across the QD box face at $\phi_m = \phi_{i-\frac{1}{2}}$:

$$I_1^q(i - \frac{1}{2}, \ell, k) = \int_{|\lambda_{q(\ell+\frac{1}{2})}|}^{|\lambda_{q(\ell-\frac{1}{2})}|} \int_{r_{k-\frac{1}{2}}}^{r_{k+\frac{1}{2}}} \mathbf{a}_{1q} \cdot \mathbf{J}\ dr\ d|\lambda_q| = \int_{|\lambda_{q(\ell+\frac{1}{2})}|}^{|\lambda_{q(\ell-\frac{1}{2})}|} \int_{r_{k-\frac{1}{2}}}^{r_{k+\frac{1}{2}}} \left(\frac{r}{R}\right)^{\frac{5}{2}} \frac{RJ_{e1}}{F}\ dr\ d|\lambda_q| \tag{9.6}$$

where (from R95)

$$\mathbf{a}_{1q} = \left(\frac{r}{R}\right)^{\frac{5}{2}} \frac{R\mathbf{d}_1}{F} \tag{9.7}$$

Assume $\left(\frac{r}{R}\right)^{\frac{5}{2}} \frac{RJ_{e1}}{F}$ is approximately constant over the area of integration, so that it can be taken outside the integrals in (9.6) and the resultant integrals can be readily solved. Then

$I_1^q(i-\frac{1}{2},\ell,k)$ can be expressed as

$$I_1^q(i-\frac{1}{2},\ell,k) = M_1^q(i-\frac{1}{2},\ell,k)J_{e1}^q(i-\frac{1}{2},\ell,k) \tag{9.8}$$

$$M_1^q(i-\frac{1}{2},\ell,k) = \left(\frac{r_k}{R}\right)^{\frac{5}{2}} \frac{R(r_{k+\frac{1}{2}}-r_{k-\frac{1}{2}})(|\lambda_{q(\ell-\frac{1}{2})}|-|\lambda_{q(\ell+\frac{1}{2})}|)}{F(i-\frac{1}{2},\ell,k)} \tag{9.9}$$

Note that $M_1^q \times F$ is independent of longitude index i. Similar to (5.14), define a normalized area factor $A_1^q(\ell+\frac{1}{2})$ representing the normalized area in layer k between the pole and $|\lambda_{q(\ell+\frac{1}{2})}|$:

$$A_1^q(\ell+\frac{1}{2}) = \frac{\pi}{2} - |\lambda_{q(\ell+\frac{1}{2})}| \tag{9.10}$$

[$A_1^q(\ell+\frac{1}{2})$ is the initial calculation of `a1q_upd(l)` in `subroutine remap_weights`. Later in that subroutine `a1q_upd(l)` is temporarily multiplied by $2/\pi$ for comparison with `a1`.] Then (9.9) can be rewritten as

$$M_1^q(i-\frac{1}{2},\ell,k) = \left(\frac{r_k}{R}\right)^{\frac{5}{2}} \frac{R(r_{k+\frac{1}{2}}-r_{k-\frac{1}{2}})[A_1^q(\ell+\frac{1}{2})-A_1^q(l-\frac{1}{2})]}{F(i-\frac{1}{2},\ell,k)} \tag{9.11}$$

Define a longitude-independent area factor Q_1 [calculated in `subroutine remap_weights`] as:

$$Q_1(\ell,k) = r_k(r_{k+\frac{1}{2}}-r_{k-\frac{1}{2}})[A_1^q(\ell+\frac{1}{2})-A_1^q(\ell-\frac{1}{2})] \tag{9.12}$$

Then

$$M_1^q(i-\frac{1}{2},\ell,k) = \left(\frac{r_k}{R}\right)^{\frac{3}{2}} \frac{Q_1(\ell,k)}{F(i-\frac{1}{2},\ell,k)} \tag{9.13}$$

In order to conserve current during remapping, we work with latitude- and height-integrated eastward currents in the layer, integrated from the pole to the edges of the ρ and QD boxes. The independent variable used for interpolation is the latitudinally integrated area of the layer, again integrated from the pole to the edges of the ρ and QD boxes. [Conceptually this independent variable is nearly the same as colatitude at the center of the layer, multiplied by $r_k(r_{k+\frac{1}{2}}-r_{k-\frac{1}{2}})$, but because the box edges are not perfectly straight lines we work with areas instead of colatitudes.] For interpolation we treat as equivalent independent variables the areas having either constant ρ or constant $|\lambda_q|$ as the equator-

ward integration limit. Normalized versions of these independent variables are A_1, defined in (5.14), and A_1^q, defined in (9.10). $A1$ goes from 0 at the pole to 1 at the equator, and is therefore to be compared with $2/\pi$ times A_1^q, which has a value of $\pi/2$ at the equator. Find interpolation indices $j_1(\ell, k)$ for $\ell > 1$ (in `subroutine remap_weights`) such that

$$A_1(j_1 + \frac{1}{2}, k) \le A_1^q(\ell + \frac{1}{2}) < A_1(j_1 + \frac{3}{2}, k) \tag{9.14}$$

The fractional distance of $A_1^q(\ell + \frac{1}{2})$ from $A_1(j_1 + \frac{1}{2}, k)$ toward $A_1(j_1 + \frac{3}{2}, k)$ is

$$x_1(\ell, k) = \frac{A_1^q(\ell + \frac{1}{2}) - A_1(j_1 + \frac{1}{2}, k)}{A_1(j_1 + \frac{3}{2}, k) - A_1(j_1 + \frac{1}{2}, k)} \tag{9.15}$$

In ρ coordinates, the latitude- and height-integrated eastward current from the pole ($\rho = 0$) to $\rho_{j+\frac{1}{2}}$ and between $r_{k-\frac{1}{2}}$ and $r_{k+\frac{1}{2}}$ at longitude $\phi_{i-\frac{1}{2}}$ is

$$L_1(i - \frac{1}{2}, j + \frac{1}{2}, k) = \begin{cases} 0 & \text{if} \quad j = -1 \\ \sum_{j'=1}^{j} I_1(i - \frac{1}{2}, j', k) & \text{if} \quad 1 \le j \le J - k + 1 \end{cases} \tag{9.16}$$

where I_1 comes from (6.10) or (6.15). In QD coordinates, the latitude- and height-integrated eastward current from the pole to $|\lambda_{q(\ell+\frac{1}{2})}|$ and between $r_{k-\frac{1}{2}}$ and $r_{k+\frac{1}{2}}$ at longitude $\phi_{i-\frac{1}{2}}$, called $L_1^q(i - \frac{1}{2}, \ell + \frac{1}{2}, k)$, is obtained by interpolation of L_1. At the pole ($\ell = 0$) set

$$L_1^q(i - \frac{1}{2}, \frac{1}{2}, k) = 0 \tag{9.17}$$

Near the pole [if $A_1^q(\ell + \frac{1}{2}) < A_1(\frac{5}{2}, k)$] the interpolation is linear:

$$L_1^q(i - \frac{1}{2}, \ell + \frac{1}{2}, k) = w_1(\ell, k, 2) L_1(i - \frac{1}{2}, j_1 + \frac{1}{2}, k) + w_1(\ell, k, 3) L_1(i - \frac{1}{2}, j_1 + \frac{3}{2}, k) \tag{9.18}$$

$$w_1(\ell, k, 2) = 1 - x_1(\ell, k) \tag{9.19}$$

$$w_1(\ell, k, 3) = x_1(\ell, k) \tag{9.20}$$

It was found that linear interpolation can sometimes produce undesirably coarse results, and

so at latitudes farther from the pole we use cubic-spline interpolation:

$$L_1^q(i-\frac{1}{2},\ell+\frac{1}{2},k)=\sum_{n=1}^{4}w_1(\ell,k,n)L_1(i-\frac{1}{2},j_1-\frac{3}{2}+n,k) \tag{9.21}$$

where the weights $w_1(\ell,k,n)$ are found by fitting a third-order polynomial through a function at the four points $x_1=-1,\ 0,\ 1,\ 2$, which gives:

$$w_1(\ell,k,1)=-x_1/3+x_1^2/2-x_1^3/6 \tag{9.22}$$

$$w_1(\ell,k,2)=1-x_1/2-x_1^2+x_1^3/2 \tag{9.23}$$

$$w_1(\ell,k,3)=x_1+x_1^2/2-x_1^3/2 \tag{9.24}$$

$$w_1(\ell,k,4)=-x_1/6+x_1^3/6 \tag{9.25}$$

Once the values of L_1^q are found, the eastward current through the side face of a QD cell is found by differencing:

$$I_1^q(i-\frac{1}{2},\ell,k)=L_1^q(i-\frac{1}{2},\ell+\frac{1}{2},k)-L_1^q(i-\frac{1}{2},\ell-\frac{1}{2},k) \tag{9.26}$$

9.3 Remapping vertical currents

The remapping of vertical currents uses integrated currents over horizontal surface slices between $\phi_{i-\frac{1}{2}}$ and $\phi_{i+\frac{1}{2}}$ from the pole to a particular magnetic latitude. The independent variable for interpolation is simply ρ instead of an integrated area, because the equatorward boundaries of elements for both the (ϕ,ρ,r) and (ϕ,λ_q,r) coordinate systems are lines of constant ρ. Let $I_3^q(i,\ell,k-\frac{1}{2})$ be the current flowing upward across the bottom of the QD cell at height $h_{k-\frac{1}{2}}$ $(r=r_{k-\frac{1}{2}})$:

$$I_3^q(i,\ell,k-\frac{1}{2})=\int_{|\lambda_{q(\ell+\frac{1}{2})}|}^{|\lambda_{q(\ell-\frac{1}{2})}|}\Delta\phi\mathbf{a}_{q3}\cdot\mathbf{J}\ d|\lambda_q|=r_{k-\frac{1}{2}}^2\Delta\phi\int_{|\lambda_{q(\ell+\frac{1}{2})}|}^{|\lambda_{q(\ell-\frac{1}{2})}|}\frac{\cos\lambda_q J_r}{F}\ d|\lambda_q| \tag{9.27}$$

where (from R95)

$$\mathbf{a}_{3q} = \frac{r^2 \cos\lambda_q \mathbf{k}}{F} \tag{9.28}$$

If J_r/F is assumed to vary little over the surface, so that is can be taken outside the integral in (9.27), then (9.27) can be rewritten as

$$I_3^q(i,\ell,k-\frac{1}{2}) = M_3^q(i,\ell,k-\frac{1}{2}) J_r(i,\ell,k-\frac{1}{2}) \tag{9.29}$$

$$M_3^q(i,\ell,k-\frac{1}{2}) = \frac{r^2_{k-\frac{1}{2}} \Delta\phi(\sin|\lambda_{q(\ell-\frac{1}{2})}| - \sin|\lambda_{q(\ell+\frac{1}{2})}|)}{F(i,\ell,k-\frac{1}{2})} \tag{9.30}$$

Define a normalized area factor $A_3^q(\ell+\frac{1}{2})$ representing the normalized area between the pole and the poleward edge of a QD box, $|\lambda_{q(\ell+\frac{1}{2})}|$:

$$A_3^q(\ell+\frac{1}{2}) = 1 - \sin|\lambda_{q(\ell+\frac{1}{2})}| \tag{9.31}$$

[$A_3^q(\ell+\frac{1}{2})$ is `a3q_upd(l)` in `subroutine remap_weights`.] Then (9.30) can be rewritten as

$$M_3^q(i,\ell,k-\frac{1}{2}) = \frac{r^2_{k-\frac{1}{2}} \Delta\phi[A_3^q(\ell+\frac{1}{2}) - A_3^q(\ell-\frac{1}{2})]}{F(i,\ell,k-\frac{1}{2})} \tag{9.32}$$

[$M_3^q(i,\ell,k-\frac{1}{2})$ is calculated in `subroutine apxparm` (file `get_apex.f90`) as `qd(i,j)%M3q(k)` with ℓ represented by `j`.] Note that $M_3^q F$ is independent of longitude. Define a longitude-independent area factor Q_3 [calculated in `subroutine remap_weights`] as:

$$Q_3(\ell,k-\frac{1}{2}) = r^2_{k-\frac{1}{2}} \Delta\phi[A_3^q(\ell+\frac{1}{2}) - A_3^q(\ell-\frac{1}{2})] \tag{9.33}$$

Then

$$M_3^q(i,\ell,k-\frac{1}{2}) = \frac{Q_3(\ell,k-\frac{1}{2})}{F(i,\ell,k-\frac{1}{2})} \tag{9.34}$$

In order to conserve current during remapping, we work with integrals of upward current. Define $\rho^q(\ell+\frac{1}{2},k-\frac{1}{2})$ as the value of ρ at the equatorward edge of the bottom of the QD

cell, equal to

$$\rho^q(\ell+\frac{1}{2},k-\frac{1}{2}) = \left(\frac{R}{r_{k-\frac{1}{2}}}\right)^{\frac{1}{2}} \cos\lambda_{q(\ell+\frac{1}{2})} \tag{9.35}$$

Find interpolation indices $j_3(\ell,k)$ for $\ell > 1$ such that

$$\rho_{(j_3+\frac{1}{2})} \le \rho^q(\ell+\frac{1}{2},k-\frac{1}{2}) < \rho_{(j_3+\frac{3}{2})} \tag{9.36}$$

The fractional distance of $\rho^q(\ell+\frac{1}{2},k-\frac{1}{2})$ from $\rho_{(j_3+\frac{1}{2})}$ toward $\rho_{(j_3+\frac{3}{2})}$ is

$$x_3(\ell,k) = \frac{\rho^q(\ell+\frac{1}{2},k-\frac{1}{2}) - \rho_{(j_3+\frac{1}{2})}}{\rho_{(j_3+\frac{3}{2})} - \rho_{(j_3+\frac{1}{2})}} \tag{9.37}$$

In ρ coordinates, the latitude- and longitude-integrated upward current between $\phi_{i-\frac{1}{2}}$ and $\phi_{i+\frac{1}{2}}$ from the pole to $\rho_{j+\frac{1}{2}}$ at radius $r_{k-\frac{1}{2}}$ is

$$L_3(i,j+\frac{1}{2},k-\frac{1}{2}) = \begin{cases} 0 & \text{if} \quad j=0 \\ \sum_{j'=1}^{j} I_3(i,j',k-\frac{1}{2}) & \text{if} \quad 1 \le j \le J-k+1 \end{cases} \tag{9.38}$$

where I_3 comes from (9.1). In QD coordinates, the latitude- and longitude-integrated upward current from the pole to $|\lambda_{q(\ell+\frac{1}{2})}|$ for $1 \le \ell \le L_q$ and between $\phi_{i-\frac{1}{2}}$ and $\phi_{i+\frac{1}{2}}$ at radius $r_{k-\frac{1}{2}}$, called $L_3^q(i,\ell+\frac{1}{2},k-\frac{1}{2})$ [`L3_qd(i,l+1,k)` in `subroutine calc_Iqd`], is obtained by interpolation of L_3. At the pole ($\ell = 0$) set

$$L_3^q(i,\frac{1}{2},k-\frac{1}{2}) = 0 \tag{9.39}$$

Near the pole [if $\rho^q(\ell+\frac{1}{2},k-\frac{1}{2}) < \rho_{\frac{5}{2}}$] L_3^q tends to vary with ρ^q roughly as A_3^q, which increases parabolically with ρ^q from a value of 0 at the pole. In this region L_3^q is considered to vary as

$$L_3^q = a(\rho^q)^2 + b(\rho^q)^3 \tag{9.40}$$

By requiring this formula for L_3^q to match the values of L_3 at $\rho^q = \rho_{\frac{3}{2}}$ and at $\rho^q = \rho_{\frac{5}{2}}$, where

$\rho_{\frac{5}{2}} = 3\rho_{\frac{3}{2}}$, we find

$$a = \left[\frac{3}{2}L_3(i, \frac{3}{2}, k-\frac{1}{2}) - \frac{1}{18}L_3(i, \frac{5}{2}, k-\frac{1}{2})\right]/\rho^2_{\frac{3}{2}} \tag{9.41}$$

$$b = \left[-\frac{1}{2}L_3(i, \frac{3}{2}, k-\frac{1}{2}) + \frac{1}{18}L_3(i, \frac{5}{2}, k-\frac{1}{2})\right]/\rho^2_{\frac{3}{2}} \tag{9.42}$$

By combining (9.37) with (9.40)-(9.42) and using $\rho_{\frac{5}{2}} = 3\rho_{\frac{3}{2}}$, we find

$$L^q_3(i, \ell+\frac{1}{2}, k-\frac{1}{2}) = w_3(\ell, k-\frac{1}{2}, 2)L_3(i, \frac{3}{2}, k-\frac{1}{2}) + w_3(\ell, k-\frac{1}{2}, 3)L_3(i, \frac{5}{2}, k-\frac{1}{2}) \tag{9.43}$$

$$w_3(\ell, k-\frac{1}{2}, 2) = -4x_3^3 + 3x_3 + 1 \tag{9.44}$$

$$w_3(\ell, k-\frac{1}{2}, 3) = \frac{4}{9}x_3^3 + \frac{4}{9}x_3^2 + \frac{1}{9}x_3 \tag{9.45}$$

At lower latitudes [if $\rho^q(\ell+\frac{1}{2}, k-\frac{1}{2}) \geq \rho_{\frac{5}{2}}$] cubic-spline interpolation is used, similar to the interpolation for Ł^q_1:

$$L^q_3(i, \ell+\frac{1}{2}, k-\frac{1}{2}) = \sum_{n=1}^{4} w_3(\ell, k-\frac{1}{2}, n)L_3(i, j_1-\frac{3}{2}+n, k-\frac{1}{2}) \tag{9.46}$$

$$w_3(\ell, k-\frac{1}{2}, 1) = -x_3/3 + x_3^2/2 - x_3^3/6 \tag{9.47}$$

$$w_3(\ell, k-\frac{1}{2}, 2) = 1 - x_3/2 - x_3^2 + x_3^3/2 \tag{9.48}$$

$$w_3(\ell, k-\frac{1}{2}, 3) = x_3 + x_3^2/2 - x_3^3/2 \tag{9.49}$$

$$w_3(\ell, k-\frac{1}{2}, 4) = -x_3/6 + x_3^3/6 \tag{9.50}$$

The upward current through the bottom of a QD box with central indices i, ℓ, k is

$$I^q_3(i, \ell, k-\frac{1}{2}) = L^q_3(i, \ell+\frac{1}{2}, k-\frac{1}{2}) - L^q_1(i, \ell-\frac{1}{2}, k-\frac{1}{2}) \tag{9.51}$$

9.4 Calculating northward elemental currents

The northward QD current I_2^q is obtained from current continuity for $1 \leq \ell \leq L_q$ as

$$I_2^q(i,\ell+\frac{1}{2},k) = \pm[L_1^q(i-\frac{1}{2},\ell+\frac{1}{2},k) - L_1^q(i+\frac{1}{2},\ell+\frac{1}{2},k) + L_3^q(i,\ell+\frac{1}{2},k-\frac{1}{2}) - L_3^q(i,\ell+\frac{1}{2},k+\frac{1}{2})] \tag{9.52}$$

where the upper/lower sign is for the northern/southern hemisphere, and for $\ell = 0$ as

$$I_2^q(i,\frac{1}{2},k) = 0 \tag{9.53}$$

Define a longitude-independent area factor Q_2 [calculated in `subroutine remap_weights`] as:

$$Q_2(\ell-\frac{1}{2},k) = r_k(r_{k+\frac{1}{2}} - r_{k-\frac{1}{2}})\Delta\phi \ \cos(\lambda_{q(\ell-\frac{1}{2})}) \tag{9.54}$$

Then we can express the area factor M_2^q for the QD elemental volumes as

$$M_2^q(i,\ell-\frac{1}{2},k) = Q_2(\ell-\frac{1}{2},k) \tag{9.55}$$

Since $I_2^q(i,L_q+\frac{1}{2},k)$ and $\mp I_3(i,J-k+1,k)$ both represent the amount of northward current crossing the magnetic equator in longitude increment i and height layer k, they should have the same value. This condition can be a check on the calculations.

9.5 Calculating current densities

In Chapter 3 the current density $\mathbf{J}$ was expressed in terms of the $\mathbf{e}'_1,\ \mathbf{e}'_2,\ \mathbf{e}'_3$ base vectors. Having now converted our current elements to QD coordinates, we can express the current density in terms of QD base vectors $\mathbf{f}_1,\ \mathbf{f}_2,\ \mathbf{f}_3$, as defined by R95:

$$\mathbf{J} = J_{f1}\mathbf{f}_1 + J_{f2}\mathbf{f}_2 + J_{f3}\mathbf{f}_3 \tag{9.56}$$

$$J_{fn} = \mathbf{g}_n \cdot \mathbf{J}, \qquad n = 1, 2, 3 \tag{9.57}$$

where $\mathbf{g}_1,\ \mathbf{g}_2,\ \mathbf{g}_3$ are the complementary QD base vectors defined by R95. Since $\mathbf{g}_3 = F\mathbf{k}$, where $\mathbf{k}$ is a unit radial vector and F is a scale factor not too different from 1,

$$J_{f3} = F J_r \tag{9.58}$$

The vectors $\mathbf{f}_1,\ \mathbf{f}_2,\ \mathbf{g}_1,\ \mathbf{g}_2$ are available numerically from the Magnetic Apex software. To calculate $\mathbf{J}$ we need the current density components $J_{f1},\ J_{f2},\ J_r$ at common locations, whereas we have so far determined $I_1^q,\ I_2^q,\ I_3^q$ at different faces of the QD volume elements. Let us first calculate $J_{f1},\ J_{f2},\ J_r$ from $I_1^q,\ I_2^q,\ I_3^q$ at those different faces, and then interpolate them to common points on a geographic grid.

For eastward currents, note that J_{f1} is directly related to J_{e1}:

$$J_{f1} = \mathbf{g}_1 \cdot \mathbf{J} = \left(\frac{r}{R}\right)^{\frac{3}{2}} \frac{\mathbf{d}_1 \cdot \mathbf{J}}{F} = \left(\frac{r}{R}\right)^{\frac{3}{2}} \frac{J_{e1}}{F} \tag{9.59}$$

The value of J_{f1} at location $(\phi_{i-\frac{1}{2}}, \lambda_{q\ell}, r_k)$ is obtained by equating J_{e1}^q in (9.8) with J_{e1} in (9.59), noting that the superscript q on J_{e1}^q simply denotes that the indices refer to QD coordinates (ϕ_q, λ_q, r) instead of coordinates (ϕ_m, ρ, r) (only the second coordinate differs here, since $\phi_q = \phi_m$):

$$J_{f1}(i - \frac{1}{2}, \ell, k) = \left(\frac{r_k}{R}\right)^{\frac{3}{2}} \frac{I_1^q(i - \frac{1}{2}, \ell, k)}{F(i - \frac{1}{2}, \ell, k) M_1^q(i - \frac{1}{2}, \ell, k)} = \frac{I_1^q(i - \frac{1}{2}, \ell, k)}{Q_1(\ell, k)} \tag{9.60}$$

where Q_1 is given by (9.12).

For northward currents, note that I_2^q is related to J_{f2}:

$$I_2^q(i, \ell - \frac{1}{2}, k) = \int_{\phi_{i-\frac{1}{2}}}^{\phi_{i+\frac{1}{2}}} \int_{r_{k-\frac{1}{2}}}^{r_{k+\frac{1}{2}}} \mathbf{a}_{2q} \cdot \mathbf{J}\ dr\ d\phi_m = \int_{\phi_{i-\frac{1}{2}}}^{\phi_{i+\frac{1}{2}}} \int_{r_{k-\frac{1}{2}}}^{r_{k+\frac{1}{2}}} r \cos\lambda_q\ J_{f2}\ dr\ d\phi_m \tag{9.61}$$

If J_{f2} is assumed approximately constant over the integration area, then

$$I_2^q(i, \ell - \frac{1}{2}, k) \quad = \quad \Delta\phi \cos\lambda_{q\ell-\frac{1}{2}} r_k (r_{k+\frac{1}{2}} - r_{k-\frac{1}{2}}) J_{f2}(i, \ell - \frac{1}{2}, k)$$

$$= \quad Q_2^q(\ell - \frac{1}{2}, k) J_{f2}(i, \ell - \frac{1}{2}, k) \tag{9.62}$$

where Q_2 is given by (9.54). Then

$$J_{f2}(i, \ell - \frac{1}{2}, k) = \frac{I_2^q(i, \ell - \frac{1}{2}, k)}{Q_2(\ell - \frac{1}{2}, k)} \tag{9.63}$$

For upward currents, (9.29) gives

$$J_r(i, \ell, k - \frac{1}{2}) = \frac{I_3^q(i, \ell, k - \frac{1}{2})}{M_3^q(i, \ell, k - \frac{1}{2})} \tag{9.64}$$

where $M_3^q(i, \ell, k - \frac{1}{2})$ comes from (9.32).

The vector current density **J** at the center of a QD elemental volume can be obtained from (9.56) and (9.58) if J_{f1} from (9.60), J_{f2} from (9.63), and J_r from (9.64) are averaged between the respective QD elemental volume sides to the center.

Chapter 10

Magnetic effects of currents above the top of the model

10.1 Introduction

Our calculation of magnetic perturbations utilizes the well-developed techniques of spherical harmonic analysis for an assumed spherical Earth. The errors introduced by neglecting Earth's oblateness are expected to be small in comparison with errors associated with other approximations and simplifications that are made, such as the neglect of currents flowing perpendicular to geomagnetic-field lines above the top of the model (e.g., ring current, tail current, magnetopause current), dipolar geometry for field-aligned currents above the top of the model, and simplifications in the calculation of currents induced in the Earth.

Physically meaningful magnetic perturbations can only be calculated from complete divergence-free current systems. Conceptually, we construct two complete current systems by imagining that two oppositely directed divergent, curl-free current sheets lie on a spherical shell at height

$$h_{\text{top}} = h_{k^{\text{top}}+\frac{1}{2}} \tag{10.1}$$

where

$$1 < k^{\text{top}} \leq K \tag{10.2}$$

That is, these imaginary current sheets lie at or below the top of the model and above the base of the model, nominally including at least most of the current flowing perpendicular to $\mathbf{B}_0$. One of these current sheets connects to the radial current below, while the other oppositely directed current sheet connects to the radial component of field-aligned current above h_{top}. Both the lower and upper current systems are divergence-free in three dimensions, and can thus be handled separately when calculating magnetic perturbations. Our algorithm calculates toroidal magnetic perturbations from the radial component of current density and poloidal magnetic perturbations from the toroidal (horizontal divergence-free) component of current density, and is not affected by any horizontal curl-free currents, so the imaginary current sheets contribute nothing to the magnetic perturbations.

Magnetic perturbations associated with field-aligned currents flowing above h_{top} are calculated using the formalism of Richmond (1974), which assumes a dipolar geometry for these currents and performs a spherical harmonic analysis of the toroidal component of current density. We extend Richmond's (1974) formalism to include hemispherically symmetric field-aligned currents that flow from h_{top} out to the dipolar field-line apex, and then flow radially to infinity with no toroidal component.

Since geomagnetic-field lines are not exactly dipolar, Richmond's (1974) formalism is inaccurate. However, two considerations partly mitigate errors introduced by the assumption of purely dipolar field-aligned currents above h_{top}. First, h_{top} can be chosen to lie considerably above ($\sim$ 1000 km) Earth's surface, where the non-dipolar distortions of the main geomagnetic field are weaker than at lower altitudes. Second, the magnetic perturbations are represented by an equivalent current sheet at h_{top} that is organized with respect to QD coordinates, and at any location on this equivalent current sheet the calculated equivalent current is most strongly influenced by nearby field-aligned currents that are fairly well organized with respect to QD coordinates, so that the pattern of computed equivalent current has a tendency to be organized appropriately over the equivalent current shell.

10.2 Spherical harmonics

For spherical-harmonic calculations with respect to colatitude θ and east longitude ϕ we use the fully normalized real spherical harmonics Y_n^m as described in Richmond (1974):

$$Y_n^m(\theta,\phi) = \frac{1}{\sqrt{4\pi}} P_n^m(\cos\theta) f_m(\phi) \tag{10.3}$$

$$f_m(\phi) = \begin{cases} \sqrt{2}\sin(m\phi) & \text{if} \quad m > 0 \\ 1 & \text{if} \quad m = 0 \\ \sqrt{2}\cos(m\phi) & \text{if} \quad m < 0 \end{cases} \tag{10.4}$$

$$P_0^0(\cos\theta) = 1 \tag{10.5}$$

$$P_m^m(\cos\theta) = \sqrt{\frac{2m+1}{2m}}\sin\theta P_{m-1}^{m-1}(\cos\theta) = \frac{\sqrt{(2m+1)!}}{2^m m!}\sin^m\theta \tag{10.6}$$

$$P_n^m(\cos\theta) = [\cos\theta P_{n-1}^m(\cos\theta) - R_{n-1}^m P_{n-2}^m(\cos\theta)]/R_n^m, \qquad n > m \geq 0 \tag{10.7}$$

$$R_n^m = \sqrt{\frac{n^2-m^2}{4n^2-1}} \tag{10.8}$$

$$P_n^{-m}(\cos\theta) = P_n^m(\cos\theta) \tag{10.9}$$

By using the real functions $f_m(\phi)$ given by (10.4) we can avoid the need for complex functions like $\exp(\pm im\phi)$. The associated Legendre polynomials P_n^m can be generated recursively using (10.5)-(10.9). Both f_m and P_n^m have root-mean-square values of 1 over the sphere, so Y_n^m has a root-mean-square value of $1/\sqrt{4\pi}$. The derivative of P_n^m with respect to θ is

$$\frac{dP_n^m(\cos\theta)}{d\theta} = n\cos\theta\frac{P_n^m(\cos\theta)}{\sin\theta} - (2n+1)R_n^m\frac{P_{n-1}^m(\cos\theta)}{\sin\theta}, \qquad n \geq m \geq 0 \tag{10.10}$$

The horizontal derivatives of Y_n^m are

$$\frac{\partial Y_n^m(\theta,\phi)}{\partial\theta} = \frac{1}{\sqrt{4\pi}}\frac{dP_n^m(\cos\theta)}{d\theta} f_m(\phi) \tag{10.11}$$

$$\frac{\partial Y_n^m(\theta,\phi)}{\partial\phi} = \frac{m}{\sqrt{4\pi}} P_n^m(\cos\theta) f_{-m}(\phi) \tag{10.12}$$

The spherical harmonics Y_n^m are orthonormal when integrated over the sphere:

$$\int Y_n^m Y_{n'}^{m'} \, d\Omega = \begin{cases} 1 & \text{if} \quad m = m' \text{ and } n = n' \\ 0 & \text{if} \quad m \neq m' \text{ or } n \neq n' \end{cases} \tag{10.13}$$

where $d\Omega$ is an element of solid angle. Vector spherical harmonics derived from the Y_n^ms are orthogonal over a sphere of radius r:

$$\int \nabla Y_n^m \cdot \nabla Y_{n'}^{m'} \, da = \begin{cases} n(n+1) & \text{if} \quad m = m' \text{ and } n = n' \\ 0 & \text{if} \quad m \neq m' \text{ or } n \neq n' \end{cases} \tag{10.14}$$

$$\int (\mathbf{k} \times \nabla Y_n^m) \cdot (\mathbf{k} \times \nabla Y_{n'}^{m'}) \, da = \begin{cases} n(n+1) & \text{if} \quad m = m' \text{ and } n = n' \\ 0 & \text{if} \quad m \neq m' \text{ or } n \neq n' \end{cases} \tag{10.15}$$

where an element of area da equals $r^2 d\Omega$. We will also make use of the fact that

$$\int (\mathbf{k} \times \nabla \psi) \cdot \nabla \xi \, da = 0 \tag{10.16}$$

for any well-behaved functions ψ and ξ.

10.3 Equivalent current function of field-aligned currents above h_{top}

The height-integrated equivalent current density $\mathbf{K}_{\text{FAC}}^{\text{equiv}}$ in the shell at the model top ($h = h_{\text{top}}$, $r = r_{\text{top}} \equiv R_E + h_{\text{top}}$) is

$$\mathbf{K}_{\text{FAC}}^{\text{equiv}} = \mathbf{k} \times \nabla \eta_{\text{FAC}} \tag{10.17}$$

The equivalent current function η_{FAC} is expanded in a spherical harmonic series as

$$\eta_{\text{FAC}}(\theta_q, \phi_q) = \sum_{n=1}^{n_{\max}} \sum_{m=-n}^{n} c_n^m \, Y_n^m(\theta_q, \phi_q) \tag{10.18}$$

where θ_q is QD colatitude, ϕ_q is QD longitude, and c_n^m is a spherical-harmonic coefficient.

Equations (27), (28), and (30) of Richmond (1974) yield the following expression for the coefficients c_n^m in (10.18):

$$c_n^m = \frac{-r_{\text{top}}^2}{n(n+1)\sqrt{4\pi}} \int_0^{2\pi} \int_0^{\pi} Q_n^m(\theta_q) f_{-m}(\phi_q)\ J_r\ \sin\theta_q\ d\theta_q\ d\phi_q \tag{10.19}$$

$$Q_n^m(\theta) = m \sin^{2n}\theta \int_\theta^{\pi/2} \frac{P_n^m(\cos\theta')}{\sin^{2n+1}\theta'} d\theta' \tag{10.20}$$

10.4 Compute Q_n^m

By expressing $P_n^m(\cos\theta)$ either as a power series in $\sin\theta$ (if $n-m$ is an even number) or as $\cos\theta$ times a power series in $\sin\theta$ (if $n-m$ is an odd number) we can obtain analytical expressions for the Q_n^m functions.

1. $n-m$ **even** $(n \geq m)$

$$P_n^m(\cos\theta) = \sin^m\theta \sum_{p=0,2}^{n-m} a_{nmp} \sin^p\theta \tag{10.21}$$

To determine the coefficients a_{nmp} we first create a recursion relation for P_n^m in terms of P_{n-2}^m and P_{n-4}^m using (10.7) twice:

$$\begin{aligned} P_n^m &= \frac{1}{R_n^m}\left\{\frac{\cos\theta}{R_{n-1}^m}\left[\cos\theta P_{n-2}^m - R_{n-2}^m P_{n-3}^m\right] - R_{n-1}^m P_{n-2}^m\right\} \\ &= \frac{1}{R_n^m}\left\{\left[\frac{(1-\sin^2\theta)}{R_{n-1}^m} - R_{n-1}^m\right] P_{n-2}^m - \frac{R_{n-2}^m}{R_{n-1}^m}\left[R_{n-2}^m P_{n-2}^m + R_{n-3}^m P_{n-4}^m\right]\right\} \\ &= \frac{1}{R_n^m R_{n-1}^m}\left[(1 - R_{n-1}^{m2} - R_{n-2}^{m2} - \sin^2\theta) P_{n-2}^m - R_{n-2}^m R_{n-3}^m P_{n-4}^m\right] \end{aligned} \tag{10.22}$$

If $n = m$ only one coefficient of the series in (10.21) is non-zero, for $p = 0$:

$$P_m^m = a_{mm0} \sin^m\theta \tag{10.23}$$

Comparison with (10.6) shows that

$$a_{mm0} = \frac{\sqrt{(2m+1)!}}{2^m m!} \tag{10.24}$$

We can derive a recursion relation for other coefficients a_{nmp} by using (10.21) in (10.22) to obtain

$$\begin{aligned} \sin^m\theta \sum_{p=0,2}^{n-m} a_{nmp} \sin^p\theta &= \frac{1}{R_n^m R_{n-1}^m}\left[(1 - R_{n-1}^{m2} - R_{n-2}^{m2} - \sin^2\theta)\sin^m\theta \sum_{p=0,2}^{n-m-2} a_{(n-2)mp}\sin^p\theta \right. \\ &- \left. R_{n-2}^m R_{n-3}^m \sin^m\theta \sum_{p=0,2}^{n-m-4} a_{(n-4)mp}\sin^p\theta\right] \end{aligned} \tag{10.25}$$

If we define

$$a_{nmp} = 0, \quad p > n - m \tag{10.26}$$

then we can equate the coefficients of the same powers of $\sin\theta$ to obtain the recursion relation

$$a_{nmp} = \frac{1}{R_n^m R_{n-1}^m}\left[(1 - R_{n-1}^{m2} - R_{n-2}^{m2})a_{(n-2)mp} - a_{(n-2)m(p-2)} - R_{n-2}^m R_{n-3}^m a_{(n-4)mp}\right], \tag{10.27}$$

$$p = 0,\ 2,\ \ldots\ n - m \tag{10.28}$$

For a given m the a_{nmp} values are generated recursively from (10.27) by stepping through the p values in increments of 2, first for $n = m + 2$, then for $n = m + 4$, and so on, up to the maximum value of n.

Equation (10.20) becomes

$$Q_n^m(\theta) = m\sin^{2n}\theta \sum_{p=0,2}^{n-m} a_{nmp} \int_\theta^{\pi/2} \frac{d\theta'}{\sin^{2n-m-p+1}\theta'} \tag{10.29}$$

We can use the following look-up formulas to evaluate the integrals in (10.29):

$$\int \frac{d\theta}{\sin\theta} = \ln\tan\frac{\theta}{2} \tag{10.30}$$

$$\int \frac{d\theta}{\sin^2\theta} = -\frac{\cos\theta}{\sin\theta} \tag{10.31}$$

$$\int \frac{d\theta}{\sin^\ell\theta} = \frac{-\cos\theta}{(\ell-1)\sin^{\ell-1}\theta} + \frac{\ell-2}{\ell-1}\int \frac{d\theta}{\sin^{\ell-2}\theta}, \quad \ell \geq 2 \tag{10.32}$$

Repeated iteration of (10.32) to reduce the power of $\sin\theta$ in the denominator of the integrand ends with a power of either 1 or 2, for which the integral can be evaluated using (10.30) or (10.31). Taking this into consideration, we can note that the functions on the right-hand sides of (10.30)-(10.32) all go to 0 for $\theta = \pi/2$, which is the upper limit of the integrals in (10.29).

If m is even then $(2n-m-p+1)$ is odd, since p is always even in (10.29), and repeated application of (10.32) gives

$$\begin{aligned}\int_\theta^{\pi/2} \frac{d\theta'}{\sin^{2n-m-p+1}\theta'} &= \frac{\cos\theta}{2n-m-p}\left[\frac{1}{\sin^{2n-m-p}\theta}\right. \\ &+ \left.\sum_{k=1}^{n-1-\frac{m}{2}-\frac{p}{2}} \frac{(2n-m-p-1)(2n-m-p-3)\cdots(2n-m-p-2k+1)}{(2n-m-p-2)(2n-m-p-4)\cdots(2n-m-p-2k)\sin^{2n-m-p-2k}\theta}\right] \\ &- \frac{(2n-m-p-1)(2n-m-p-3)\cdots(1)}{(2n-m-p)(2n-m-p-2)\cdots(2)}\ln\tan\frac{\theta}{2}, \quad m \text{ even}\end{aligned} \tag{10.33}$$

If m is odd then $(2n-m-p+1)$ is even, since p is always even in (10.29), and repeated application of (10.32) gives

$$\begin{aligned}\int_\theta^{\pi/2} \frac{d\theta'}{\sin^{2n-m-p+1}\theta'} &= \frac{\cos\theta}{2n-m-p}\left[\frac{1}{\sin^{2n-m-p}\theta}\right. \\ &+ \left.\sum_{k=1}^{n-\frac{1}{2}-\frac{m}{2}-\frac{p}{2}} \frac{(2n-m-p-1)(2n-m-p-3)\cdots(2n-m-p-2k+1)}{(2n-m-p-2)(2n-m-p-4)\cdots(2n-m-p-2k)\sin^{2n-m-p-2k}\theta}\right], \\ &m \quad \text{odd}\end{aligned} \tag{10.34}$$

Q_n^m ($n-m$ even) is then calculated from (10.29) using the coefficients a_{nmp} and either (10.33) (m even) or (10.34) (m odd).

2. $n-m$ **odd** $(n>m)$

$$P_n^m(\cos\theta)=\cos\theta\sin^m\theta\sum_{p=0,2}^{n-m-1}a_{nmp}\sin^p\theta \tag{10.35}$$

(Note that the values of the subscripts for a_{nmp} are different in (10.21) and (10.35), so the same notation can be used in both equations without conflict.) If $n=m+1$ only one coefficient of the series in (10.35) is non-zero, for $p=0$:

$$P_{m+1}^m=a_{(m+1)m0}\cos\theta\sin^m\theta \tag{10.36}$$

For $n=m+1$ (10.7) and (10.6) give (noting that $R_m^m=0$):

$$P_{m+1}^m=\cos\theta P_m^m/R_{m+1}^m=\frac{\sqrt{(2m+1)!}}{2^m m!R_{m+1}^m}\cos\theta\sin^m\theta \tag{10.37}$$

Comparison with (10.36) shows that

$$a_{(m+1)m0}=\frac{\sqrt{(2m+1)!}}{2^m m!R_{m+1}^m} \tag{10.38}$$

We can derive a recursion relation for other coefficients a_{nmp} by using (10.35) in (10.22) to obtain

$$\begin{aligned}\cos\theta\sin^m\theta\sum_{p=0,2}^{n-m-1}a_{nmp}\sin^p\theta=&\\ \frac{1}{R_n^mR_{n-1}^m}\Bigg[&(1-R_{n-1}^{m2}-R_{n-2}^{m2}-\sin^2\theta)\cos\theta\sin^m\theta\sum_{p=0,2}^{n-m-3}a_{(n-2)mp}\sin^p\theta\\ &-R_{n-2}^mR_{n-3}^m\cos\theta\sin^m\theta\sum_{p=0,2}^{n-m-5}a_{(n-4)mp}\sin^p\theta\Bigg]\end{aligned} \tag{10.39}$$

If we define

$$a_{nmp}=0,\quad p>n-m-1 \tag{10.40}$$

then we can equate the coefficients of the same powers of $\sin\theta$ in (10.39) to obtain the identical recursion relation (10.27) as when $n-m$ is even. For a given m the a_{nmp} values

are generated recursively from (10.27) by stepping through the p values in increments of 2, first for $n = m+3$, then for $n = m+5$, and so on, up to the maximum value of n. Equation (10.20) becomes

$$\begin{aligned} Q_n^m(\theta) &= m\sin^{2n}\theta \sum_{p=0,2}^{n-m-1} a_{nmp} \int_\theta^{\pi/2} \frac{\cos\theta' d\theta'}{\sin^{2n-m-p+1}\theta'} \\ &= m\sin^{2n}\theta \sum_{p=0,2}^{n-m-1} a_{nmp} \left[\frac{-1}{(2n-m-p)\sin^{2n-m-p}}\theta \right]_\theta^{\pi/2} \\ &= m \sum_{p=0,2}^{n-m-1} a_{nmp} \left[\frac{\sin^{m+p}\theta - \sin^{2n}\theta}{2n-m-p} \right], \quad n-m \text{ odd} \end{aligned} \tag{10.41}$$

which is much simpler than the formulas for Q_n^m when $n-m$ is even.

Chapter 11

Map currents to geographic grid

We use the SPHEREPACK 3.2 code package to perform scalar and vector spherical-harmonic analysis of the currents and magnetic perturbations. This code assumes a perfect sphere with regular grid points equally spaced in geographic longitude, which facilitates fast-Fourier transforms with respect to longitude. Our geographic grid has `nggjlon` evenly spaced longitudes, from 0° to 360°$(1 - 1/$`nggjlon`$)$. In the latitude direction, SPHEREPACK 3.2 has the option of conducting Gaussian quadrature if the input values are provided at Gauss points, which is the choice we make. Our geographic grid has an even number `nggjlat` of Gauss points between (but not including) the geographic South and North Poles. Current components are in geographic directions. (It would be possible to relax the requirements of having the currents transferred to a geographic grid and expressed in geographic directions, but that is not the approach we have taken.) This chapter explains how the current densities obtained at the sides of QD elemental volumes are interpolated to a regular geographic grid, where they are then converted to current densities in geographic directions.

11.1 Grouping current layers to reduce computations

Calculating magnetic perturbations from a three-dimensional current distribution is computationally expensive. To reduce the amount of computation needed, the code offers the possibility of reducing the number of currrent layers by summing subsets of the original high-resolution layers into fewer thick layers. This should reduce the accuracy of computed magnetic perturbations only slightly in regions distant from the thick layers where magnetic observations are usually made: at the ground and at low-Earth-orbit altitudes above about 300 km. For example, 80-150 km currents could all be placed at 110 km. This lowest layer probably needs higher resolution in λ_q than higher layers because it is where the electrojets lie, so different $\Delta\lambda_q$s could be used in different layers. Currently, our algorithm uses the same latitude resolution for all layers.

The selection of which thin layers to group into thick layers is made in `module params_module` and `subroutine gen_ggj_grid`. Let k_g be the height index of a thick layer, with $1 \leq k_g \leq k_g^{\max}$. (Subscript g signifies "geographic", since the thick layers are created for use on the geographic grid. In `subroutine calc_Iqd` $k_g^{\max}$ is named `nggjht`.) Let $n_t(k_g)$ be the cumulative number of thin layers up to the top of thick layer k_g, and define $n_t(0) = 0$. The top of thick layer k_g lies at height and radius

$$h_{k_g}^{\text{top}} = h_{n_t(k_g)+\frac{1}{2}} \tag{11.1}$$

$$r_{k_g}^{\text{top}} = h_{k_g}^{\text{top}} + R_E \tag{11.2}$$

The bottom of thick layer k_g lies at height and radius

$$h_{k_g}^{\text{bot}} = \begin{cases} h_{k_g-1}^{\text{top}}, & k_g > 1 \\ h_R, & k_g = 1 \end{cases} \tag{11.3}$$

$$r_{k_g}^{\text{bot}} = h_{k_g}^{\text{bot}} + R_E \tag{11.4}$$

In `module delB_module` $h_{k_g}^{\text{bot}}$ is `ggjbot`. The nominal radius of thick layer k_g is $r_{k_g}^t$, specified

in `subroutine gen_ggj_grid` such that

$$r_{k_g}^{\rm bot} < r_{k_g}^t < r_{k_g}^{\rm top} \tag{11.5}$$

The height-integrated horizontal current density components K_{f1} and K_{f2} for a thick layer are

$$K_{f1}(i-\frac{1}{2},\ell^{sn},k_g) = \sum_{k=n_t(k_g-1)}^{n_t(k_g)} J_{f1}(i-\frac{1}{2},\ell,k)(h_{k+\frac{1}{2}}-h_{k-\frac{1}{2}}) \tag{11.6}$$

$$K_{f2}(i,\ell^{sn}-\frac{1}{2},k_g) = \sum_{k=n_t(k_g-1)}^{n_t(k_g)} J_{f2}(i,\ell-\frac{1}{2},k)(h_{k+\frac{1}{2}}-h_{k-\frac{1}{2}}) \tag{11.7}$$

$$\ell^{sn} = \begin{cases} \ell, & \text{southern hemisphere} \\ 2L_q+1-\ell, & \text{northern hemisphere} \end{cases} \tag{11.8}$$

[In `subroutine calc_Iqd` $K_{f1}(i-\frac{1}{2},\ell,k_g)$ is `Kf1qd(i,l,k)` and $K_{f2}(i,\ell-\frac{1}{2},k_g)$ is `Kf2qd(i,l,k)`. $J_{f1}(i-\frac{1}{2},\ell,k)$ and $J_{f2}(i-\frac{1}{2},\ell,k)$ are `Jf1qd(i,l,k,isn)` and `Jf2qd(i,l,k,isn)`, respectively, with `isn` = 1 for the southern hemisphere and 2 for the northern hemisphere.] The radial current density at the top of thick layer k_g is defined as

$$J_r^t(i,\ell^{sn},k_g) = J_r[i,\ell,n_t(k_g)+\frac{1}{2}] \tag{11.9}$$

[In `subroutine calc_Iqd` $J_r^t(i,\ell^{sn},k_g)$ is `Jrtopqd(i,l,k)`. Note that $J_r(i,\ell,k-\frac{1}{2})$ in (9.64) is defined to be the radial current density at the *bottom* of the kth thin layer, which is why 1 is added to the height index on the right-hand side of (11.9).] We define a "QD cell" with indices i,ℓ^{sn},k_g as the volume delimited on the west and east by $\phi_{q(i-\frac{1}{2})}$ and $\phi_{q(i+\frac{1}{2})}$, on the south and north by $\lambda_{q(\ell^{sn}-\frac{1}{2})}$ and $\lambda_{q(\ell^{sn}+\frac{1}{2})}$, and on the bottom and top by $h_{k_g}^{\rm bot}$ and $h_{k_g}^{\rm top}$ (or $r_{k_g}^{\rm bot}$ and $r_{k_g}^{\rm top}$) for use in the next section.

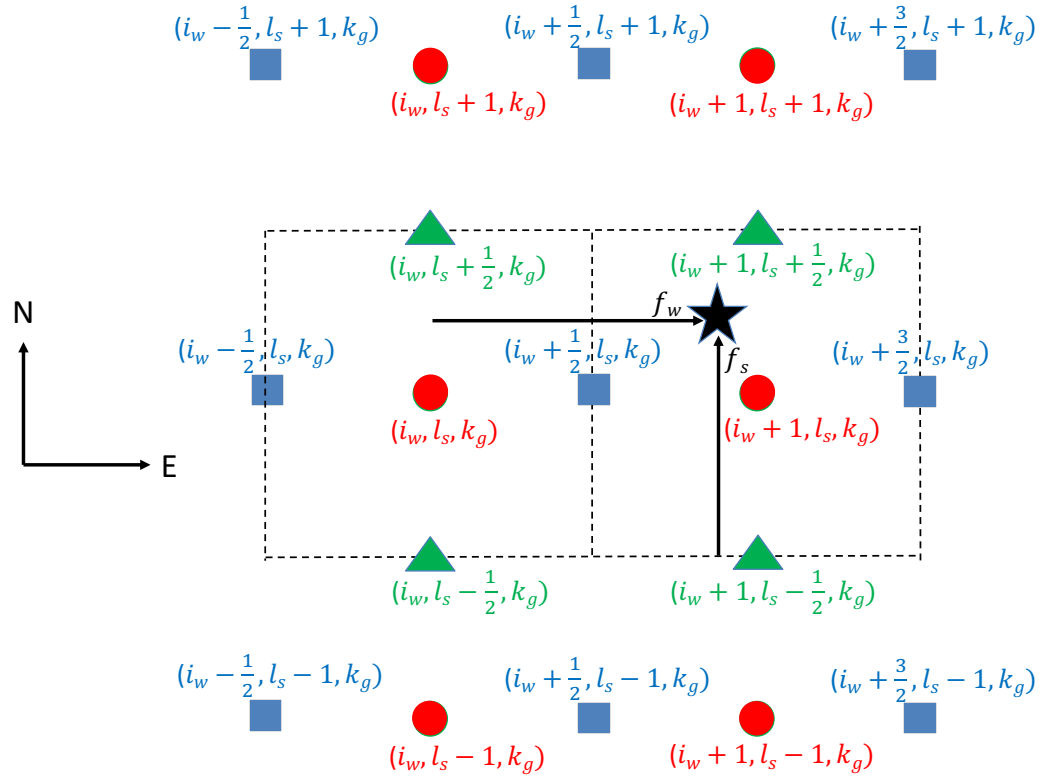

Figure 11.1: Schematic diagram showing how current components are interpolated from the QD grid to a geographic grid point. All points here are at the same thick-layer height level k_g. The geographic point to which current components are interpolated is the black star, where f_w gives its fractional distance from ϕ_{i_w} to ϕ_{i_w+1} and f_s gives its fractional distance from $\lambda_{l_s-\frac{1}{2}}$ to $\lambda_{l_s+\frac{1}{2}}$. In the case illustrated $f_w > 0.5$ and $f_s > 0.5$. Red circular dots represent the centers of QD cells, two of which are outlined with dashed lines. Green triangles represent the southern and northern edges of QD cells. Blue squares represent the western and eastern edges of QD cells.

11.2 Bilinear interpolation from QD to geographic grid

Figure 11.1 illustrates how QD and geographic grid points are matched. In `subroutine apxparm` (file `get_apex.f90`) a given geographic grid point (black dot) with geographic indices (i_g, j_g, k_g) at thick-layer height k_g is located between QD longitudes ϕ_{qi_w} and $\phi_{q(i_w+1)}$ (at the centers of QD cells) and between QD latitudes $\lambda_{q(l_s-\frac{1}{2})}$ and $\lambda_{q(l_s+\frac{1}{2})}$ (at the southern and northern edges of QD cells). Note that the referenced QD longitudes run through the centers of QD cells, while the referenced QD latitudes are at the southern and northern edges of these QD cells. The fractional QD longitude distance of the black star from ϕ_{qi_w} toward $\phi_{q(i_w+1)}$ is f_w. Its fractional QD latitude distance from $\lambda_{q(l_s-\frac{1}{2})}$ toward $\lambda_{q(l_s+\frac{1}{2})}$ is f_s. All of the quantities $i_w,\ l_s,\ f_w,\ f_s$ depend on the geographic indices $i_g,\ j_g,\ k_g$.

The three current components to be interpolated, $K_{f1},\ K_{f2},\ J_r^t$ have been computed at different faces of the QD cells. In order to minimize artificial numerical diffusion of the currents during interpolation, the QD current components are first individually interpolated bilinearly in the horizontal plane to the geographic grid before being vectorially combined and converted to geographic directions. (In retrospect, this modest benefit was probably not worth the extra complications caused by requiring three different interpolations instead of a single interpolation that could have been used if K_{f1} and K_{f2} had first been averaged to the centers of the QD cells.) In each case bilinear interpolation is carried out from the four locations surrounding the geographic point. For a given current component different locations may be selected depending on whether f_w and f_s are less than or greater than $\frac{1}{2}$. Values from the points to the south are weighted by w_s; those from the north by w_n; those from the west by w_w; and those from the east by w_e. These weights satisfy

$$w_n = 1 - w_s \tag{11.10}$$

$$w_e = 1 - w_w \tag{11.11}$$

The following sections describe how the locations for interpolation are selected and how their weights are calculated for each current component.

11.3 Interpolation of K_{f2}

K_{f2} has been calculated at the southern and northern faces of the QD cells, as represented by the green triangles in Figure 11.1. The western and eastern selected green triangles have longitude indices

$$\begin{aligned} i^- &= i_w \\ i^+ &= i_w + 1 \end{aligned} \tag{11.12}$$

(modified as needed to account for wrap-around longitudes). The southern and northern selected green triangles have latitude indices

$$\begin{aligned} l^- &= l_s - \frac{1}{2} \\ l^+ &= l_s + \frac{1}{2} \end{aligned} \tag{11.13}$$

The western and eastern weights are

$$\begin{aligned} w_w &= 1 - f_w \\ w_e &= f_w \end{aligned} \tag{11.14}$$

The southern and northern weights are

$$\begin{aligned} w_s &= 1 - f_s \\ w_n &= f_s \end{aligned} \tag{11.15}$$

The value of K_{f2} interpolated to the black star is

$$\begin{aligned} K^g_{f2}(i_g, j_g, k_g) &= w_w w_s K_{f2}(i^-, l^-, k_g) + w_w w_n K_{f2}(i^-, l^+, k_g) \\ &+ w_e w_s K_{f2}(i^+, l^-, k_g) + w_e w_n K_{f2}(i^+, l^+, k_g) \end{aligned} \tag{11.16}$$

11.4 Interpolation of J_r^t and η_{FAC}

J_r^t has been calculated at the top faces of the QD cells, above the red circular dots in Figure 11.1. The western and eastern selected red dots have longitude indices

$$\begin{aligned} i^- &= i_w \\ i^+ &= i_w + 1 \end{aligned} \tag{11.17}$$

The western and eastern weights are

$$\begin{aligned} w_w &= 1 - f_w \\ w_e &= f_w \end{aligned} \tag{11.18}$$

If $f_s > \frac{1}{2}$ as in Figure 11.1 the southern and northern latitude indices are

$$\begin{aligned} l^- &= l_s \\ l^+ &= l_s + 1 \end{aligned} \tag{11.19}$$

and the southern and northern weights are

$$\begin{aligned} w_s &= \frac{3}{2} - f_s \\ w_n &= f_s - \frac{1}{2} \end{aligned} \tag{11.20}$$

(Special considerations apply near the north QD pole.)

If $f_s < \frac{1}{2}$ the selected red dots move one index southward, so that the southern and northern latitude indices are

$$\begin{aligned} l^- &= l_s - 1 \\ l^+ &= l_s \end{aligned} \tag{11.21}$$

and the southern and northern weights are

$$\begin{aligned} w_s &= \frac{1}{2} - f_s \\ w_n &= f_s + \frac{1}{2} \end{aligned} \tag{11.22}$$

(Special considerations apply near the south QD pole.)

The value of upward current density at the top of the thick layer on the geographic grid is

$$\begin{aligned} J_r^{gt}(i_g, j_g, k_g) &= w_w w_s J_r^t(i^-, l^-, k_g) + w_w w_n J_r^t(i^-, l^+, k_g) \\ &+ w_e w_s J_r^t(i^+, l^-, k_g) + w_e w_n J_r^t(i^+, l^+, k_g) \end{aligned} \tag{11.23}$$

At the top of the topmost layer ($k_g = k_g^{\max}$, $h = h_{\text{top}}$) the equivalent current function η_{FAC} representing magnetic effects of field-aligned currents above this height is interpolated to the geographic grid using the same indices and weights as for J_r^{gt} at this height. In geographic coordinates this equivalent current function is labeled η_{FAC}^g [`etagg` in `subroutine calc_Iqd`].

11.5 Interpolation of K_{f1}

K_{f1} has been calculated at the western and eastern faces of the QD cells, as represented by the blue squares in Figure 11.1. When $f_s > \frac{1}{2}$, as in Figure 11.1, then the southern and northern selected blue squares have latitude indices

$$l^- = l_s \tag{11.24}$$

$$l^+ = l_s + 1 \tag{11.25}$$

The southern and northern weights are

$$w_s = \frac{3}{2} - f_s \tag{11.26}$$

$$w_n = f_s - \frac{1}{2} \tag{11.27}$$

If $f_s < \frac{1}{2}$ the selected blue squares move one grid point southward, with latitude indices

$$l^- = l_s - 1 \tag{11.28}$$

$$l^+ = l_s \tag{11.29}$$

The southern and northern weights are

$$w_s = \frac{1}{2} - f_s \tag{11.30}$$

$$w_n = f_s + \frac{1}{2} \tag{11.31}$$

(Special considerations apply at the poles.)

When $f_w > \frac{1}{2}$, as in Figure 11.1, then the western and eastern selected blue squares have longitude indices

$$i^- = i_w + \frac{1}{2} \tag{11.32}$$

$$i^+ = i_w + \frac{3}{2} \tag{11.33}$$

The western and eastern weights are

$$w_w = \frac{3}{2} - f_w \tag{11.34}$$

$$w_e = f_w - \frac{1}{2} \tag{11.35}$$

If $f_w < \frac{1}{2}$ the selected blue squares move one grid point westward, with longitude indices

$$i^- = i_w - \frac{1}{2} \tag{11.36}$$

$$i^+ = i_w + \frac{1}{2} \tag{11.37}$$

The western and eastern weights are

$$w_w = \frac{1}{2} - f_w \tag{11.38}$$

$$w_e = f_w + \frac{1}{2} \tag{11.39}$$

The interpolated value of K_{f1} at the black star is

$$\begin{aligned} K^g_{f1}(i_g, j_g, k_g) &= w_w w_s K_{f1}(i^-, l^-, k_g) + w_w w_n K_{f1}(i^-, l^+, k_g) \\ &+ w_e w_s K_{f1}(i^+, l^-, k_t) + w_e w_n K_{f1}(i^+, l^+, k_t) \end{aligned} \tag{11.40}$$

11.6 Layer currents in geographic directions

The radial current density (11.23) is already expressed in a geographic (upward) direction. In this section we express the horizontal layer currents in geographic directions. SPHEREPACK 3.2 takes inputs in the eastward and southward directions. The eastward and southward horizontal layer current densities $K_{\text{east}}(i_g, j_g, k_g)$ and $K_{\text{south}}(i_g, j_g, k_g)$ have contributions from all three QD current components, because $\mathbf{f}_3$ in (9.56) has small horizontal components, in general.

The average value of J_r in a current layer is taken to be the average of J^{gt}_r from (11.23) at the bottom and top of the layer. Then

$$\begin{aligned} K_{\text{east}}(i_g, j_g, k_g) &= f_{11}(i_g, j_g, k_g) K^g_{f1}(i_g, j_g, k_g) + f_{21}(i_g, j_g, k_g) K^g_{f2}(i_g, j_g, k_g) \\ &+ 0.5[f_{31}/F](i_g, j_g, k_g)[J^{gt}_r(i_g, j_g, k_g - 1) + J^{gt}_r(i_g, j_g, k_g)]\Delta h_{k_g} \end{aligned} \tag{11.41}$$

$$\begin{aligned} K_{\text{south}}(i_g, j_g, k_g) &= -f_{12}(i_g, j_g, k_g) K^g_{f1}(i_g, j_g, k_g) - f_{22}(i_g, j_g, k_g) K^g_{f2}(i_g, j_g, k_g) \\ &- 0.5[f_{32}/F](i_g, j_g, k_g)[J^{gt}_r(i_g, j_g, k_g - 1) + J^{gt}_r(i_g, j_g, k_g)]\Delta h_{k_g} \end{aligned} \tag{11.42}$$

where f_{11} and f_{12} are the geographic eastward and northward components of the basis vector

$\mathbf{f}_1$; f_{21} and f_{22} are the corresponding components of $\mathbf{f}_2$; f_{31} and f_{32} are the corresponding components of $\mathbf{f}_3$; $F = |\mathbf{f}_1 \times \mathbf{f}_2|$; and

$$\Delta h_{k_g} = h_{k_g}^{\text{top}} - h_{k_g}^{\text{bot}} \tag{11.43}$$

where $h_{k_g}^{\text{top}}$ and $h_{k_g}^{\text{bot}}$ are given by (11.1) and (11.3).

Chapter 12

Calculating Magnetic Perturbations

12.1 Spherical-harmonic expansion of current components

Represent the height-integrated horizontal current in the layer k_g as

$$\mathbf{K}_{k_g}(\theta_g, \phi_g) = \mathbf{k} \times \nabla \eta_{k_g}(\theta_g, \phi_g) + \nabla_h \xi_{k_g}(\theta_g, \phi_g) \tag{12.1}$$

where θ_g, ϕ_g are geographic colatitude and longitude and ∇_h is the horizontal gradient operator $-\mathbf{k} \times (\mathbf{k} \times \nabla\ )$. The first term on the right-hand side of (12.1) represents toroidal current, while the second term represents the horizontal component of poloidal current. Toroidal currents produce poloidal magnetic perturbations that have a radial component and can be sensed below the current region, while poloidal currents produce toroidal magnetic perturbations that have no radial component and are not sensed below the current region.

Expand η_{k_g} in a spherical-harmonic series in geographic coordinates as

$$\eta_{k_g}(\theta_g, \phi_g) = \sum_{n=1}^{N} \sum_{m=-n}^{n} c_n^m(k_g) Y_n^m(\theta_g, \phi_g) \tag{12.2}$$

where Y_n^m is a spherical harmonic as defined in Section 10.2. Using (12.2) in (12.1) and making use of (10.15) and (10.16), we find

$$\int (\mathbf{k} \times \nabla Y_n^m) \cdot \mathbf{K}_{k_g} \, da = n(n+1) c_n^m(k_g) = \int \left[\frac{1}{r} \frac{\partial Y_n^m}{\partial \theta_g} \mathbf{i} + \frac{1}{r \sin\theta_g} \frac{\partial Y_n^m}{\partial \phi_g} \mathbf{j} \right] \cdot \mathbf{K}_{k_g} \, da \tag{12.3}$$

$$c_n^m(k_g) = \frac{1}{n(n+1)} \int \left[\frac{K_{k_g\theta_g}}{r} \frac{\partial Y_n^m}{\partial \theta_g} + \frac{K_{k_g\phi_g}}{r \sin\theta_g} \frac{\partial Y_n^m}{\partial \phi_g} \right] da \tag{12.4}$$

where $\mathbf{i}$ and $\mathbf{j}$ are unit vectors in the geographic eastward and northward directions. Consider the equivalent current function η^g_{FAC} associated with field-aligned currents above r_{top} to be the (k_g+1)th layer:

$$\eta^g_{\mathrm{FAC}}(\theta_g, \phi_g) = \sum_{n=1}^{N} \sum_{m=-n}^{n} c_n^m(k_g^{\max}+1) Y_n^m(\theta_g, \phi_g) \tag{12.5}$$

$$c_n^m(k_g^{\max}+1) = \int \eta^g_{\mathrm{FAC}}(\theta_g, \phi_g) Y_n^m(\theta_g, \phi_g) \, \frac{da}{r_{\mathrm{top}}^2} \tag{12.6}$$

The area integrals in (12.4) and (12.6) could be carried out either in QD or geographic coordinates; we choose the latter (although the former would avoid the necessity of interpolating from the QD grid to the geographic grid).

The radial current density J_r at radius r can be expanded in a spherical-harmonic series as

$$J_r(r, \theta_g, \phi_g) = \sum_{n=1}^{N} \sum_{m=-n}^{n} \frac{b_n^m(r)}{r^2} Y_n^m(\theta_g, \phi_g) \tag{12.7}$$

$$b_n^m(r) = \int J_r(r, \theta_g, \phi_g) Y_n^m(\theta_g, \phi_g) \, da \tag{12.8}$$

Note that to get $b_n^m(r_{k_g}^{\mathrm{bot}})$ at the base of thick current layer k_g it is the gridded values of J_r at the *top* of the thick layer *below*, $J_r^{gt}(i_g, j_g, k_g - 1)$ [see (11.23)] that need to be used in the integral of (12.8). To get $b_n^m(r_{k_g^{\max}+1}^{\mathrm{bot}})$ at the top of thick current layer $k_g^{\max}$ it is gridded values of J_r at the *top* of the top thick layer $(k_g^{\max})$, $J_r^{gt}(i_g, j_g, k_g)$ that is used in the integral of (12.8).

The current potential function ξ_{k_g} in (12.1) could also be expanded in a spherical-harmonic series, but it is not needed to calculate magnetic perturbations.

12.2 Spherical-harmonic expansion of magnetic-perturbation components

The model calculates magnetic perturbations $\mathbf{\Delta B}$ at the ground and at the boundaries between current layers, from where the perturbations can be interpolated to other heights within the ionosphere for simulation of magnetic perturbations at the locations of Low-Earth-Orbit (LEO) spacecraft. At the ground the magnetic-perturbation field is curl-free and can be expressed as the negative gradient of a scalar potential V, but at LEO the presence of local currents means $\mathbf{\Delta B}$ is not curl-free there. We idealize the three-dimensional current density within the ionosphere as composed of thin horizontal current layers at heights $h^t_{k_g}$ (radii $r^t_{k_g}$, where the superscript t indicates that the subscript is for a thick layer as defined in Section 11.1, not for a thin layer as in Section 4.4) that carry all of the horizontal current in the k_gth layer, connected by radial current density flowing between layers. The toroidal height-integrated current in layer k_g is $\mathbf{k} \times \nabla\eta(k_g, \theta_g, \phi_g)$, which produces potential-field magnetic perturbations above and below. The radial current density produces a toroidal magnetic perturbation that is solely horizontal. For all locations *except* locations right at the idealized current sheets, we can write the magnetic perturbation field as

$$\mathbf{\Delta B} = \nabla_h V(r, \theta_g, \phi_g) - \mathbf{k} \times \nabla\tau(r, \theta_g, \phi_g) + \mathbf{k}\ \Delta B_r(r, \theta_g, \phi_g) \tag{12.9}$$

(This is not valid right at the current sheets, because the curl of $\nabla_h V$ does not yield the toroidal current density in the sheets, although the difference of $\nabla_h V$ calculated immediately below and above a current sheet, when rotated 90° horizontally, does yield the height-integrated toroidal current density in the sheet. Since we calculate $\mathbf{\Delta B}$ from (12.9) only at the ground and at the boundaries between the thick current layers, this limitation of (12.9) poses no problem. Note that the magnetic potential V is used only for horizontal magnetic perturbations and not for calculating the radial magnetic perturbation ΔB_r.) V, τ, and ΔB_r are expanded in spherical-harmonic series as

$$V(r, \theta_g, \phi_g) = \sum_{n=1}^{N} \sum_{m=-n}^{n} v_n^m(r)\ Y_n^m(\theta_g, \phi_g) \tag{12.10}$$

$$\tau(r,\theta_g,\phi_g) = \sum_{n=1}^{N}\sum_{m=-n}^{n} t_n^m(r)\ Y_n^m(\theta_g,\phi_g) \tag{12.11}$$

$$\Delta B_r(r,\theta_g,\phi_g) = \sum_{n=1}^{N}\sum_{m=-n}^{n} \beta_n^m(r)\ Y_n^m(\theta_g,\phi_g) \tag{12.12}$$

The coefficients t_n^m at a given height are directly obtained from the spherical-harmonic coefficients b_n^m in (12.8) at that height, since

$$\mu_0 J_r = \mathbf{k}\cdot\nabla\times\mathbf{\Delta B} = -\nabla\cdot(\mathbf{k}\times\mathbf{\Delta B}) = -\nabla_h^2\tau \tag{12.13}$$

where ∇_h^2 is the horizontal Laplacian. Note that

$$\nabla_h^2 Y_n^m = -\frac{n(n+1)}{r^2}Y_n^m \tag{12.14}$$

Then

$$\frac{\mu_0}{r^2}\sum_{n=1}^{N}\sum_{m=-n}^{n} b_n^m(r)Y_n^m(\theta_g,\phi_g) = \sum_{n=1}^{N}\sum_{m=-n}^{n}\frac{n(n+1)}{r^2}t_n^m(r)Y_n^m(\theta_g,\phi_g) \tag{12.15}$$

$$t_n^m(r) = \frac{\mu_0}{n(n+1)}b_n^m(r) \tag{12.16}$$

The magnetic potential V and the radial magnetic perturbation ΔB_r are calculated from the toroidal current sheets $\mathbf{k}\times\nabla\eta_{k_g}(\theta_g,\phi_g)$ in (12.1). The current layer at r_g^t produces a magnetic potential with coefficients

$$v_{nk_g}^m(r) = -\frac{\mu_0\ c_n^m(k_g)}{2n+1}\times\begin{cases} n\ \left(\frac{r_{k_g}^t}{r}\right)^{n+1}, & r > r_{k_g}^t \\ (n+1)\left(\frac{r}{r_{k_g}^t}\right)^n, & r < r_{k_g}^t \end{cases} \tag{12.17}$$

and radial magnetic perturbation coefficients

$$\beta_{nk_g}^m(r) = -\frac{\partial v_{nk_g}^m(r)}{\partial r} = -\frac{\mu_0 n(n+1)c_n^m(k_g)}{r(2n+1)}\times\begin{cases} \left(\frac{r_{k_g}^t}{r}\right)^{n+1}, & r \geq r_{k_g}^t \\ \left(\frac{r}{r_{k_g}^t}\right)^n, & r \leq r_{k_g}^t \end{cases} \tag{12.18}$$

At ground level the "external" coefficients associated with the ionospheric and field-

aligned magnetospheric currents are obtained by summing the contributions from all layers:

$$\frac{v_n^m(R_E)^{\rm ext}}{R_E} = \frac{\mu_0\ (n+1)}{(2n+1)R_E} \sum_{k'=1}^{k_g^{\rm max}+1} c_n^m(k') \left(\frac{R_E}{r_{k'}^t}\right)^n \tag{12.19}$$

$$\beta_n^m(R_E)^{\rm ext} = \frac{-\mu_0\ n(n+1)}{(2n+1)R_E} \sum_{k'=1}^{k_g^{\rm max}+1} c_n^m(k') \left(\frac{R_E}{r_{k'}^t}\right)^n = -n\frac{v_n^m(R_E)^{\rm ext}}{R_E} \tag{12.20}$$

The time-varying external magnetic perturbations induce currents within the Earth that create "internal" magnetic perturbations, which can be represented by coefficients $v_n^m(r)^{\rm int}$ and $\beta_n^m(r)^{\rm int}$. Section 12.4 gives a simple model of the internal coefficients. Between the Earth's surface and the base of the model ($R_E < r < R_E + h_R$) the coefficients are

$$v_n^m(r) = v_n^m(R_E)^{\rm ext} \left(\frac{r}{R_E}\right)^n + v_n^m(R_E)^{\rm int} \left(\frac{R_E}{r}\right)^{(n+1)} \tag{12.21}$$

$$\beta_n^m(r) = \beta_n^m(R_E)^{\rm ext} \left(\frac{r}{R_E}\right)^n + \beta_n^m(R_E)^{\rm int} \left(\frac{R_E}{r}\right)^{(n+1)} \tag{12.22}$$

$$t_n^m(r) = 0 \tag{12.23}$$

Within the ionosphere ($R_E + h_R < R < r_{\rm top}$) the model calculates the coefficients at the bases of the thick layers ($r = r_{k_g}^{\rm bot},\ 1 \le k_g \le k_g^{\rm max}+1$). Summing up the effects at $r_{k_g}^{\rm bot}$ from currents in all layers plus the effects of "internal" magnetic perturbations gives

$$\begin{aligned} \frac{v_n^m(r_{k_g}^{\rm bot})}{r_{k_g}^{\rm bot}} &= \frac{\mu_0}{(2n+1)r_{k_g}^{\rm bot}} \left[-n \sum_{k'=1}^{k_g-1} c_n^m(k') \left(\frac{r_{k'}^t}{r_{k_g}^{\rm bot}}\right)^{n+1} + (n+1) \sum_{k'=k_g}^{k_g^{\rm max}+1} c_n^m(k') \left(\frac{r_{k_g}^{\rm bot}}{r_{k'}^t}\right)^n \right] \\ &+ \frac{v_n^m(R_E)^{\rm int}}{r_{k_g}^{\rm bot}} \left(\frac{R_E}{r_{k_g}^{\rm bot}}\right)^{(n+1)} \end{aligned} \tag{12.24}$$

$$\begin{aligned} \beta_n^m(r_{k_g}^{\rm bot}) &= \frac{-\mu_0\ n(n+1)}{(2n+1)r_{k_g}^{\rm bot}} \left[\sum_{k'=1}^{k_g-1} c_n^m(k') \left(\frac{r_{k'}^t}{r_{k_g}^{\rm bot}}\right)^{n+1} + \sum_{k'=k_g}^{k_g^{\rm max}+1} c_n^m(k') \left(\frac{r_{k_g}^{\rm bot}}{r_{k'}^t}\right)^n \right] \\ &+ \beta_n^m(R_E)^{\rm int} \left(\frac{R_E}{r_{k_g}^{\rm bot}}\right)^{(n+1)} \end{aligned} \tag{12.25}$$

where

$$r^{\rm bot}_{k_g^{\rm max}+1} \equiv r_{\rm top} \tag{12.26}$$

The coefficients $t_n^m(r_{k_g}^{\rm bot})$ at the base of thick layer k_g are obtained from (12.8) and (12.16). For heights (radii) other than $r_{k_g}^{\rm bot}$ within the ionosphere ($r_1^{\rm bot} < r < r_{\rm top}$) the quantities v_n^m/r, β_n^m, and t_n^m are linearly interpolated between the values at the layer interfaces below and above.

When the coefficients have been calculated, the magnetic perturbatons at any location from the ground to the top of the model can be calculated from (12.9)-(12.12).

12.3 Equivalent current function at 110 km

The coefficients $v_n^m(R_E)^{\rm ext}$ from 12.19 and $\beta_n^m(R_E)^{\rm ext}$ from 12.20 are identical to what would be produced by a thin layer of divergence-free horizontal current $\mathbf{K}_{110}^{\rm equiv}$ flowing at an altitude of 110 km, represented by an equivalent current function η_{110}:

$$\mathbf{K}_{110}^{\rm equiv} = \mathbf{k} \times \nabla \eta_{110} \tag{12.27}$$

$$\eta_{110}(\theta_g, \phi_g) = \sum_{n=1}^{n_{\rm max}} \sum_{m=-n}^{n} c_{n110}^m Y_n^m(\theta_g, \phi_g) \tag{12.28}$$

$$c_{n110}^m = \frac{2n+1}{(n+1)\mu_0} \left(\frac{R_E + 110 \text{ km}}{R_E} \right)^n v_n^m(R_E)^{\rm ext} \tag{12.29}$$

12.4 Simple model of "internal" magnetic perturbations

As the "external" magnetic field varies in time, it effectively diffuses into the conducting Earth. This diffusion is accompanied by electric currents within the Earth that flow in such a way as to prevent the combined "external" field and the magnetic field produced by the Earth currents from rapidly penetrating deep into the Earth. For an "external" field that is suddenly switched on, the Earth currents tend to flow horizontally in a direction

opposite to the equivalent ionospheric current, such that the vertical components of the magnetic perturbation due to the ionospheric and induced Earth currents tend to partially cancel each other. The larger the electrical conductivity of the Earth at a particular depth, the more difficult it is for the total perturbation magnetic field to penetrate rapidly. The oceans can be partially penetrated in a few minutes. The upper Earth's mantle has lower conductivity than ocean water, but the mantle conductivity generally increases with depth. On a time scale of hours magnetic fields can penetrate to a depth of 500 km or more. A very simple model of Earth conductivity has zero conductivity down to a certain depth, about 600 km for typicaly daily magnetic variations, transitioning abruptly to infinite conductivity at that depth. An "external" field can penetrate unimpeded to that depth, where it will induce current at the surface of the infinite conductor such that ΔB_r vanishes at that depth. The horizontal component of magnetic perturbation associated with the current is such that the total magnetic perturbation below the current vanishes, while the magnetic perturbation above it increases. These effects are instantaneous, without a time lag that would exist if the conductivity were finite. In reality the induced Earth currents neither set up instantaneously nor decay instantaneously if the "external" field is suddenly removed.

If the radius of the perfect conductor is c then this simple model gives

$$v_n^m(R_E)^{\text{int}} = \left(\frac{c}{R_E}\right)^{(2n+1)} v_n^m(R_E)^{\text{ext}} \tag{12.30}$$

$$\beta_n^m(R_E)^{\text{int}} = -\left(\frac{c}{R_E}\right)^{(2n+1)} \beta_n^m(R_E)^{\text{ext}} \tag{12.31}$$

12.5 Application of SPHEREPACK 3.2

Although the SPHEREPACK 3.2 code uses an ancient version of FORTRAN (F77), it calculates both the scalar and vector spherical harmonics we need. Some constraints are that the code requires equally spaced points in longitude and (in our implementation) latitude points corresponding to Gaussian quadrature. We needed to modify only one aspect of the code to make it work with modern FORTRAN compilers: changing the final dimension of certain

subroutine arrays from a nominal value of "1" (used only as a pointer to the first element of the array) to "$*$" (signifying that this array dimension is set by the calling routine).

The mathematics underlying this code are documented for an earlier version (SPHEREPACK 2.0) in *Adams and Swartzrauber* (1997). The documentation uses unnormalized associated Legendre functions $P_n^m{}_{\text{unnormalized}}$, which are related to the normalized functions we define in (10.5)-(10.9) by

$$P_n^m = \sqrt{(2n+1)\frac{(n-m)!}{(n+m)!}}\; P_n^m{}_{\text{unnormalized}} \tag{12.32}$$

Adams and Swartzrauber (1997) and comments in the SPHEREPACK 3.2 code also reference normalized associated Legendre functions, and it is not clear whether these normalized functions might used in the code. (THIS SHOULD BE CHECKED WITH SOME TESTS.) Also, the documentation uses cosine and sine functions to express longitude structure, as opposed to the normalized longitude functions f_m of (10.4), which have an average squared value of 1. Because of these differences, the spherical-harmonic coefficients directly obtained from calls to SPHEREPACK 3.2 routines may have multiplicative factors dependent on n and m with respect to the coefficients of the present document. However, as long as the SPHEREPACK 3.2 routines are also used to reconstruct the current and magnetic-perturbation fields, effectively using the same multiplicative factors, the final fields should be compatable with what would be obtained using the equations in this document.

One thing to note when combining SPHEREPACK 3.2's spherical-harmonic coefficients calculated for scalar functions like those in (12.2) with coefficients calculated using area integrals involving gradients of spherical harmonics like those in (12.4) is that SPHEREPACK 3.2 first multiplies the gradients of the spherical harmonics in `subroutine vhags` by $r/\sqrt{[n(n+1)]}$. Therefore, we multiply the coefficient arrays returned from `subroutine vhags` by $\sqrt{[n(n+1)]}/r$ when used to calculate c_n^m as in (12.4).

Chapter 13

References

International Geomagnetic Reference Field: the 13th generation, Alken, P., Thébault, E., Beggan, C.D. et al. International Geomagnetic Reference Field: the thirteenth generation. Earth Planets Space 73, 49 (2021). doi: 10.1186/s40623-020-01288-x

Richmond, A.D. (1995). Ionospheric electrodynamics using Magnetic Apex Coordinates. *Journal of Geomagnetism and Geoelectricity, 47*, 191-212. https://doi.org/10.5636/jgg.47.191

Richmond, A.D. (2016). Ionospheric electrodynamics. In G.V. Khazanov (Ed.), *Space Weather Fundamentals*, Chapter 14, 245-259. Boca Raton, FL: CRC Press.